# Early-Stage Ship Design Operational Considerations as a Thin Abstraction Enabled by a Grid-Supported Markov Decision Process Directional Decision Ensemble Framework

by

Hao Yuan

A dissertation submitted in partial fulfillment
of the requirements for the degree of
Doctor of Philosophy
(Naval Architecture and Marine Engineering)
in the University of Michigan
2021

Doctoral Committee:

Associate Professor David J. Singer, Chair
Associate Professor Matthew D. Collette
Associate Professor Kevin J. Maki
Professor Romesh Saigal

Hao Yuan

haoyuanl@umich.edu

ORCID iD: 0000-0002-3272-6901

© Hao Yuan 2021

To my family and friends.

# ACKNOWLEDGEMENTS

First and foremost, I would like to thank my advisor, Dr. David Singer, who guided me to the field of design and has been providing me with support inside and outside the research. I will not reach this point without his guidance and encouragement.

I would like to thank my committee, for their insightful comments and suggestions on my research and thesis development.

I would like to thank China Scholarship Council, for providing me with the funding to pursue the Ph.D. study.

I would like to thank my lab mates, for lending me their wisdom to brainstorm new ideas whenever I needed help.

I would like to thank my family and friends, for giving me unparalleled love, trust, and support throughout my life.

# TABLE OF CONTENTS

# LIST OF TABLES

**Table**

# LIST OF FIGURES

**Figure**

# LIST OF ABBREVIATIONS

**MDP** Markov Decision Process

**GS-MDP** Grid-Supported Markov Decision Process

**CFD** Computational Fluid Dynamics

**FEA** Finite Element Analysis

**RMS** Root Mean Square

**SSA** Significant Single Amplitude

**OCV** Offshore Construction Vessel

# ABSTRACT

Design always works with a reduction of the problem's complexity. Independent of the design stage, design always involves a reduction in fidelity from the final operational product. This fact is even more prevalent in the design of large marine products. The reduction of the designed vessel's complexity is also known as an abstraction, and designers utilize abstractions during all phases of design. The term abstraction means that designers connect "the world of events that actually occurred or can occur" and "the imagined world of hypothetical descriptions". Currently, researchers have focused on creating thick abstractions through specific frameworks, which can richly describe a certain scenario of the event with as much detail as possible. However, little has been done to enable thin abstractions, which only reserve key factors to ensure condensed but not scenario-specific descriptions of the event. Because of this gap, it becomes challenging to understand the operational performances of a conceptual design with adequate multidisciplinary trade-offs. If suitable key factors exist, designers would then be able to model ship operations at a reduced-order level, consistent with what a conceptual design supports but rich in the implications of how multiple disciplines are synthetically balanced. In the evaluation of ship operations, thick abstractions are the predominant approach being taken. The research presented in this thesis focuses on the creation of a novel thin abstraction of ship operations so that the appropriate key factors of describing sea transport performances in concept design can be obtained.

The Grid-Supported Markov Decision Process (GS-MDP) framework has been developed to analyze ship operations as a thin abstraction. The framework blends a newly developed gridding approach, Markov Decision Process (MDP), and frequency-

domain seakeeping codes. The GS-MDP framework uniquely identifies directional decisions as the key factor required to execute operational evaluation as a thin abstraction. A directional decision is the determination of whether a direction at a location deserves to be maintained or adjusted with respect to reaching the destination. By setting up MDP based on a novel ocean grid, a vessel can be simulated to make directional decisions for all directions at all locations over the entire ocean under any circumstance. Linking frequency-domain seakeeping codes to MDP ensures the incorporation of physics-based ship motions to the sea transport simulations. Furthermore, aggregating directional decisions solutions across a large simulation space creates thin abstraction operation ensembles. The operation ensemble can provide valuable knowledge for designers to understand a conceptual design.

Beyond the novel framework, new decision metrics have been developed that enable design decisions utilizing the thin abstraction. Based on the utilization and statistical analysis of an operation ensemble, these metrics enable the designer to understand the potentials of operational efficiency or operational difficulty. The ability to quantify efficiency or difficulty allows designers to explain the underlying causation associated with the operational potentials. Two case studies are presented in this thesis. The first case study discusses the usefulness of the GS-MDP framework in identifying main contributors and underlying contexts with respect to certain operational outcomes. The second case study expands the application of this framework and maps it onto both transit events and on-site operational events, which illustrates the value of a thin abstraction.

# CHAPTER I

# Introduction

## 1.1 Background

### 1.1.1 Concept Design

The ship design process, referenced by (*Tupper*, 2013; *Rawson and Tupper*, 2001), utilizes various terminology, but the intent is consistent across the literature. (*Tupper*, 2013) describes the three main design stages as follows.

- Concept design. It is generally agreed that this is the earliest and most important design stage during which designers start to translate the customer requirements to potential solutions. Naval architects need to conceive rough hull form parameters and analyze aspects of the hull form at the appropriate level of detail.

- Contract design. Design solutions must be further developed to allow a contract to be negotiated for building the vessel. Calculations that apply high-fidelity methods such as Computational Fluid Dynamics (CFD) and Finite Element Analysis (FEA) will be carried out. Model tests will also be conducted when the final hull form emerges.

- Detail design. Based on the contract design, the shipyard's staff will work on

detailed engineering drawings and production plans. This stage may overlap with the construction of the vessel.

The research focus of this thesis is on the concept design stage. One unique aspect of marine products, when compared to traditional engineering products, is their scale and complexity. The scale and complexity of large ships make the use of high-fidelity tools and detail modeling prohibitive at the early design stages. Out of necessity, abstraction plays a significant role in concept design. Abstraction, if properly executed, can reduce complexity and mitigate the risk of being trapped in psychological inertia (*Kamarudin et al.*, 2016).

*Kamarudin et al.* (2016) have summarized several different definitions (*Dictionary.com*, n.d.; *Merriam-Webster*, n.d.; *Lexico.com*, n.d.) of abstraction and stated that "the term theorizing complements abstraction in design science". Theorizing means that people make a connection between "the world of observed events, such as falling apples, and the imagined world of hypothetical concepts, such as gravity" (*Folger and Turillo*, 1999). The process of theorizing can be supported by constructing events with thickness or thinness.

- Thickness. A thick abstraction is one that richly describes a scenario of the event, allowing a person to understand the scenario, the event, and the potential or real outcomes side-by-side. A thick abstraction allows people to gain limited theoretical insights due to the fact that they can only compare outcomes directly to a described scenario (*Pinker*, 1997). In the marine domain, this is akin to developing a detailed model of a transit scenario. Ship owners and designers often desire to understand which vessel design will provide the best fuel efficiency or produce the most profit over a trade route. To achieve this goal, the designers will create a model that tries to capture as much detail as possible, including all the factors that they believe potentially impact the cost or revenue. Once the model is completed, they will apply the model to various design scenarios and

compare the results. They may even complete a sensitivity study so that they can understand the impact of assumptions or parameters on the conclusions. Even though the model created by the designers would contain many details, it is still an abstraction of what the vessel would actually experience. This example can be considered as a thick abstraction due to the details included and the direct side-by-side comparisons that can be made.

- Thinness. A thin abstraction is a highly condensed description of an event, which allows people to disregard irrelevant details that are not required to make a conclusion and reserve key factors. The critical difference between thick and thin is that thinness removes the focus on the results of a particular scenario. The shift of focus away from results allows a thin abstraction to be mapped onto several scenarios due to the simple fact that results are scenario-specific. Thin abstractions are purposely rich not in details but in implications (*Folger and Turillo*, 1999). An adequate extraction of all the key factors ensures that thin abstractions are rich in implications. The research presented in this thesis provides the framework and methods for a thin abstraction of maritime operations.

The Kolb learning cycle (*Kolb*, 2014) further demonstrates that abstraction is a necessary learning mode to gain knowledge. Within this cycle, people's understanding will become complete when they reflectively observe concrete experiences and form abstract theories (*Sharlanova*, 2004). The concrete experiences that naval architects can observe are broad. For example, if they tend to abstract sea transport operations, concrete experiences for observation may refer to routes or the ship's stepwise movements. There are no good or bad concrete experiences. As long as they are appropriately generated and organized based on a particular perspective, people can gain valuable knowledge from them. Moreover, according to the problems that ship designers work on, the demand for concrete experiences varies. For a simple marine

design, such as a standard bulk carrier, what the designers expect to gain from the engineering activities has a high probability of matching what previous engineering activities have actually produced. Since there is a large number of bulk carriers designed and produced each year, the designers only require a small number of personal concrete experiences to produce a reliable abstraction. This is due to the fact that they can leverage the experiences of others and treat them as their own and use them as a reference for abstraction. However, when designing a complex or novel marine product, it is unclear to predict the future influence of design decisions since no common reference exists. Hereby, the number of experiences, not specifically concrete toward a result or a specific outcome, needs to dramatically expand if the designers want to create a robust abstraction. Broadly speaking, observing concrete experiences is helpful for designers to proceed to more general and even formal design theories (*Urquhart et al.*, 2010). As such, if it is computationally accessible, building a vast repository of concrete experiences will significantly assist the abstraction. The situation does remain for novel designs where the ability to create concrete experiences does not, or can not, exist.

Additionally, it is worth noticing that the knowledge derived from abstraction is somewhat bound to the abstraction background (*Gregor et al.*, 2013). Designers should be aware of the context, the objective, or the scope of abstraction before generating and using corresponding knowledge. The presented work demonstrates the development and execution of a novel thin abstraction of ship operations within the conceptual design construct. Through the use of a thin abstraction, the research creates an ensemble of potential operational experiences that a ship might encounter, which provides a source of experiences, while are not concrete or result-specific, for the designers to use for operational knowledge development.

Within the early-stage design, thick abstractions are often pursued due to the desire to provide specific information needed to satisfy certain contractual objectives.

It is common for the thick abstraction to be a literal translation of a deliverable. The reality is that in many design problems, abstractions are simply needed to provide knowledge for designers to understand objective fulfillment but not to provide a result value. Several relevant objectives (*Gale*, 2003) of this stage are listed in Table 1.1. All the listed objectives ask for one or more outcomes. In other words, quantify, validate, or establish certain outcomes. For the completion of such objectives, designers have to create appropriate knowledge to understand the implications associated with each outcome before they can make a determination. Designers need to use thin abstractions to create the appropriate knowledge for understanding implications while using thick abstractions for determination. A thin abstraction of ship operations will enrich novel knowledge concerning ship performances and serve as a complement to the thick abstractions already in use. An alternative method for creating ship operational experiences is an important part of analyzing ship configurations, thus indirectly promoting the understanding of ship main hull design decisions.

Table 1.1: Several design objectives of the concept stage

| | |
|---|---|
| **1** | Quantify ship performance. |
| **2** | Validate the top-level ship performance requirements and develop second-tier requirements. |
| **3** | Establish ship size and overall configuration. |

### 1.1.2 Abstraction of Ship Operations

Ship operations often rely on many disciplines, such as mechanics (*Couser*, 2000), logistics (*McLean and Biles*, 2008), and economic valuations (*Michalski*, 2014). One of the basic operations is ocean transit, when the ship's response to the ocean environment creates adverse motions that affect its behavior of maintaining desirable trajectories and decrease its operational performance. Therefore, in early design it is beneficial for designers to abstract transit operations with the impact of ship motions

in consideration.

Current methods, which range in complexity and quality, support a thick abstraction of transit. Even in the concept stage when designers cannot completely describe the thickness of the transit operation that they want to investigate, designers will focus on a specific discipline of interest related to the transit problem and infer the impact of that discipline on an operational scenario. For example, some researchers (*McLean and Biles*, 2008) in the field of industrial engineering idealize the ship motions, specify a given shipping network with several routes, and use discrete-event models to simulate the ship's transit efficiency. In terms of marine engineering, there exists research (*Couser*, 2000) that overlays low-fidelity methods of estimating seakeeping responses based on specific routes and the sea conditions along the routes. When using these reduced-order methods, designers attempt to describe the relevant events along the route based on what they perceive to be the best modeling, data, and information available to them. There is also another category of methods, high-fidelity methods, whose characteristic is to require and output thickness. These methods integrate complex physics and other disciplines related to a route to create operational simulations of a design with substantially more details in both the modeling as well as the vessel itself. Nevertheless, typically early-stage design cannot offer the vessel details that high-fidelity methods require. Even if the designers assume and supplement the details, the time to create, run, and analyze these thick abstractions are longer than the available time allotted for decision-making.

As mentioned before, the usefulness of abstraction cannot be detached from its background. If the abstraction of transit operations is created based on a current reduced-order model, the background mainly involves rough hull form approximations and few disciplinary connections. Such abstraction realizes a quick and versatile understanding of an isolated discipline. In terms of the abstraction derived from a current high-fidelity model, the background usually covers explicit hull form details.

What this abstraction achieves is a detailed understanding of how multiple disciplines synthetically impose influence on the ship's transit. Although this abstraction provides a detailed understanding from a multidisciplinary perspective, this understanding is not versatile. A versatile abstraction is one that is not only capable of doing many things competently, or possessing varied uses or many functions, but also changeable without loss of its initial quality. If properly conceived, a thin abstraction is a versatile one. If designers evaluate a high-fidelity thick transport abstraction, any change to the ship, the modeling assumptions, or the modeling parameters will fundamentally change the results and thus the conclusions that can be made. Moreover, the previous results of the original thick abstraction can not be compared to the new modified thick abstraction. They are unique instances whose multidisciplinary influences cannot be compared with each other, simply because the multidisciplinary influences are tied to each abstraction independently. Since properly developed thin abstractions are formulated by using only key factors and removing irrelevant details, they can be applied in multiple studies as long as the key factors do not change. Thus, the following question remains. How can it be true that thin abstractions can handle changes while thick ones cannot? This aspect of the thin and thick abstraction is also stated by *Folger and Turillo* (1999): the model built based on thinness "can be mapped onto several situations, all of which share the same relevant features, even if irrelevant features make them appear dissimilar". There is obviously a gap between the current thin and thick abstractions used within the marine domain. Given the current abstractions of transit operations, the author wonders if it is possible to create an abstraction on the basis of rough hull form approximations and sufficient disciplinary interactions such as ship motions grounded in physics. This new background condition to learn conceptual ship designs, which cannot be fully addressed by the existing method, requires innovative methods with their own usefulness to abstract transit operations.

The primary challenge for designers is that they are too accustomed to referring to something that has been proven helpful for understanding the transit, but seldom think over what the key factors to the design problem should be and whether they are really focusing on the appropriate key factors. For example, if the designers want to learn the ship's transport efficiency, they often make a conscious effort to estimate the transit time, fuel consumption, or operating costs. Then it is their natural intent to extract a few routes where the transport may occur, so that (1) analyzing route distances together with in-transit speed loss enables the transit time; (2) considering weather effect and relevant resistance variations supports the prediction of fuel consumption; (3) multiplying the transit time with daily costs yields the total operating costs. Nevertheless, the current thoughts from the designers involve many irrelevant details to the concept design, such as route distances, in-transit speed loss, or temporal resistance variations. These thoughts have not yet clarified the key factors directly, but there are hints that the key factors should be structured in a way independent of routes. Therefore, the designers are supposed to dig a little deeper into the exploration of appropriate key factors. Posing and answering questions about observations and experiences is a powerful technique to trace important design context factors (*Wood Daudelin*, 1996; *Reymen*, 2001). The next section will proceed with asking *why* questions to realize the exploration.

## 1.2 Motivation

### 1.2.1 *What* versus *Why*

In this thesis, the term *what* represents the *what* questions that naval architects may ask, and indeed correspond to the resultant phenomena of marine operations. The term *why* means the *why* questions related to the underlying explanations or mechanism of certain resultant phenomena. These two terms are relative to each

other, and they create an iterative learning loop for naval architects to understand complex designs.

This research stipulates the following axioms to help people concentrate on the real *why* questions that explore the thinness and not the thickness related to a *what* question.

- The first axiom is that *why* questions originate from the *what* questions. The context of *why* questions should be the reflective observations on certain resultant phenomena.

- The second axiom is that *why* questions must only pertain to and include the traceable model, data, and analysis, against which the resultant phenomena have been generated. In other words, the original design problem has prescribed the boundary of exploring thinness, while adding thickness beyond the boundary is not allowed.

- The third axiom is that *why* questions must avoid subjective preferences. For example, if designers explain the resultant phenomena by imposing their own opinions of reality, they will be distracted from the *why* understanding.

In terms of transit operations, the author exemplifies two traditional *what* questions here. (1) *What is the transit time from port A to port B?* The answer to this question may demonstrate that hull form X has shorter transit time than hull form Y. (2) *What are the ship motions caused by the wave conditions from port A to port B?* Solving this question may inform the designers that hull form Y experiences fewer adverse motions than hull form X. These two *what* questions make one thing clear that depending on the decision criterion and the type of resultant phenomenon the designers cannot have a clear decision. Under this circumstance, delving into the *why* questions that hold to the axioms will assist the design process.

Suppose that hull form Y is relatively slender compared to hull form X and the two hull forms have the same design speed.

- First *why* - *Why is the transit time of hull form Y longer?*

  Analysis - Transit time is a function of distances and speeds. Since the design speeds of the two hulls are the same, the route of hull form Y is longer than hull form X.

- Second *why* - *Why is the route of hull form Y longer?*

  Analysis - The waypoints of hull form X from port A to port B are along the shortest path, but hull form Y needs to zigzag away from the shortest path.

- Third *why* - *Why does hull form Y have to zigzag?*

  Analysis - Hull form Y is more slender than hull form X, so hull form Y is more likely to suffer substantial ship motions, especially large roll motions in beam seas. At most of its waypoints, hull form Y has to choose the directions that do not follow the shortest path but only cause mild ship motions. This is also why hull form Y experiences fewer adverse motions than hull form X.

The description above is a suppositional example, but it conveys a useful message about ship transit. The transit is basically a ship staying or not staying on the anticipated trajectories (most often the shortest trajectories) at every single waypoint. As discussed in the analysis of the second *why* question, observing all the waypoints allows people to know what the whole transit looks like. In light of the third *why* question, determining directions at a waypoint has natural connections with physics. Indeed, this message articulates the key factor to abstract transit operations from the thinness perspective. Even for the different situations mentioned in Section 1.1.2, they can be expressed via this key factor. For example, the percentage of a ship staying at the shortest trajectories reflects the route distances. The speed loss during the transit may be a result of propeller emergence, which is influenced by the relative motions

between the ship and waves. Then knowing the physical responses and sea conditions at each waypoint along the trajectory facilitates the prediction of the overall speed loss. The temporal resistance variations can also be translated to the evaluations of how often and how difficult the ship stays on the shortest trajectories. Furthermore, this key factor necessitates some systematic representations of waypoints, directions, and what can happen at a waypoint or a direction, which will be discussed in the next section.

### 1.2.2 Directional Decisions and an Operation Ensemble

The presented thesis now introduces a new concept called directional decisions. If directional decisions are described as determining a direction to go at each location, they will be almost equivalent to routes. However, the thesis defines directional decisions from a different viewpoint. Each one of all the directions at a location should be respectively analyzed to decide if it deserves to be maintained or not. Then there will be directional decisions that cover the feasible and infeasible choices during sea transport. This definition enables a significant distinction between directional decisions and routes. Additionally, directional decisions are the micro-level components before a route comes into being.

A single directional decision only represents if the ship moves or not within the scope of one location and one direction. It is impossible to generalize transit operations with only a few directional decisions. To achieve the thin abstraction through directional decisions, designers should aggregate plenty of them. Ideally, any port-to-port transit under any weather environment can be represented by a series of directional decisions at varying locations. Therefore, if "all" the directional decisions are gathered together, it will be convenient to either reoccur an operation or abstract the overall operations. "All" directional decisions refer to evaluating all directions at all locations over the entire ocean under all circumstances. What the designers

should create is an operation ensemble, which is concretely defined as follows.

"***An operation ensemble*** *of a ship design represents the extensive directional decisions generated in all directions at all locations over the entire ocean, disassociated from any case-specific settings (such as weather conditions, origins, or destinations), based on integrated considerations of physics and other needed disciplines.*"

To technically produce the operation ensemble, this thesis establishes a Grid-Supported Markov Decision Process (GS-MDP) framework, which blends a gridding approach, Markov Decision Process (MDP), and appropriate physical analysis codes. The function of the gridding approach is to replace the spherical surface of the earth with distributed locations and trajectories as the foundation for thin abstraction, and the MDP is the main body to simulate sea transport as a vessel sequentially making directional decisions. The ability of the MDP to generate predictive design data has been proven by *Niese et al.* (2015) in a Ship-Centric Markov Decision Process framework. In addition, although the MDP does not possess physics itself, its structure is flexible to incorporate the implications of physics.

In short, the development of an operation ensemble is motivated by the thinness perspective of abstraction and is supported by the GS-MDP framework. The unique features embedded in the operation ensemble make it powerful to create knowledge about causation. According to what *Goldthorpe* (2001) has stated, causation can be understood in three broad and non-technical ways.

- Causation as robust dependence. Two things will be considered to have robust dependence if their causation relationship cannot be weakened or eliminated through one or more other things being introduced into the analysis (*Simon*, 1954; *Suppes*, 1970). Thus, learning causation needs "all data". "All data" refers to everything that has been accumulated up to the point when the effects occur. In the operation ensemble, the directional decisions are explicitly linked with the associated data, including weather conditions and physical experiences.

- Causation as consequential manipulation. The indication of causation is that if one thing is manipulated, then, given appropriate controls, a systematic effect will be produced on another thing (*Goldthorpe*, 2001). Thus, what is crucial for learning causation is that "adequate data" is structured. Concerning the framework that produces the operation ensemble, the MDP is able to impose appropriate controls. For example, physics can be incorporated in the transition probabilities while other aspects are in the rewards. As such, the impact of physics can be examined by only modifying the transition probabilities.

- Causation as a generative process. It has been suggested (*Simon and Iwasaki*, 1988) to reveal the causation by some mechanism operating at a more microscopic level than that at which the causation emerges. As mentioned above, the directional decisions are at a more microscopic level than the level at which the routes change. Hence the operation ensemble contains data to demonstrate generative process variations.

To sum up, the operation ensemble contains valuable resources to understand operational performances and further delves into the corresponding causation relationships.

## 1.3 Overview of the Thesis

### 1.3.1 Contributions

With a focus on creating and utilizing thin abstractions, this thesis has made several contributions to the conceptual design, which are briefly mentioned as follows.

1. Introduced the concept of thick and thin abstractions to ship design and identified the need for thin abstractions.

2. Developed directional decisions and operation ensembles as key factors to en-

able the thin abstraction for ship operations. The thin abstraction generically represented diverse operational cases, situations, and scenarios.

3. Developed the GS-MDP framework to achieve the thin abstraction.

   (i) Developed a novel gridding approach that enabled an adequate representation of the ocean domain to include all the potential trajectories and transit status.

   (ii) Developed a method of tying the implications of ship motions to operational simulations within the MDP transition probabilities.

   (iii) Presented the feature of desirable ship operations through the MDP rewards and Bellman equation.

4. Created unique metrics to enable multi-attribute operational evaluations.

   (i) Identified the principles that new metrics should follow and reserved the possibility of adding more metrics whenever necessary.

   (ii) Developed new metrics to reflect transit selections, efficiency, robustness, and on-site working status.

5. Enabled deep investigation of operational outcomes. Concerning certain operational phenomena or metric results, the GS-MDP framework provided an in-depth exploration of all relevant data, underlying dynamics, and causal contexts.

### 1.3.2 Organization

The remainder of this thesis consists of six chapters and is organized as follows.

- Chapter II presents the basic background about the methods that are related to the establishment of the GS-MDP framework, including ocean gridding, Markov Decision Process, and frequency-based analysis.

- Chapter III describes how a new ocean gridding approach and the MDP structure are synthetically used to form a thin abstraction of ship operations, and how an operation ensemble is generated from the GS-MDP framework.

- Chapter IV defines a series of new metrics that allow the exploration of operational potentials based on the operation ensemble.

- Chapter V shows a representative case study that created an operation ensemble for a given ship design. This operation ensemble consisted of transit scenarios to an assigned destination under manually specified wave conditions with different seakeeping considerations. The results of this case study verify and validate the GS-MDP framework.

- Chapter VI demonstrates a case study that evaluated an offshore construction vessel based on an operation ensemble including both transit and on-site operational scenarios. This case study introduces how to model transit and on-site operations both within the GS-MDP framework, which illustrates the advantage and value of the thin abstraction.

- Chapter VII details the contributions of this thesis and offers suggestions for future work.

# CHAPTER II

# Methodology

The GS-MDP framework applies Markov Decision Process (MDP) as its main body. Thus its primary mathematical model depends on MDP. Then, what makes this framework unique is to set up MDP based on a novel ocean gridding approach, which can fundamentally support the creation of an operation ensemble. Since MDP does not possess physics itself, frequency-domain seakeeping methods are convenient to link MDP with physics in the concept design. Finally, a suitable technique to handle an operation ensemble is statistical analysis. Thus, this chapter covers the background methodology behind ocean gridding, MDP, and frequency-domain analyses.

## 2.1 Ocean Gridding

Ocean gridding is the technique that enables a discrete representation of an ocean domain. It is typically used when there is a desire to save computational resources while attempting to maintain estimation accuracy. Ocean gridding is a mature methodology and is used in many research areas, including ocean circulation (*Fox-Kemper et al.*, 2019), fluid mechanics (*Kim*, 2011), and vessel tracking (*Fiorini et al.*, 2016).

### 2.1.1 Structured and Unstructured Grid

In general, regardless of the analysis domain to which the ocean gridding is applied, there are two categories of ocean grids: structured and unstructured grids. In the case of two-dimensional representations, structured grids are characterized by regular connectivity with quadrilateral elements (*Castillo et al.*, 1987); unstructured grids are characterized by irregular connectivity, employing triangles as elements (*Mavriplis*, 1996). Figure 2.1 is a typical example extracted from the work of *Trotta et al.* (2016), which represents a certain ocean area by the structured and unstructured ocean grid, respectively.

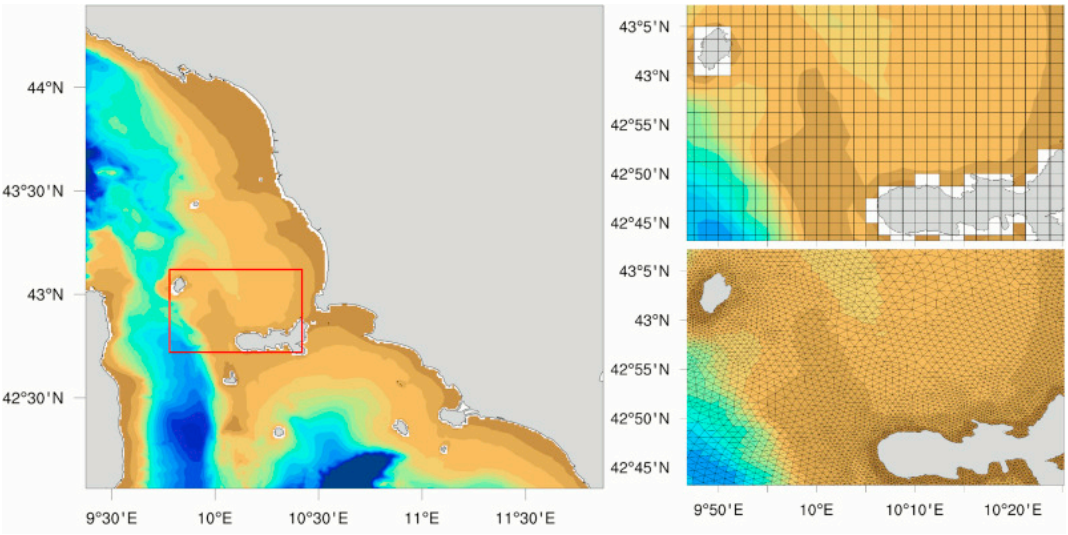


Figure 2.1: The structured and unstructured ocean grid of an ocean domain created by *Trotta et al.* (2016)

Depending on the analysis goals, researchers can choose to use the two categories separately or together. As an example, structured and unstructured grids are both used independently for the analysis of ocean circulation. To be specific, the nesting of certain structured meshes, such as ROMS (*Shchepetkin and McWilliams*, 2005) and NEMO-AGRIF (*Debreu et al.*, 2008), has demonstrated usefulness in simultaneously modeling small-scale processes and large basins. The development in some

unstructured meshes, such as FVCOM(*Chen et al.*, 2003), has made the incorporation of multi-resolution possible. Hybrid mesh generations also exist (*Lane et al.*, 2009), which employed structured grids to model waves and utilized unstructured grids for tides and storms. In this thesis, ocean gridding is a fundamental component that is uniquely used for the simulation of transit operations. While the development and application of ocean gridding in this research are unique, there are some relevant papers (*Prochazka and Adland*, 2019) that have used particular ocean grid realizations to mimic shipping routes. What differentiates the research developed for this thesis from existing research utilizing ocean grid techniques is that existing research and methods are focused on the ship routing problem, but this research is not specifically focused on the routing problem. The similarity between the published work and the novel approach contained within is only in the intent of using nodes and arcs as the transport foundation. A detailed discussion of the gridding approach used in this research will be demonstrated in the next chapter.

### 2.1.2 Resolution

The resolution of the ocean grids is one of the critical factors that determine the computational time and estimation accuracy and should be appropriately balanced. The advantage of fine-mesh ocean grids is to enlarge the operation ensemble. Additionally, the resolution not only determines how precise or coarse the grid is, but also influences the amount of other relevant data, such as weather data, that can be bound to the ocean grid. However, the disadvantage is that higher resolutions will induce computational explosion that may, or may not, be a barrier. Thus, the final value of the resolution should appropriately balance the magnitude of the operation ensemble, the computational time, and the accuracy requirements associated with the conclusion desired.

## 2.2 Markov Decision Process

### 2.2.1 Structure

Markov Decision Process (MDP) is a model that solves sequential decision-making problems in regard to stochastic environments. A fully observable MDP consists of states, actions, transition probabilities, and rewards, which are written as a 4-tuple $< \mathcal{S}, \mathcal{A}, \mathcal{P}, \mathcal{R} >$. Figure 2.2 illustrates a diagram of the MDP, where action $a$ is selected for state $s$, affecting a transition to the next state $s'$ with $P(s'|s, a)$ and obtaining $R(s, s')$ from this transition.

- $\mathcal{S} = \{s\}$, is a finite set of states that the environment contains;
- $\mathcal{A} = \{a\}$, is a finite set of actions that can be executed at the states;
- $\mathcal{P}$ is the space of transition probabilities, and $\mathrm{P}(s'|s, a)$ represents the transition probability of achieving state $s'$ from state $s$ through the execution of action $a$;
- $\mathcal{R}$ is the space of rewards, and $\mathrm{R}(s, s')$ represents the immediate reward obtained because of the transition from state $s$ to state $s'$.

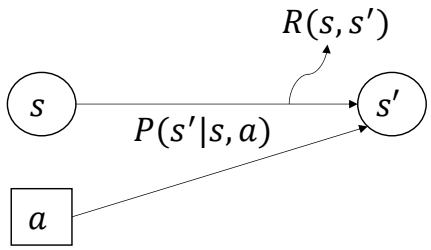


Figure 2.2: A diagram of the MDP

The value of an MDP is that decision-making results are partially influenced by randomness and partially under the control of the decision maker. The decision maker's objective is to select actions that maximize the long-term cumulative rewards

of the states. To present this objective within the model, the MDP also comprises the following two definitions.

- $\gamma \in [0,1]$, is a discount factor that reflects different preferences between immediate rewards and future rewards;
- $\pi$ is a policy that specifies each of the states an action.

For this thesis, only infinite horizon MDP will be applied. The term "infinite horizon" refers to the case in which there is no fixed deadline to let all the states stop executing actions at a homogeneous time step (*Russell and Norvig*, 2010). In particular, an MDP which contains a terminate state is an example of infinite-horizon MDPs. Without a fixed deadline, there is no need for the same state to take different actions at different time steps, which indicates that the optimal policy would be stationary. The existence of a stationary optimal policy has been proven by *Puterman* (1994). Furthermore, by definition (*Puterman*, 1994), a stationary policy is always Markovian. Markovian is a memoryless property that specifies that the future states of a stochastic process only depend on the present state. In other words, given the present state, the action that a policy assigns to this state should be independent of the actions that have been assigned to the previous states.

### 2.2.2 Value Iteration

Value iteration is an efficient algorithm that is commonly used to solve an infinite horizon MDP. The value function $V^{\pi}(s)$ expressed in Equation (2.1) defines the long-term expected reward by executing policy $\pi$ starting at state $s$ with $s_0 = s$. The Bellman equation (*Bellman*, 1957) further yields a recursive estimation of $V^{\pi}(s)$, which is shown in Equation (2.2). It is the basis of the value iteration algorithm.

$$V^{\pi}(s) = E[\sum_{t=0}^{\infty} \gamma^t R(s_t, s'_t)] \tag{2.1}$$

$$V^{\pi}(s) = \sum_{s'}[P(s'|s,a) \times (R(s,s') + \gamma V^{\pi}(s'))] \tag{2.2}$$

When the value iteration converges, optimal value function $V^*(s)$ and optimal policy $\pi^*(s)$, which maximize the long-term expected reward, can be expressed as follows:

$$V^*(s) = max\{\sum_{s'}[P(s'|s,a) \times (R(s,s') + \gamma V(s'))]\} \tag{2.3}$$

$$\pi^*(s) = argmax_{a\in\mathcal{A}}\{\sum_{s'}[P(s'|s,a) \times (R(s,s') + \gamma V(s'))]\} \tag{2.4}$$

Unless non-standard methods are used, once the MDP is solved, only the optimal action $\pi^*(s)$ and the corresponding cumulative reward $V^*(s)$ at a specific state are retained. Figure 2.3 explicitly displays $\pi^*(s)$, $V^*(s)$, and the associated data that supports the calculation of the optimum occurring at state $s$.

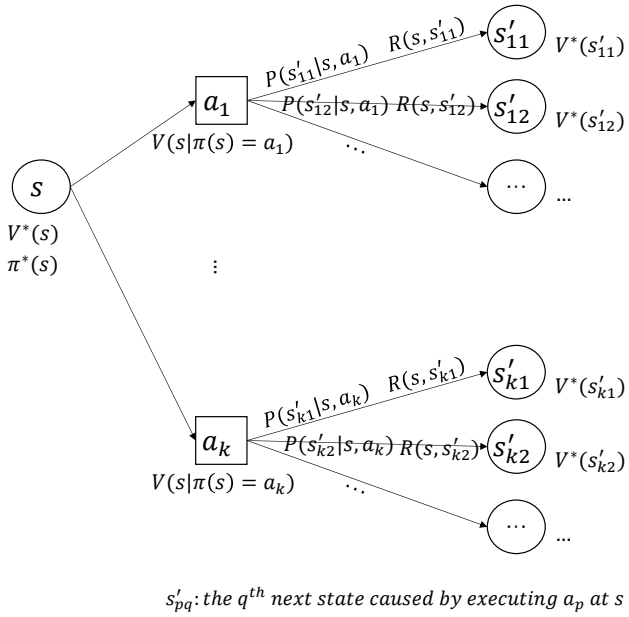


Figure 2.3: State and data association within MDP

Since practical decision-making problems vary, there are also other classes of the MDP structures. For example, the model may incorporate multiple decision makers. Additionally, continuous time, imprecise transition probabilities, imprecise rewards,

and partial observability generalize certain definitions within the MDP. In general, all MDPs utilize the logic rooted in the value function to find optimal solutions. Heuristic approaches, dynamic programming, and other solution techniques all exist within the MDP literature.

### 2.2.3 Application

The MDP has been widely applied in a variety of areas such as robotics, maintenance operations, and design theory. A common explanatory application in the area of robotics is to assist a robot in navigating itself under imperfect movement circumstances (*Russell and Norvig*, 2010). In the field of maintenance operations, MDP has been used to model bridge component deterioration and an optimization strategy between maintenance and replacement (*Robelin and Madanat*, 2007). Within the marine field, the Ship-Centric Markov Decision Process (SC-MDP) framework is a significant application to inspire design insights.

SC-MDP is a unique design framework created by *Niese* (2012) to enable a designer to uncover lifecycle decision paths. Its initial study of the lifecycle decision paths was on the implementation of vessel ballast water treatment in light of environmental policy changes. This framework serves as a reference to identify lifecycle path dependencies and relate them back to the early-stage ship design decisions, which provides the design data needed to avoid design lock-in (*Niese and Singer*, 2013). Furthermore, researchers (*Kana and Singer*, 2016) advance this framework by using eigenvalue spectral analysis to explain the causation of various decision paths. The work in the existing papers demonstrates the applicability and flexibility of SC-MDP in evaluating ship operational events, and the current developments explore the impact of environmental policies (*Niese and Singer*, 2013), economic benefits (*Niese and Singer*, 2014), and safety factors (*Kana and Droste*, 2019) on the ship design process. On the basis of the SC-MDP mindset, it is possible and promising to modify an MDP,

to be used as an early-stage surrogate framework, which incorporates the interaction between physics and other operational expectations, simulates ship operations, and produces adequate design data.

## 2.3 Frequency-Based Analysis

Frequency-based analysis has great significance in control systems, physics, statistics, and so on. It refers to the analysis of phenomena, signals, or functions with respect to frequencies (*Broughton and Bryan*, 2008). Compared to time-based analysis that demonstrates variations over time, the frequency-domain analysis focuses on summarizing the occurrences of different individuals. Within the scope of this thesis, frequency-based analysis will be used in two aspects.

### 2.3.1 Frequency-Domain Seakeeping Method

Frequency-domain seakeeping methods allow one to compute the ship motions to harmonic waves of different wave lengths and wave directions in the frequency domain (*Bertram*, 2012). For this case, irregular waves are represented by a wave spectrum utilizing the Fourier Transform and other spectral techniques. Frequency-domain seakeeping methods allow designers to convert the wave spectrum to energy spectra of different physical responses. These spectra further provide values of statistical parameters, such as the root mean square response, significant response, and average of the 1/10 highest responses.

Using frequency-domain seakeeping methods is an excellent way of estimating physics for a conceptual design where the scale of the operation assigned to the vessel does not warrant detailed analysis (*Couser*, 2000). Because of its calculation speed, it is convenient to link the reliable and rapid estimations from these methods to the MDP structure.

### 2.3.2 Statistical Evaluation of Operation Ensembles

Through the creation of operation ensembles, frequency distributions can be generated and statistically evaluated. Statistical evaluations enable the generation of frequency distributions according to the operation ensemble. A frequency distribution is a summarized grouping of operational data, which records the mutually exclusive categories and the number of occurrences in each category (*Freund et al.*, 2010). Once a frequency distribution is created, operational data can be directly extracted from the operation ensemble or modified. Furthermore, the statistical evaluation of the ensemble frequency distribution provides descriptive statistics, including measures of central tendency, measures of dispersion, and percentile values. Understanding the operation ensemble largely depends on these statistics, especially the measures of central tendency. Central tendency is often the most useful single characteristic of a distribution, which provides representative values of all the data within the distribution. For example, mean and median are two commonly used measures of central tendency.

# CHAPTER III

# GS-MDP Framework

The first two chapters of this thesis have established the unique requirements for a novel thin abstraction of ship operations for early-stage design. Additionally, the foundational technology needed for developing a thin abstraction has been discussed. This chapter will discuss the development and details of the GS-MDP framework, which enables the execution of abstracting ship operations from the thinness perspective for use in early-stage design.

## 3.1 Gridding Approach

A critical and novel aspect of the GS-MDP is the gridding approach which represents the spherical surface of the earth into the requisite thin abstraction components. In this thesis, the spherical surface is broken into two components, distributed locations and trajectories that connect any of the two adjacent locations. These two components provide the foundation needed to conduct sea transport simulations in any ocean domain. As such, this thesis develops a gridding approach that specifies the following steps.

The first step in creating the ocean grid is to discretize the longitude and latitude range of interest uniformly. The discrete values of longitude and latitude, which are

$x$ and $y$, are placed in two corresponding sets *Lon* and *Lat*.

$$Lon = \{x : x \in longitude\ values,\ 0^\circ \leq x < 360^\circ\} \tag{3.1}$$

$$Lat = \{y : y \in latitude\ values,\ -90^\circ \leq y \leq 90^\circ\} \tag{3.2}$$

Through the Cartesian product of *Lon* and *Lat*, the set *Node* that represents all the distributed locations of the ocean grid is then obtained.

$$Node = Lon \times Lat = \{(x, y) : x \in Lon\ , y \in Lat\} \tag{3.3}$$

The next step in the gridding process is to connect the distributed locations. Each location is surrounded by several other locations. For example, if it is in the interior, it will be surrounded by 8 locations; if it is at the boundary but not the corner of the space, it will be surrounded by 5 locations; if it is at the corner, it will be surrounded by 3 locations. For each pair of the adjacent locations $(x_i, y_i)$ and $(x_j, y_j)$, the ocean grid prescribes a trajectory that connects them. This thesis assumes that the trajectory between $(x_i, y_i)$ and $(x_j, y_j)$ is an arc with a constant direction as measured relative to magnetic north, which means that it follows a rhumb line. The set *Arc* represents all the trajectories between adjacent nodes of the ocean grid.

$$Arc = \{rhumb\ line[(x_i, y_i), (x_j, y_j)] : (x_i, y_i), (x_j, y_j)\ are\ adjacent \in Node\} \tag{3.4}$$

This gridding approach provides an ocean grid shown in Figure 3.1. Based on the ocean grid, vessel transit can be simulated at all locations within the grid toward all available directions. The last thing worth noting is that the presented gridding approach should be applied to ocean areas away from the coastlines in order to avoid erroneous results. If coastline gridding is required, only true available trajectories must be included at every relevant node location.

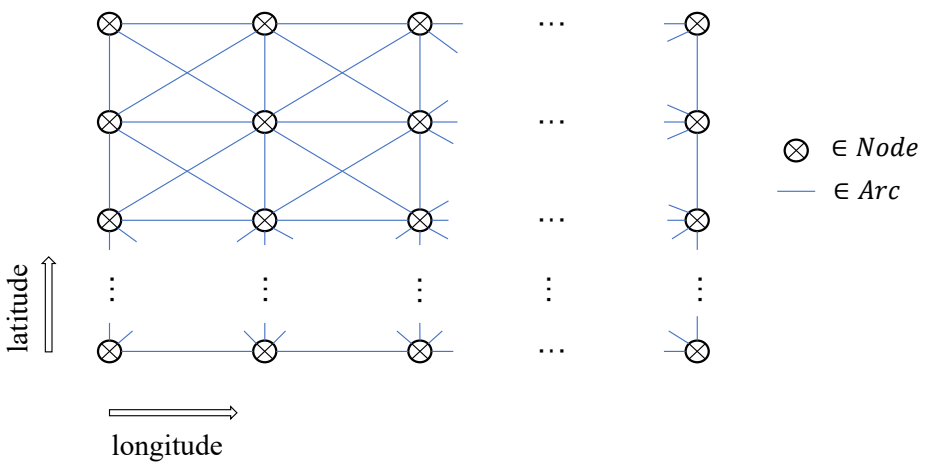


Figure 3.1: The ocean grid created by the presented gridding approach

## 3.2 MDP Structure of the GS-MDP

### 3.2.1 States

Within the GS-MDP framework a state is defined as "a ship at a specific location toward a specific direction". As defined, the location of a state is determined by the grid, but the determination of the direction has not yet been established. This section will describe methods used to establish the directions needed for MDP states.

There are two conditions to determine the ship's heading direction based on the ship's current location and corresponding adjacent locations. First, the ship is at a location $(x, y)$ in the interior of the ocean grid. Its adjacent locations can be sequentially expressed as $(x_{ai}, y_{ai})|(x, y)$ where index $i$=1,2...,8. Different indices refer to different relative positions between $(x_{ai}, y_{ai})|(x, y)$ and $(x, y)$. When index $i$ is equal to 1, $(x_{a1}, y_{a1})|(x, y)$ denotes the adjacent location that is to the north of location $(x, y)$, and then one after another, $(x_{a2}, y_{a2})|(x, y)$ till $(x_{a8}, y_{a8})|(x, y)$ denote the other adjacent locations clockwise. Figure 3.2 is an illustration of location $(x, y)$ that is in the interior of the ocean grid and its adjacent locations from $(x_{a1}, y_{a1})|(x, y)$ to $(x_{a8}, y_{a8})|(x, y)$.

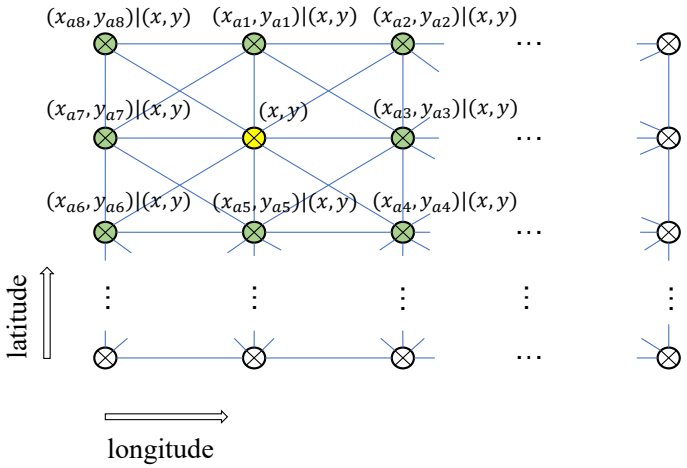


Figure 3.2: Location $(x, y)$ in the interior of the ocean grid and its corresponding adjacent locations from $(x_{a1}, y_{a1})|(x, y)$ to $(x_{a8}, y_{a8})|(x, y)$

As can be seen in Figure 3.2, there are 8 available heading directions at location $(x, y)$. The eight heading directions are defined as the rhumb line azimuths from location $(x, y)$ to the next adjacent locations $(x_{ai}, y_{ai})|(x, y)$. The azimuths mentioned here are the true north-based azimuths. Thus, the ocean grid discretizes the continuous heading directions at location $(x, y)$ into 8 discrete ones $\theta_i$ by referring to the 8 corresponding adjacent locations $(x_{ai}, y_{ai})|(x, y)$, where $i$=1,2...8. In addition, $\theta_1$=0°, $\theta_3$=90°, $\theta_5$=180°, and $\theta_7$=270° are always true.

$$\begin{gathered} \theta_i = \textit{rhumb line azimuth}[(x,y) \rightarrow (x_{ai}, y_{ai})|(x,y)] \\ (x_{ai}, y_{ai})|(x,y) \textit{ represents the next adjacent location}, \quad i = 1, 2...8 \end{gathered} \tag{3.5}$$

Second, if the ship is at location $(x, y)$ that is at the boundary of the ocean grid, there will be only 5 or 3 adjacent locations. Before applying Equation (3.5), one more step is needed. It is necessary to temporarily make the adjacent locations that are beyond the range of the ocean grid available by following the same rules of the gridding approach. Thus, such a location can be presumed to have all 8 adjacent locations, and then the corresponding $\theta_i$ can be calculated by Equation (3.5). For example,

as shown in Figure 3.3, $(x, y)$ is a location at the northwest corner of the ocean grid. The adjacent locations that truly exist are $(x_{a3}, y_{a3})|(x, y)$, $(x_{a4}, y_{a4})|(x, y)$, and $(x_{a5}, y_{a5})|(x, y)$, while the others are temporarily added that merely serve as references to determine the heading directions.

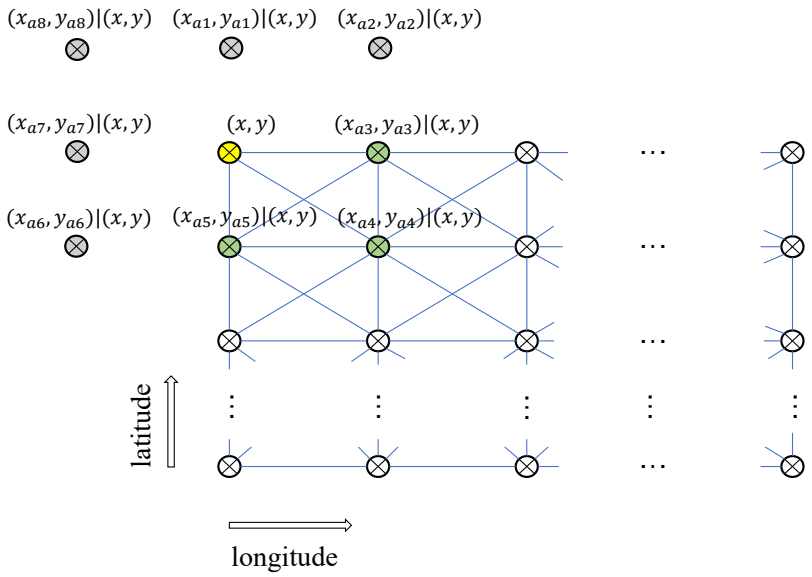


Figure 3.3: Location $(x, y)$ at the northwest corner of the ocean grid with its true and temporarily added adjacent locations

Therefore, with the help of the ocean grid, the set *Node* signifies all the locations which the ship may be at, and the heading directions of the ship depend on the azimuths along the rhumb lines that are defined in the set *Arc*. A state $s$ in the set $\mathcal{S}$ means "a ship at $(x, y)$ toward $\theta_i$". An example of $s$ is demonstrated in Figure 3.4.

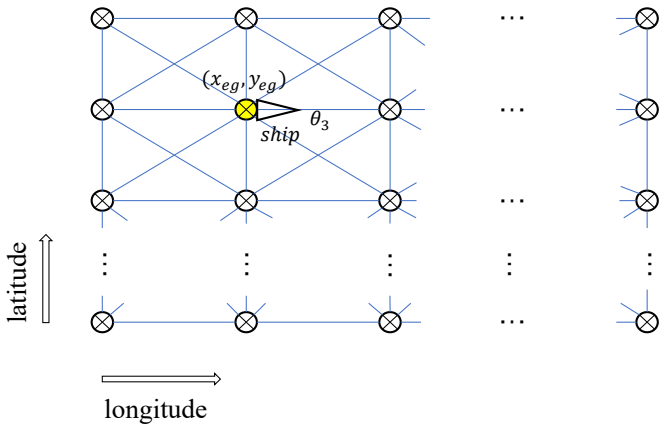


Figure 3.4: An exemplified state $s$, "a ship at ($x_{eg}$,$y_{eg}$) toward $\theta_3$"

The two primary dimensions of data that a state contains are the ship's location $(x, y)$ and heading direction $\theta_i$. Furthermore, relevant ocean weather data and seakeeping data can also be linked to a state. The ocean weather data at location $(x, y)$ can be extracted from the public database such as NOAA or ECMWF, which may involve significant wave heights $H_s$, mean wave periods $T$, mean wave directions $\theta_{wave}$, and so on. The seakeeping data can be obtained through frequency-domain estimations as follows. First, based on the ocean weather data at location $(x, y)$, a wave spectrum $S_W(\omega)$ is attainable, where $\omega$ is the wave frequency in radians per second. Then in combination with the hull form and ship's heading direction $\theta_i$, the wave spectrum $S_W(\omega)$ can be converted to the encounter frequency spectrum $S_W(\omega_E)$. After that, Equation (3.6) enables the computation of the energy spectrum $S_{motion}(\omega_E)$ for any given ship motion. In this equation, $\omega_E$ is the encounter frequency in radians per second and $RAO_{motion}(\omega_E)$ is the response amplitude operator of the corresponding motion. At last, the seakeeping data, such as Root Mean Square (RMS) of the motion amplitudes, becomes available to reflect the physical experiences at a state. To sum up, each state in this MDP has a vector of data as shown in Figure 3.5.

$$S_{motion}(\omega_E) = [RAO_{motion}(\omega_E)]^2 S_W(\omega_E) \tag{3.6}$$

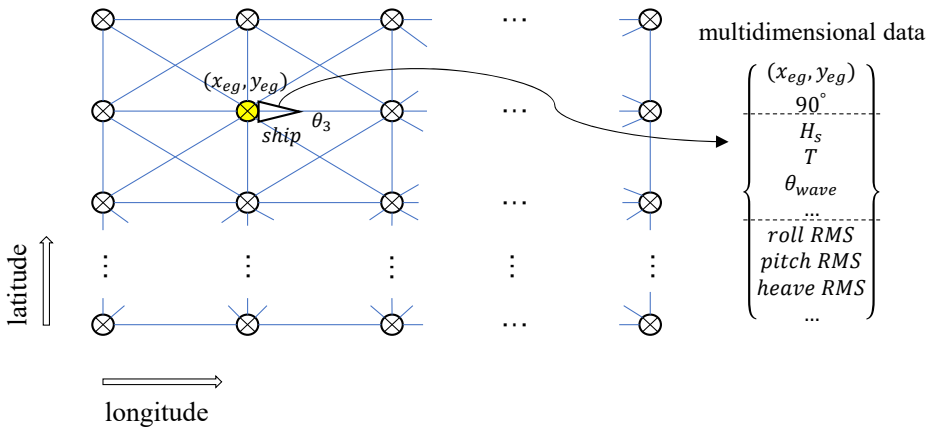


Figure 3.5: The multidimensional data associated with the exemplified state $s$ "a ship at $(x_{eg}$,$y_{eg})$ toward $\theta_3$"

### 3.2.2 Actions

The MDP simulates the "captain's options" as actions at each state during a possible sea transport process. There are two options available to the "captain", moving on to the next location on a path or adjusting the heading to new paths. Based on ship motion results, the availability of actions is determined as well as the transitions between states. These two actions, together with relevant ship motions, determine the transitions among states.

- Action 1 (move on, written as $a_1$): The vessel moves on to the next location on its trajectory. Whether the movement can be achieved depends on the comparison of physical motions against certain seakeeping criteria.

- Action 2 (adjust the heading, written as $a_2$): The vessel adjusts the heading toward a different trajectory. The outcomes of the adjustment depend on the relative magnitudes of the physical motions. The ship is more willing to shift to a heading direction that is linked to relatively smaller ship motions rather than larger ones.

To be more specific, if $a_1$ is executed at state $s$ "a ship at $(x, y)$ toward $\theta_i$", there will be 2 possible transitions. First, if the movement is not achieved the next state $s'|s, a_1$ will be the same as $s$. Second, if the movement is achieved, the next state will be "a ship at the corresponding adjacent location of $s$ toward the same direction as $s$", i.e. "a ship at $(x_{ai}, y_{ai})|(x, y)$ toward $\theta_i$". For example, for the state shown in Figure 3.4, the according $s'|s, a_1$ will be "a ship at ($x_{eg}$,$y_{eg}$) toward $\theta_3$" or "a ship at $(x_{a3}, y_{a3})|(x_{eg}, y_{eg})$ toward $\theta_3$". Figure 3.6 further depicts these two outcomes. However, there is a special circumstance where the movement may be restricted by the boundary of the ocean grid. If this circumstance occurs, then that movement will be invalid and the ship will just stay at its current state.

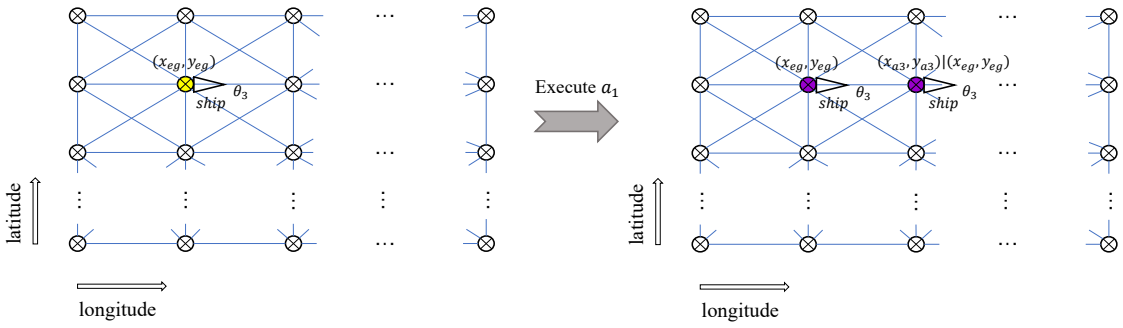


Figure 3.6: The two transition outcomes caused by $a_1$

If $a_2$ is executed at state $s$ "a ship at $(x, y)$ toward $\theta_i$", there will be 8 possible transitions. The next state $s'|s, a_2$ will be "a ship at the same location as $s$ toward the same or another direction", i.e. "a ship at $(x, y)$ toward $\theta_{j=1,2,...8}$". The outcome of "a ship staying at the same location toward the same direction" still exists, but it is caused by action $a_2$ and will be related to a new transition probability. Using the exemplified state in Figure 3.4 again, the ship may still maintain $\theta_3$, or adjust to $\theta_2$, $\theta_4$, or shift to even farther states $\theta_1$, $\theta_5$, $\theta_8$, $\theta_6$, or $\theta_7$. Figure 3.7 illustrates the corresponding $s'|s, a_2$ due to these transitions.

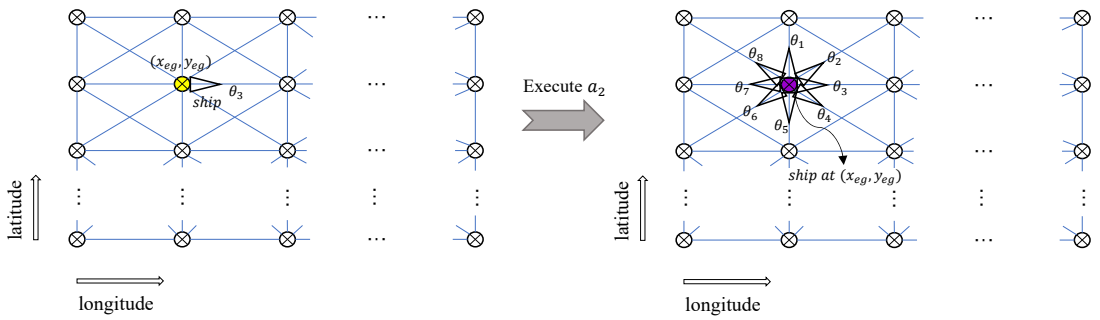


Figure 3.7: The eight transition outcomes caused by $a_2$

### 3.2.3 Transition Probabilities

As stated earlier, the state-to-state transition incorporates the influence of physical motions into the MDP. The transition probability values of $P(s'|s, a_1)$ and $P(s'|s, a_2)$ are calculated through the steps described below.

To calculate $P(s'|s, a_1)$, which is the transition probability of moving to state $s'$ from state $s$ ("a ship at $(x, y)$ toward $\theta_i$") through action $a_1$, a threshold $\lambda$ is defined. The $\lambda$ value depends on a certain operation criterion, determined by a designer, for a given ship motion. The intent of introducing $\lambda$ is that the ship's movement is considered to be impeded when the given ship motion exceeds $\lambda$. Furthermore, the probability of the given ship motion exceeding $\lambda$ is defined through Equation (3.7), which is an equation derived in the reference book (*Molland*, 2008). In this equation, *Amp* represents the random amplitudes of the given ship motion that can be roll, pitch, or heave; $RMS$ represents the Root Mean Square value of the given ship motion, which can be extracted from the multidimensional data associated with state $s$.

$$P(Amp > \lambda) = exp(-\frac{\lambda^2}{2 \times RMS^2}) \tag{3.7}$$

Thus, Equation (3.8) will provide the value of $P(s'|s, a_1)$ if the movement is not restricted by the boundary of the ocean grid. For the special circumstance where

the movement is restricted because of the boundary, Equation (3.9) should be used to express the invalid movement. In both equations, $s$ represents "a ship at $(x, y)$ toward $\theta_i$" and $a_1$ represents moving on.

$$P(s'|s, a_1) = \begin{cases} P(Amp > \lambda) = exp(-\frac{\lambda^2}{2 \times RMS^2}) \\ \qquad \text{when } s' = \textit{"a ship at (x,y) toward } \theta_i\textit{"} \\ P(Amp \leq \lambda) = 1 - exp(-\frac{\lambda^2}{2 \times RMS^2}) \\ \qquad \text{when } s' = \textit{"a ship at } (x_{ai}, y_{ai})|(x, y) \textit{ toward } \theta_i\textit{"} \end{cases} \tag{3.8}$$

$$P(s'|s, a_1) = 1 \quad s' = \textit{"a ship at (x,y) toward } \theta_i\textit{"} \tag{3.9}$$

As for the calculation of $P(s'|s, a_2)$, this thesis has established a mechanism of adjusting heading directions according to relative variations of the ship motions. When $a_2$ is executed at a state $s$ ("a ship at $(x, y)$ toward $\theta_i$"), the ship may maintain its current heading $\theta_i$, shift clockwise to $\theta_{ic}$, or shift counter-clockwise to $\theta_{icc}$. All the $\theta_{ic}$ and $\theta_{icc}$ are determined from $\theta_i$, which is the ship's current heading direction. When the ship shifts to another direction clockwise, there will be seven potential outcomes, written as $\theta_{ic}(1)$, $\theta_{ic}(2)$... $\theta_{ic}(7)$ in sequence. If the ship shifts to other directions counter-clockwise, there will also be seven outcomes, which can be written as $\theta_{icc}(1)$, $\theta_{icc}(2)$... $\theta_{icc}(7)$ in sequence. Furthermore, $\theta_{ic}(1)$ and $\theta_{icc}(7)$ represent the same heading direction; $\theta_{ic}(2)$ and $\theta_{icc}(6)$ represent the same heading direction; $\theta_{ic}(3)$ and $\theta_{icc}(5)$ represent the same heading direction; $\theta_{ic}(4)$ and $\theta_{icc}(4)$ represent the same heading direction. For instance, Figure 3.8 depicts $\theta_{ic}(1)$ to $\theta_{ic}(7)$ and $\theta_{icc}(1)$ to $\theta_{icc}(7)$ when $i$=3. There are 15 unique heading sequences to obtain different adjustment outcomes, which are listed below. For each sequence, the ship shifts its heading direction step by step, which means that each sequence is composed of one or more one-step shifts.

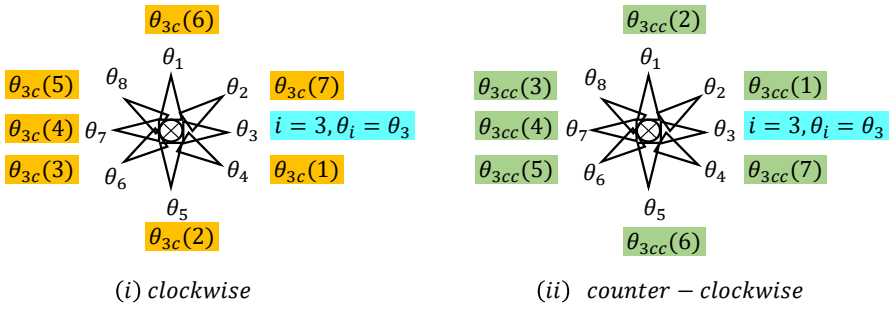


Figure 3.8: The subsequent directions clockwise and counter-clockwise for $\theta_3$, namely $\theta_{3c}(1)$ to $\theta_{3c}(7)$ and $\theta_{3cc}(1)$ to $\theta_{3cc}(7)$

The probabilities of these 15 sequences are important for the ultimate determination of $P(s'|s, a_2)$. Except for the outcome of heading the same direction, each specific adjustment outcome can be obtained through either a clockwise shift or a counter-clockwise shift. Based on the ship motions, the MDP determines which sequence of the adjustment has the higher probability of obtaining specific outcomes. For instance, $\theta_{ic}(1)$ and $\theta_{icc}(7)$ represent the same heading direction, so either the second sequence or the fifteenth sequence will be selected as the transition of this outcome.

1. $\theta_i \rightarrow \theta_i$
2. $\theta_i \rightarrow \theta_{ic}(1)$
3. $\theta_i \rightarrow \theta_{ic}(1) \rightarrow \theta_{ic}(2)$
4. $\theta_i \rightarrow \theta_{ic}(1) \rightarrow \theta_{ic}(2) \rightarrow \theta_{ic}(3)$
5. $\theta_i \rightarrow \theta_{ic}(1) \rightarrow \theta_{ic}(2) \rightarrow \theta_{ic}(3) \rightarrow \theta_{ic}(4)$
6. $\theta_i \rightarrow \theta_{ic}(1) \rightarrow \theta_{ic}(2) \rightarrow \theta_{ic}(3) \rightarrow \theta_{ic}(4) \rightarrow \theta_{ic}(5)$
7. $\theta_i \rightarrow \theta_{ic}(1) \rightarrow \theta_{ic}(2) \rightarrow \theta_{ic}(3) \rightarrow \theta_{ic}(4) \rightarrow \theta_{ic}(5) \rightarrow \theta_{ic}(6)$
8. $\theta_i \rightarrow \theta_{ic}(1) \rightarrow \theta_{ic}(2) \rightarrow \theta_{ic}(3) \rightarrow \theta_{ic}(4) \rightarrow \theta_{ic}(5) \rightarrow \theta_{ic}(6) \rightarrow \theta_{ic}(7)$

9. $\theta_i \rightarrow \theta_{icc}(1)$

10. $\theta_i \rightarrow \theta_{icc}(1) \rightarrow \theta_{icc}(2)$

11. $\theta_i \rightarrow \theta_{icc}(1) \rightarrow \theta_{icc}(2) \rightarrow \theta_{icc}(3)$

12. $\theta_i \rightarrow \theta_{icc}(1) \rightarrow \theta_{icc}(2) \rightarrow \theta_{icc}(3) \rightarrow \theta_{icc}(4)$

13. $\theta_i \rightarrow \theta_{icc}(1) \rightarrow \theta_{icc}(2) \rightarrow \theta_{icc}(3) \rightarrow \theta_{icc}(4) \rightarrow \theta_{icc}(5)$

14. $\theta_i \rightarrow \theta_{icc}(1) \rightarrow \theta_{icc}(2) \rightarrow \theta_{icc}(3) \rightarrow \theta_{icc}(4) \rightarrow \theta_{icc}(5) \rightarrow \theta_{icc}(6)$

15. $\theta_i \rightarrow \theta_{icc}(1) \rightarrow \theta_{icc}(2) \rightarrow \theta_{icc}(3) \rightarrow \theta_{icc}(4) \rightarrow \theta_{icc}(5) \rightarrow \theta_{icc}(6) \rightarrow \theta_{icc}(7)$

The key to determine the probabilities of the 15 sequences listed above is a seakeeping matrix $Q$ created at location $(x, y)$. The seakeeping matrix stores the relative ship motion results at each heading direction. The size of the seakeeping matrix is $8\times8\times3$. Row indices denote the heading directions before the shift, and column indices denote the heading directions after the shift. The 3 different layers are the ship motion differences between two available states of the adjustment, preference utilities of the motion differences, and the probabilities of the one-step shifts occurred in the 15 sequences, respectively. Each layer of the seakeeping matrix has the same format that is shown in Figure 3.9. The positions that are not shaded in gray correspond to all the one-step shifts from the "row" to the "column". These positions should be filled with values utilizing Equations (3.10) to (3.12).

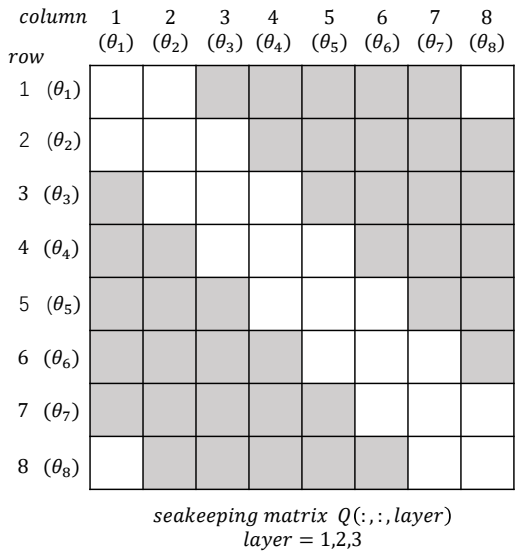


Figure 3.9: Format of the seakeeping matrix $Q$

$$\begin{aligned} Q(row, column, 1) = \textit{seakeeping data (a ship at (x,y) toward } \theta_{row}\textit{)} \\ -\textit{seakeeping data (a ship at (x,y) toward } \theta_{column}\textit{)} \end{aligned} \tag{3.10}$$

$$Q(row, column, 2) = exp(\alpha \times Q(row, column, 1)), \quad \alpha \geq 0 \tag{3.11}$$

$$Q(row, column, 3) = \frac{Q(row, column, 2)}{\sum Q(row, :, 2)} \tag{3.12}$$

In addition, $\alpha$ in Equation (3.11) is a parameter that defines the level of difficulty in adjusting the heading direction. Modifying the value of parameter $\alpha$ imposes different levels of seakeeping impact on the adjustment of heading directions. If $\alpha$ equals zero, then seakeeping impact will be removed as a limiting factor. The influence of seakeeping will accordingly rise with the increase of $\alpha$.

Since shifting the heading direction is assumed to occur in sequence, this thesis further defines that the probability of reaching an adjustment outcome should be the multiplication between the probability of shifting to this heading direction and the probability of not changing this heading direction after shifting to it. First, the

probability of shifting to a certain heading direction can be expressed based on the chain rule $P(\bigcap_{k=1}^{n} X_k) = \prod_{k=1}^{n} P(X_k|\bigcap_{j=1}^{k-1} X_j)$. In this expression, $X_1$ denotes the current heading direction $\theta_i$. After (n-1) steps, the adjustment passes the heading directions denoted by $X_2$, $X_3$, ...$X_{n-1}$ and ultimately achieves the heading direction denoted by $X_n$. As demonstrated in the seakeeping matrix $Q$, each step of shifting the heading direction is independent, so $P(X_k|\bigcap_{j=1}^{k-1} X_j)$ can be reduced as $P(X_k|X_{k-1})$. Furthermore, $P(X_n|X_n)$ represents the probability of not changing the heading direction after shifting to it. $P(X_n|X_n)$ needs to be considered because it means the probability of staying in a heading direction. A sequence of heading direction adjustment can be achieved only when the ship finally stays in that adjustment outcome. Therefore, the probability of reaching an adjustment outcome based on one of the 15 sequences mentioned above, written as $P(sequence\ number)$, can be described via the following Equation (3.13). Seakeeping matrix $Q(:,:,3)$ provides all the values that are needed in this equation.

$$P(sequence\ number) = [\prod_{k=1}^{n} P(X_k|X_{k-1})] \times P(X_n|X_n) \qquad (3.13)$$
$$where: n \geq 1,\ P(X_1|X_0) = P(X_1)$$

For example, $P(sequence\ 15)$ illustrates an application of this equation in detail where $n$=8, $X_1$=$\theta_i$, $X_2$=$\theta_{icc}(1)$, $X_3$=$\theta_{icc}(2)$, ... $X_8$=$\theta_{icc}(7)$. It is known that the current heading direction is $\theta_i$, so $P(\theta_i) = 1$ is always true.

$$\begin{aligned} P(sequence\ 15) &= P(\theta_i\ , \theta_{icc}(1)\ , \theta_{icc}(2)\ ...\theta_{icc}(7)) \times P(\theta_{icc}(7)\ |\theta_{icc}(7)) \\ &= P(\theta_i) \times P(\theta_{icc}(1)\ |\theta_i)... \times P(\theta_{icc}(7)|\theta_{icc}(6)) \times P(\theta_{icc}(7)\ |\theta_{icc}(7)) \\ &= P(\theta_{icc}(1)\ |\theta_i)... \times P(\theta_{icc}(7)|\theta_{icc}(6)) \times P(\theta_{icc}(7)\ |\theta_{icc}(7)) \end{aligned}$$

Up to now, $P(sequence\ 1)$ to $P(sequence\ 15)$ have become available. The se-

quences and associated probabilities of transiting to 8 different adjustment outcomes are listed as follows. The last step of determining $P(s'|s, a_2)$ is to normalize these associated probabilities based on Equation (3.14).

- adjustment outcome 1: "a ship at $(x, y)$ toward $\theta_i$"
  $p_1$=$P(sequence\ 1)$
- adjustment outcome 2: "a ship at $(x, y)$ toward $\theta_{ic}(1)$ or $\theta_{icc}(7)$"
  $p_2$=max$\{P(sequence\ 2),\ P(sequence\ 15)\}$
- adjustment outcome 3: "a ship at $(x, y)$ toward $\theta_{ic}(2)$ or $\theta_{icc}(6)$"
  $p_3$=max$\{P(sequence\ 3),\ P(sequence\ 14)\}$
- adjustment outcome 4: "a ship at $(x, y)$ toward $\theta_{ic}(3)$ or $\theta_{icc}(5)$"
  $p_4$=max$\{P(sequence\ 4),\ P(sequence\ 13)\}$
- adjustment outcome 5: "a ship at $(x, y)$ toward $\theta_{ic}(4)$ or $\theta_{icc}(4)$"
  $p_5$=max$\{P(sequence\ 5),\ P(sequence\ 12)\}$
- adjustment outcome 6: "a ship at $(x, y)$ toward $\theta_{ic}(5)$ or $\theta_{icc}(3)$"
  $p_6$=max$\{P(sequence\ 6),\ P(sequence\ 11)\}$
- adjustment outcome 7: "a ship at $(x, y)$ toward $\theta_{ic}(6)$ or $\theta_{icc}(2)$"
  $p_7$=max$\{P(sequence\ 7),\ P(sequence\ 10)\}$
- adjustment outcome 8: "a ship at $(x, y)$ toward $\theta_{ic}(7)$ or $\theta_{icc}(1)$"
  $p_8$=max$\{P(sequence\ 8),\ P(sequence\ 9)\}$

$$P(s'|s, a_2) = \frac{p_j}{\sum_{m=1}^{8} p_m} \quad s'=adjustment\ outcome\ j,\ j = 1, 2, ...8 \tag{3.14}$$

### 3.2.4 Rewards

The MDP rewards quantify the movements or adjustments caused by the actions. The rewards of movements and adjustments are both defined as normalized values to

ensure that they are of the same magnitude. First, if the transition is a movement from location $(x, y)$ to another location, as what $a_1$ has defined, the ship will transit the distance between two adjacent locations on the trajectory. Normalizing this distance by Equation (3.15) yields the corresponding $R(s, s')$. The denominator is the maximum distance among the trajectories between adjacent locations over the defined ocean domain. This equation is suitable for the movement that is not restricted by the boundary of the ocean grid. State $s'$ represents either "a ship at $(x, y)$ toward $\theta_i$" or "a ship at $(x_{ai}, y_{ai})|(x, y)$ toward $\theta_i$".

$$R(s, s') = -\frac{rhumb\ line\ distance(s\ to\ s')}{max\{rhumb\ line\ distance(L), L \in \mathcal{A}rc\}} \tag{3.15}$$

Specially, when the movement is restricted because the ship cannot move beyond the boundary of the ocean grid, the reward will be set as negative infinity to signify an invalid movement. In Equation (3.16), $s'$ can only be the same as $s$, which is "a ship at $(x, y)$ toward $\theta_i$".

$$R(s, s') = -inf \tag{3.16}$$

Second, if the transition refers to an adjustment from one heading direction to another one within location $(x, y)$, as what $a_2$ has defined, a corresponding angle in degrees will be formed. $R(s, s')$ can be determined by normalizing this angle according to Equation (3.17). In this equation, $s'$ represents "a ship at $(x, y)$ toward $\theta_{j=1,2,...8}$", and whether the angle from $s$ to $s'$ is obtained clockwise or counter-clockwise has already been decided during the previous calculation of $P(s'|s, a_2)$.

$$R(s, s') = -\frac{angle\ from\ s\ to\ s'}{360^\circ} \tag{3.17}$$

### 3.2.5 Optimal Policy

When a destination, a particular weather environment, a $\lambda$ value, and an $\alpha$ value are assigned to the MDP, the MDP will generate a corresponding optimal policy $\pi$. A destination is required to allow the MDP to determine the optimal policy. A weather environment specifies the transit circumstance that induces seakeeping responses of the ship. $\lambda$ and $\alpha$ are two parameters that control the influence of seakeeping on the ship's transit MDP solution. When the MDP is launched, an optimal policy $\pi$ is obtained based on the Bellman equation and value iteration algorithm by maximizing the cumulative rewards at all the states, which have been discussed in Section 2.2.2. Furthermore, $\pi(s)$ is the directional decision of state $s$ "a ship at $(x, y)$ toward $\theta_i$". By maximizing the cumulative reward, $\pi(s)$ is the action, $a_1$ or $a_2$, that supports the transit to be conducted by means of the shortest distances and least adjustments from state $s$ to the destination. Therefore, in this framework, the optimal policy $\pi$ defines the directional decisions at all states.

Figure 3.10 shows an example of the optimal policy for one transit scenario that contains the directional decisions, destination, weather environment, $\lambda$ value, and $\alpha$ value. In this figure, if an arrow is plotted for a direction at a location, the corresponding directional decision of that state is $a_1$, which is the move-on action. Otherwise, directional decisions are $a_2$, which is the action of adjusting the heading.

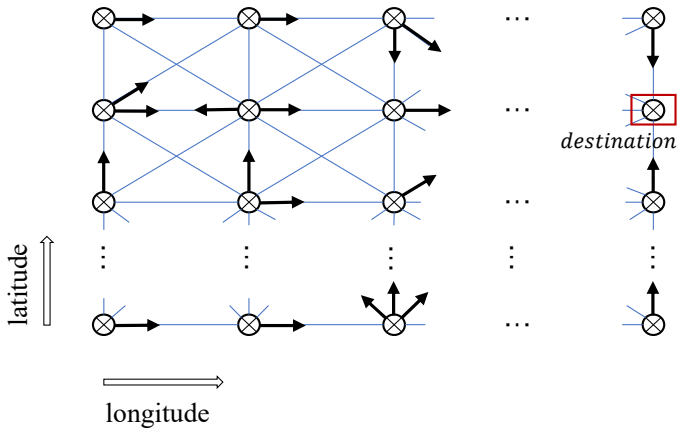


Figure 3.10: The optimal policy generated by the MDP

### 3.2.6 MDP Output

In the GS-MDP framework, the following data associated with each MDP transit simulation will be stored.

- Optimal policy $\pi$, i.e., directional decisions at all states.
- Transition probability matrix $T_1$ that is based on $a_1$, moving on.
- Transition probability matrix $T_2$ that is based on $a_2$, adjusting the heading.
- A matrix $\Phi$ that stores the directional decisions at all locations. The rows and columns of this matrix are the latitude points and longitude points of the ocean grid, respectively. The dimension of this matrix should be equivalent to the ocean grid. Each element of this matrix is an 8×1 vector $\overrightarrow{d}$ that stores the 8 directional decisions at a location.
- A matrix $\Psi$ that stores the seakeeping responses at all locations. The dimension of $\Psi$ is also the same as the ocean grid. Each element of this matrix is an 8×1 vector $\overrightarrow{skp}$ that stores the roll, pitch, or heave amplitudes along the eight directions at a location.

## 3.3 Formation of an Operation Ensemble

As previously mentioned, the MDP will yield different optimal policies for different destinations, weather environments, $\lambda$ values, or $\alpha$ values. If the MDP is executed for a large set of combinations of these four operational setups, the MDP will produce a set of diverse transit scenarios. Thus, the GS-MDP framework produces an operation ensemble that contains a variety of optimal policies that contain directional decisions. Moreover, for all the transit simulations, the GS-MDP framework saves their associated data mentioned in Section 3.2.6. By including multiple destinations and weather conditions, the created ensembles provide the data required to understand the impact of parameters and relative weights on the transit operation MDP outputs. $\lambda$ and $\alpha$ reflect the designer's perception of risk tolerance relative to ship motions during the sea transport. Assigning different values to them allows one to understand the impact of their range due to seakeeping considerations within the ensemble.

## 3.4 Summary

There are three unique contributions of the GS-MDP framework. Firstly, in terms of the simulation foundation, this framework develops a novel gridding approach that sets an adequate representation of the ocean domain. This representation enables the inclusion of all the potential trajectories, weather conditions, and transport status. Therefore, naval architects can have an extensive set of resources to sample operational behaviors and statistically quantify the operational performances for a thin abstraction. Secondly, with respect to the modeling approach, the GS-MDP framework focuses on the novel concept of directional decisions rather than traditional routes. This framework provides a systematic way of decomposing transit procedures and integrating essential physics as a means for understanding the impacts on operational performances. This modeling approach provides designers the ability to

combine various ship operational considerations, thus generating a novel set of data that enables the understanding for early-stage design decisions. Thirdly, as for the MDP application, the presented framework treats the MDP as a mechanism of data generation versus its common use that is traditionally focused on simply calculating optimal policy solutions. All the MDP components, namely states, actions, transition probabilities, rewards, and optimal policies, represent the key factors for a thin abstraction of transit operations. The operational data and the associated ensembles created by these components are valuable to learn the causation of specific ship performance outcomes.

# CHAPTER IV

# *COEM* Metrics

In order to abstract design value from the developed operational ensembles, designers need appropriate metrics. Traditional metrics, such as the transit distance of a route, are appropriate for a thick abstraction but are not directly transferable to a thin abstraction and thus do not fit the GS-MDP framework. This chapter defines several new metrics that enable one to understand operational performances utilizing thin abstraction data. The metrics described in this chapter utilize individual location analysis output data to generate knowledge associated with operational potentials such as transport efficiency, difficulty, and so on.

## 4.1 *Metric(C)*: Closeness to Ideal Transit

As discussed in Section 3.3 designers can modify $\lambda$ values, $\alpha$ values, weather conditions, and destinations to create unique operation ensembles. The modification of $\lambda$ and $\alpha$ controls the extent to which ship motions drive the MDP's solution. By assigning positive infinity to $\lambda$ and zero to $\alpha$, designers can make the MDP solution unaffected by seakeeping responses. Unlike traditional operational thick abstractions, which require the model to be re-run for every unique case, the GS-MDP framework allows a designer to evaluate representative sea state cases without the need for additional model computation time. Within the framework the ($\lambda$=$\infty$, $\alpha$=0) case provides

the benchmark used to evaluate ship transit operations at a set of destinations while concurrently considering weather conditions and seakeeping responses. In this section *metric(C)* will be discussed. This metric measures the closeness to ideal transit. To be specific, the definition of *metric(C)* is that it compares the $a_1$-directional decisions at a location influenced by seakeeping responses to the non-seakeeping ideal case.

Figure 4.1 delineates the directional decisions to a destination with and without seakeeping impact. The directional decisions with the seakeeping impact are on the left side of the figure, and they are going to be benchmarked with the ideal ones on the right side, which do not consider the seakeeping impact. According to the associated data at a single location $(x, y)$, the determination of *metric(C)* is as follows.

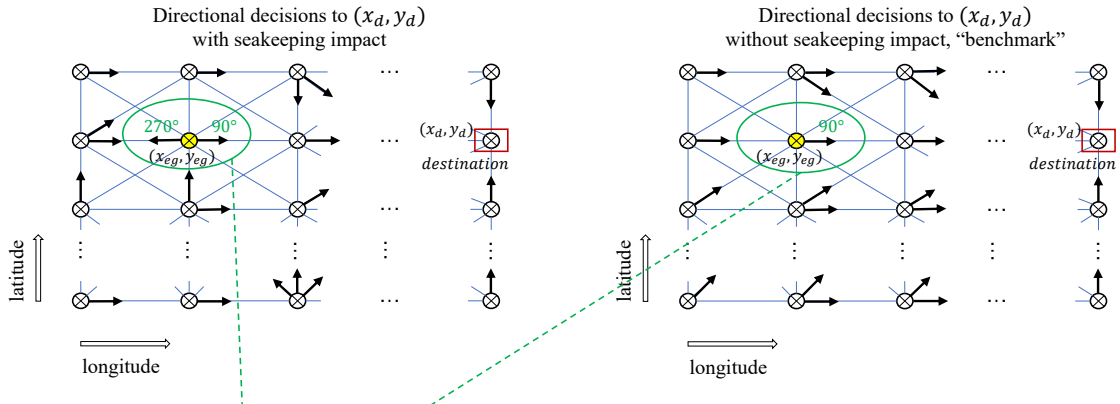


| at $(x_{eg}, y_{eg})$ $\theta_{skp}$ | nearest benchmark | deviation degree $md(\theta_{skp})$ | closeness score $score(\theta_{skp})$ | $metric(C) = \overline{score(\theta_{skp})}$ |
|---|---|---|---|---|
| 90° → | 90° → | 0° | 1 | 0 |
| 270° ← | 90° → | 180° | $-\frac{180°}{180°} = -1$ | |

Figure 4.1: An example of calculating *metric(C)*

First, extract the azimuths of $a_1$-directional decisions at location $(x, y)$ and save these azimuths in the set $M$ (short for Moving-on azimuths). Furthermore, $M_{skp}$ corresponds to a transit scenario that considers the seakeeping impact, while $M_{ideal}$ corresponds to the transit that does not consider the seakeeping impact. For instance,

at the exemplified location $(x_{eg}, y_{eg})$ in Figure 4.1, $M_{skp}$={90°, 270°} and $M_{ideal}$={90°}.

$$M = \{\theta_i : \pi(s_i|(x, y)) = a_1\} \tag{4.1}$$

Then, measure how much the azimuths in the set $M_{skp}$ deviate away from the azimuths in the set $M_{ideal}$. For each element $\theta_{skp}$ in $M_{skp}$, it needs to be compared with all the elements in $M_{ideal}$ to find its nearest benchmark, which can be identified by the minimum deviation $md(\theta_{skp})$. Equation (4.2) to (4.3) express the calculation of $md(\theta_{skp})$. A small $md(\theta_{skp})$ value represents that azimuth $\theta_{skp}$ is close to ideal transit. Equation (4.4) concretely defines the closeness score of azimuth $\theta_{skp}$. Indeed, these equations set a mapping procedure from the set $M_{skp}$ to a new set $S_{skp}$ that contains the closeness scores for all the elements in $M_{skp}$. Back to the example at location $(x_{eg}, y_{eg})$: $M_{skp}$={90°, 270°} and $M_{ideal}$={90°}, so that $S_{skp}$={1, -1}.

$$md(\theta_{skp}) = Min\{f(\theta_{skp}, \theta_{ideal}), \theta_{ideal} \in M_{ideal}\} \tag{4.2}$$

$$f(\theta_{skp}, \theta_{ideal}) = \begin{cases} |\theta_{skp} - \theta_{ideal}| & \text{if } |\theta_{skp} - \theta_{ideal}| \leq 180° \\ 360° - |\theta_{skp} - \theta_{ideal}| & \text{if } |\theta_{skp} - \theta_{ideal}| > 180° \end{cases} \tag{4.3}$$

$$score(\theta_{skp}) = \begin{cases} 1 & \text{if } \theta_{skp} = 0° \\ -\frac{md(\theta_{skp})}{180°} & \text{if } \theta_{skp} \neq 0° \end{cases} \tag{4.4}$$

$$S_{skp} = \{score(\theta_{skp}) : \theta_{skp} \in M_{skp}\} \tag{4.5}$$

Finally, the value of *metric(C)* at location $(x, y)$ takes all the $a_1$-directional decisions at this location into account. The mean of closeness scores in the set $S_{skp}$ is used as the *metric(C)* value for a location. At the location $(x_{eg}, y_{eg})$ mentioned above, its

corresponding *metric(C)* value is 0.

$$\begin{aligned} metric(C) &= \overline{score(\theta_{skp})},\ score(\theta_{skp}) \in S_{skp} \\ -1 &\leq metric(C) \leq 1 \end{aligned} \tag{4.6}$$

*Metric(C)* is a thin abstraction of the deviation from ideal routes at a location, which reflects a ship's capability of transiting in an idealized way. If this metric gets small, it will inform designers that a ship design has poor potentials to follow the ideal transit trajectories due to the seakeeping impact.

## 4.2 *Metric(O)*: Outdegree of Transit

The metric of transit outdegree, *metric(O)*, measures the percent of $a_1$-directional decisions that occur at a location. Regardless of whether a transit scenario is ideal or not, it is promoted by the directional decisions selected as moving on. If the transit scenario is ideal, the $a_1$-directional decisions are decided upon a single desire, which is to reach the destination as quickly as possible. However, most of the transit scenarios simulated in the GS-MDP are not ideal, and the $a_1$-directional decisions result from balancing the desires of moving directly to the destination and experiencing acceptable ship motions. Among the eight directions at a location, the determination of *metric(O)* is based on Equation (4.7).

$$\begin{aligned} metric(O) &= \frac{|\{s_i : \pi(s_i|(x,y)) = a_1\}|}{8} \\ 0 &\leq metric(O) \leq 1 \end{aligned} \tag{4.7}$$

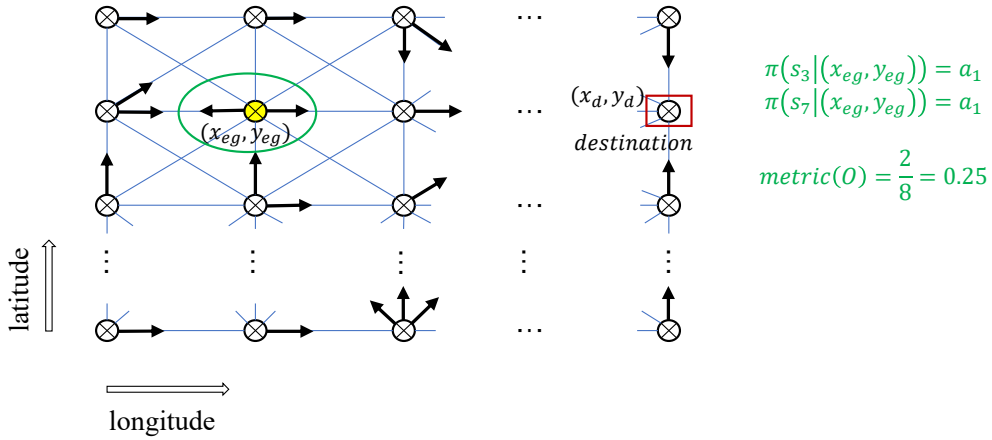


Figure 4.2: An example of calculating *metric(O)*

In Equation (4.7), the numerator is the absolute measurement of $a_1$-directional decisions at location $(x, y)$. Dividing the absolute measurement by eight normalizes this measurement. Thus, *metric(O)* is defined as the percent of $a_1$-directional decisions at a location, ranging from zero to one. As shown in Figure 4.2, *metric(O)* equals 0.25 at the exemplified location $(x_{eg}, y_{eg})$.

*Metric(O)* is a thin abstraction of potential routes. It reflects the move-on actions that promote transit operations toward the destination. The direction associated with the move-on action may put the vessel closer to the destination, or it may make the vessel move farther away from the destination. Thus the magnitude of this metric does not directly reveal the extent to which the ship's transit options bring the ship directly toward its goal. Small values of *metric(O)* may indicate ideal transit operations that only follow direct directions toward destinations, or may also correspond to some poor transit operations that present limited and undesirable movements. When the value of *metric(O)* approaches one, there is a high probability that the transit is undesirable in that at a location there are as many move-on directions that bring the vessel closer to its goal as the move-on directions that move it away. While *metric(O)* does not provide direct value, it does provide unique value when being used with other metrics.

## 4.3 *Metric(E)*: Efficiency of Transit

After a ship decides to move on at a specific location $(x, y)$, it will get either closer or farther to the destination. Only when an $a_1$-directional decision makes a ship closer to the destination can the transit be speculated as efficient. *Metric(E)*, which stands for transit efficiency, measures the ratio of occurrences that the ship gets closer to the destination versus the total number of the $a_1$-directional decisions at a location. The value of *metric(E)* is determined by Equation (4.8). Figure 4.3 further illustrates two examples of calculating this metric.

$$\begin{aligned} metric(E) &= \frac{|\{s_i : \pi(s_i|(x,y)) = a_1,\ d_{current} > d_{next}\}|}{|\{s_i : \pi(s_i|(x,y)) = a_1\}|} \\ d_{current} &= great\ circle\ distance((x,y)\ to\ destination) \\ d_{next} &= great\ circle\ distance((x_{ai}, y_{ai})|(x,y)\ to\ destination) \\ 0 &\leq metric(E) \leq 1 \end{aligned} \tag{4.8}$$

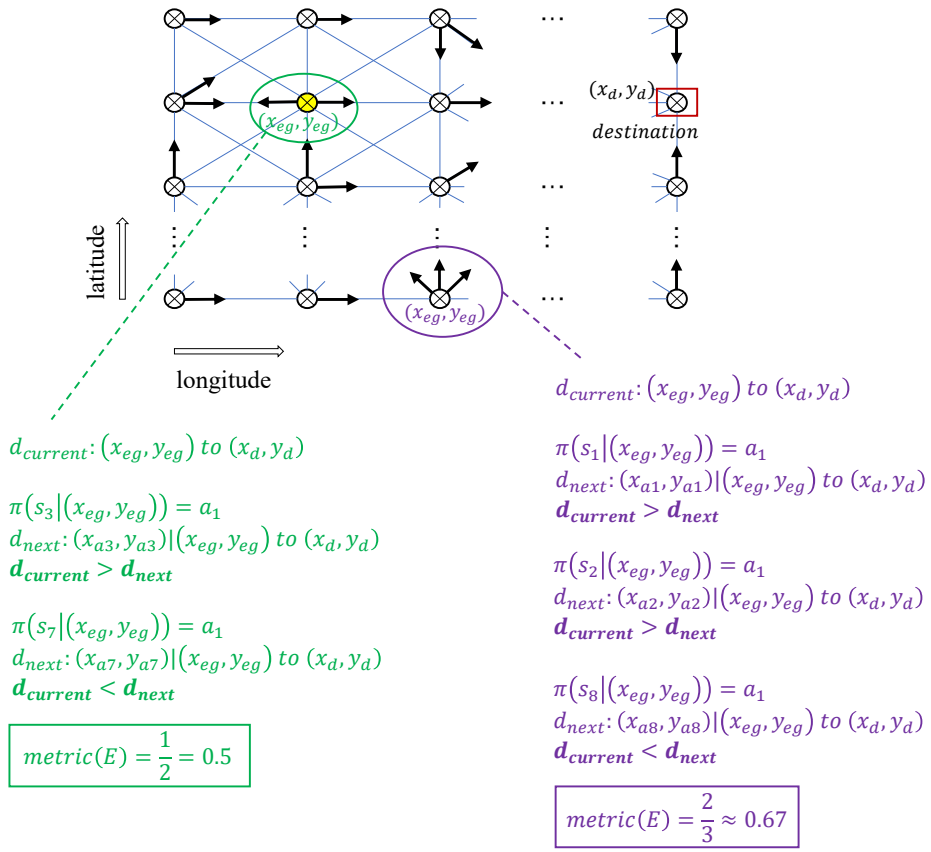


Figure 4.3: Examples of calculating *metric(E)*

As shown in Equation (4.8), the denominator is the absolute measurement of $a_1$-directional decisions at location $(x, y)$. When an $a_1$-directional decision is achieved, the ship will move from the current location to the next location. The comparison between $d_{current}$ and $d_{next}$ concretely expresses the meaning of getting closer to the destination. Among all the $a_1$-directional decisions at $(x, y)$, the ones that can lead a ship closer to the destination are counted in the numerator. In terms of the exemplified location $(x_{eg}, y_{eg})$ in green, one of the two $a_1$-directional decisions at this location can lead a ship closer to the destination, hence yielding *metric(E)* as 0.5 at this location. At another exemplified location $(x_{eg}, y_{eg})$ in purple, there is one $a_1$-directional decision that is ideal and roughly toward the northeast. There is one $a_1$-directional decision toward the north, which just slightly deviates away from the ideal direction and can

still lead a ship closer to the destination. The last $a_1$-directional decision will make a ship farther away from the destination. Therefore, *metric(E)* is 0.67 at this location.

*Metric(E)* is a thin abstraction of potential routes that are with positive operational progress. This metric reflects a ship's potential of positively continuing on transit operations. The worst efficiency score is zero, indicating that the ship is always moving away from the destination. While the best score is one, indicating that the ship is always approaching the destination and no detours occur. The variation in *metric(E)* from zero to one shows that the efficiency potential becomes more and more satisfactory.

## 4.4 *Metric(M)*: Maneuver Robustness

At a location $(x, y)$, the associated directional decisions refer to not only the ones occurring at this location, but also other ones that have connections with this location. Among the adjacent locations of location $(x, y)$, there may exist $a_1$-directional decisions that point to $(x, y)$. These $a_1$-directional decisions are also helpful to explore transit potentials. First of all, similar to the transit outdegree, the $a_1$-directional decisions that point to location $(x, y)$ enable a new metric about transit indegree, *metric(I)*. Then considering the transit indegree and outdegree together supports the consideration of potential trajectories at location $(x, y)$. Given these trajectories, designers are able to develop another new metric, *metric(M)*, and deduce a ship's potential of maneuver robustness via this metric. The development of *metric(M)* is presented below step by step.

First, only the following eight states, $p_k$ where $k$=1,2...,8, are probable to generate $a_1$-directional decisions that point to location $(x, y)$. If the optimal action at $p_k$ is $a_1$, this $a_1$-directional decision will contribute to the indegree of location $(x, y)$, and a ship will transit from state $p_k$ to state $p_k{}'$.

- $p_1$: a ship at location $(x_{a1}, y_{a1})|(x, y)$ toward $\theta_5$

  $p_1{}'$: a ship at location $(x, y)$ toward $\theta_5$

- $p_2$: a ship at location $(x_{a2}, y_{a2})|(x, y)$ toward $\theta_6$

  $p_2{}'$: a ship at location $(x, y)$ toward $\theta_6$

- $p_3$: a ship at location $(x_{a3}, y_{a3})|(x, y)$ toward $\theta_7$

  $p_3{}'$: a ship at location $(x, y)$ toward $\theta_7$

- $p_4$: a ship at location $(x_{a4}, y_{a4})|(x, y)$ toward $\theta_8$

  $p_4{}'$: a ship at location $(x, y)$ toward $\theta_8$

- $p_5$: a ship at location $(x_{a5}, y_{a5})|(x, y)$ toward $\theta_1$

  $p_5{}'$: a ship at location $(x, y)$ toward $\theta_1$

- $p_6$: a ship at location $(x_{a6}, y_{a6})|(x, y)$ toward $\theta_2$

  $p_6{}'$: a ship at location $(x, y)$ toward $\theta_2$

- $p_7$: a ship at location $(x_{a7}, y_{a7})|(x, y)$ toward $\theta_3$

  $p_7{}'$: a ship at location $(x, y)$ toward $\theta_3$

- $p_8$: a ship at location $(x_{a8}, y_{a8})|(x, y)$ toward $\theta_4$

  $p_8{}'$: a ship at location $(x, y)$ toward $\theta_4$

Therefore *metric(I)* can be computed by Equation (4.9). In addition to the value of *metric(I)*, it is also important to extract all the states $p_k{}'$ that are related to the "indegree" $a_1$-directional decisions, according to Equation (4.10).

$$metric(I) = \frac{|\{p_k : \pi(p_k) = a_1\}|}{8}$$
$$0 \leq metric(I) \leq 1 \tag{4.9}$$

$$P_{in} = \{p_k{}' : \pi(p_k) = a_1\} \tag{4.10}$$

Figure 4.4 temporarily omits the $a_1$-directional decisions at location $(x_{eg}, y_{eg})$ and just focuses on the $a_1$-directional decisions that contribute to the transit indegree of $(x_{eg}, y_{eg})$. It demonstrates the value of *metric(I)* and highlights the related states, which are $p_5$, $p_7$, $p_5'$, and $p_7'$.

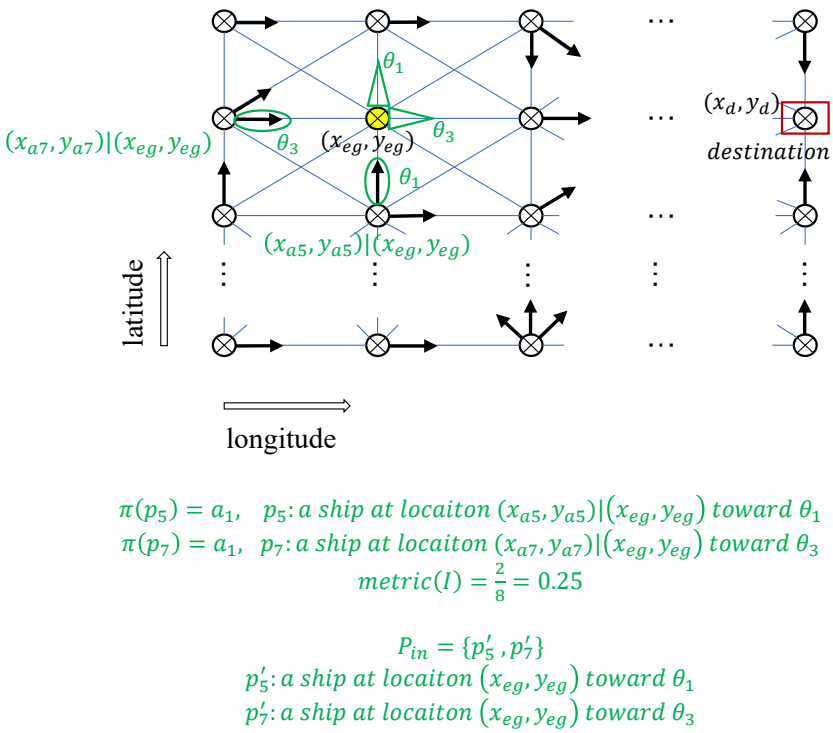


Figure 4.4: The $a_1$-directional decisions at adjacent locations contributing to the transit indegree of $(x_{eg}, y_{eg})$

Then, the observations of transit indegree and outdegree are both needed to learn the trajectories at location $(x, y)$. Use the symbol $P_{out}$ to represent the set of states that exhibit $a_1$-directional decisions at location $(x, y)$. The states in the set $P_{in}$ describe the heading directions of a ship when it arrives at location $(x, y)$. Before leaving this location, the ship may or may not have to change its heading direction. If a state in the set $P_{in}$ is also in the set $P_{out}$, it means that the ship can pass the location without changing its heading direction. However, if a state only belongs to the set $P_{in}$, it means that the ship's heading should be maneuvered according to an

$a_1$-directional decision that location $(x, y)$ allows (i.e., the set $P_{out}$ allows). In short, each trajectory can be represented by its angle value. The angle value depends on the ship's heading directions along which it transits into and out of location $(x, y)$. The set *Traj*, which is expressed in Equation (4.12), gathers all the potential trajectories at location $(x, y)$. For each state $p_k{}'$ in the set $P_{in}$, the relevant calculation of g($p_k{}'$,$s_i$) is defined by Equation (4.13). On one side, if $p_k{}'$ happens to be in the set $P_{out}$, g($p_k{}'$,$s_i$) will always be zero, which is independent of $s_i$. On the other side, if $p_k{}'$ does not belong to the set $P_{out}$, it should be compared with all the states of $P_{out}$ to gain different values of g($p_k{}'$,$s_i$). Additionally, the value of *angle along the way($p_k{}'$ to $s_i$)* should be available based on Equation (3.14) and (3.17), which are two equations defined in the GS-MDP framework. The ship's turning angle $\beta$ at a location sometimes can be large. The reason is that certain intermediate directions with adverse motions are difficult to overcome and influence the ship heading adjustment.

$$P_{out} = \{s_i : \pi(s_i|(x, y)) = a_1\} \tag{4.11}$$

$$Traj = \{\beta : \beta = g(p_k{}', s_i) \;\; p_k{}' \in P_{in} \;,\; s_i \in S_{out}\} \tag{4.12}$$

$$g(p_k{}', s_i) = \begin{cases} g(p_k{}') = 0^\circ & \text{if } p_k \in P_{out} \\ \textit{angle along the way}(p_k{}' \textit{ to } s_i) & \text{if } p_k \notin P_{out} \end{cases} \tag{4.13}$$

Finally, designers can pay attention to the trajectories with specific features to explore a ship's potential performances in maneuvering. This thesis utilizes 90° as a threshold value to identify the trajectories that are relatively smooth. The set $Traj_{smooth}$ collects all the smooth trajectories. The ratio of smooth trajectories to all the trajectories at location $(x, y)$ is a useful indicator of maneuver robustness. *Metric(M)* is defined according to this ratio in Equation (4.15). Figure 4.5 briefly

shows the determination of *metric(M)* at location $(x_{eg}, y_{eg})$.

$$Traj_{smooth} = \{\beta_{smooth} : \beta_{smooth} \in Traj\ ,\ \beta_{smooth} \leq 90°\} \tag{4.14}$$

$$\begin{gathered} metric(M) = \frac{|Traj_{smooth}|}{|Traj|} \\ 0 \leq metric(M) \leq 1 \end{gathered} \tag{4.15}$$

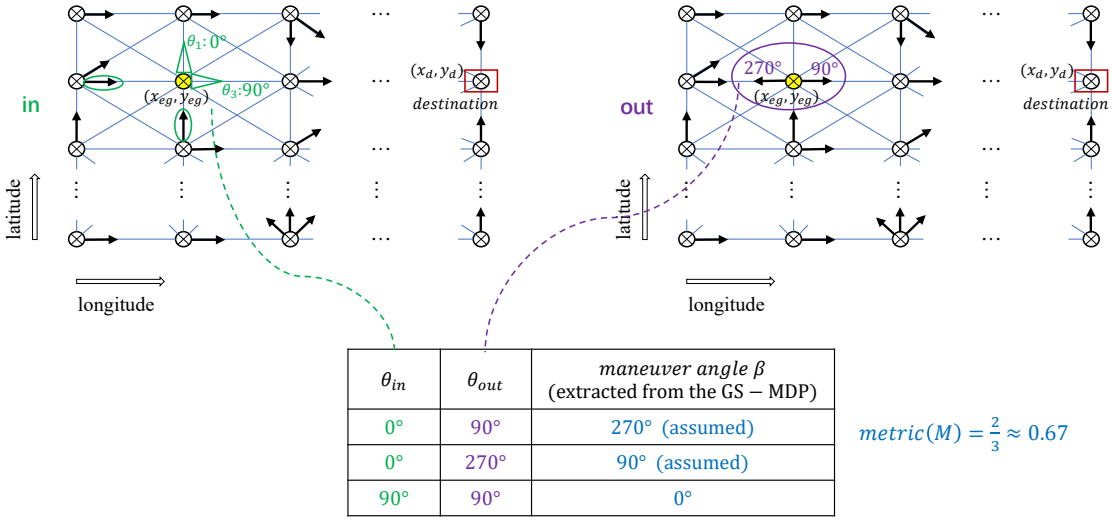


Figure 4.5: An example of calculating *metric(M)*

*Metric(M)* measures the desirable trajectories at a location, along which a ship adjusts its heading direction for 90° at most. This metric is a thin abstraction of transit course changes. It can reflect the ship's potential of smoothly continuing on transit operations with few maneuver difficulties. Its range is from zero to one. The larger *metric(M)* is, the better maneuver robustness that a ship has. Additionally, if a location is not associated with any "indegree" $a_1$-directional decisions, it is allowable to skip the calculation of *metric(M)* at this location.

## 4.5 Summary

Four novel metrics that abstract different aspects of transit operations have been developed in this chapter. These four metrics are *metric(C)*, *metric(O)*, *metric(E)*, and *metric(M)*, and will be defined utilizing the acronym *COEM*. Table 4.1 below provides a summary of their use and definitions. These metrics are consistent with the context of the operation ensemble. Ship designers can explore the metric values based on the operation ensemble and utilize statistical analyses to understand the operational performances of a conceptual design.

Table 4.1: The use and definitions of *COEM* metrics

| | |
|---|---|
| **C** | *Metric(C)* is a thin abstraction of the deviation from ideal routes. |
| | The comparison of the $a_1$-directional decisions at a location influenced by seakeeping responses to the non-seakeeping ideal case. |
| **O** | *Metric(O)* is a thin abstraction of potential routes. |
| | The percent of $a_1$-directional decisions at a location. |
| **E** | *Metric(E)* is a thin abstraction of potential routes that are with positive operational progress. |
| | The ratio of occurrences that a ship gets closer to the destination versus the total number of the $a_1$-directional decisions at a location. |
| **M** | *Metric(M)* is a thin abstraction of the difficulty related to transit course changes. |
| | The ratio of trajectories along which a ship adjusts its heading direction for 90° at most at a location. |

# CHAPTER V

# Case Study 1: Testing the GS-MDP Framework

As described in Chapter III and IV, the GS-MDP framework enables designers to evaluate a conceptual design through the corresponding operation ensemble and associated "*COEM*" metrics. In this chapter, a representative case study is presented to demonstrate the application, dynamics, and analysis of the framework. The case study presented is focused on the creation of the required operation ensemble for a given ship design, which consisted of the transit scenarios to an assigned destination under manually specified wave conditions with the seakeeping consideration of either roll, pitch, or heave. The intent of creating this special operation ensemble is to show the uniqueness of the GS-MDP framework in:

- identifying the main contributors to undesirable operational outcomes;
- explaining the underlying contexts of why certain operational phenomena exist;
- providing useful evaluations based on the newly defined operational metrics.

## 5.1 Case Setups

The global shipping density (*Wu et al.*, 2017) manifests that the North Pacific Ocean is of great interest to study sea transport operations. This case study refers to an existing container ship named Maunawili (*MarineTraffic*, n.d.) that transports

cargoes across the North Pacific Ocean, and then presumes the following conceptual design to be evaluated by the GS-MDP framework. Table 5.1 exhibits the ship's main hull parameters and the design speed for transit.

Table 5.1: Parameters of a conceptual ship design

| Ship design parameter | Value |
|---|---|
| Waterline length, LWL(m) | 217 |
| Beam, B(m) | 32 |
| Draft, T(m) | 12.8 |
| Block coefficient, $C_B$ | 0.65 |
| Displacement, $\nabla$ (tonne) | 58853 |
| Speed, $V_k$ (knot) | 22 |

### 5.1.1 Destinations and Wave Conditions

The sea transport scenarios were simulated in the North Pacific Ocean. This case study defined the longitude range from 150E to 230E and the latitude range from 10N to 50N. The resolutions along the longitude and latitude were 8 degrees and 5 degrees, respectively. The destination of the sea transport was set at (230E,40N), a location close to California. Figure 5.1 concretely plots this ocean area and this destination.

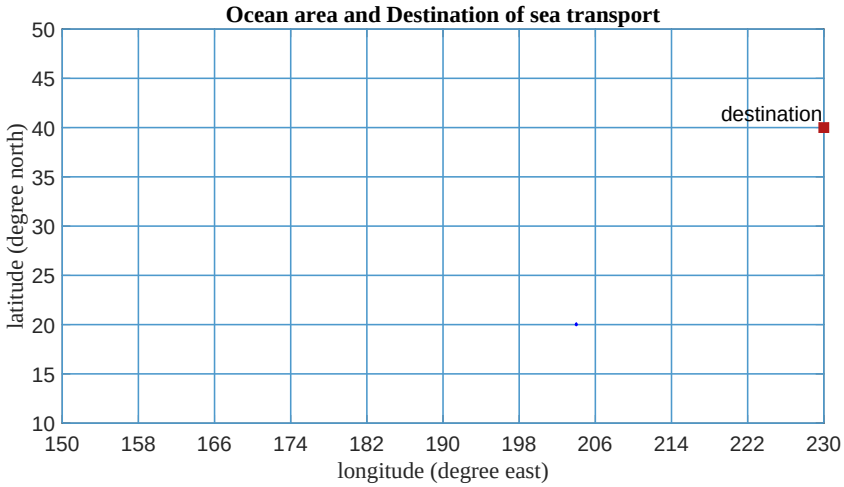


Figure 5.1: North Pacific Ocean Grid and the transit destination

In an effort to embody certain extreme wave conditions, the author manually assumed two groups of wave environments. At each location, there should be a direction that allows the ship to follow the shortest path to the destination. Geographically speaking, this direction is called the great-circle azimuth. In the first group of wave environments, the wave direction at every location was 90° more than the great-circle azimuth, and wave heights and wave periods were at the scale of sea state 7. In other words, the wave height would vary from 6 to 9 meters, and the wave period would change from 11.7 to 19.8 seconds (*Paik and Thayamballi*, 2007; *Lee et al.*, 1985). As such, if the ship went along the shortest path, it would always encounter beam seas. In the second group, the wave conditions were still at the scale of sea state 7, while the wave direction at each location was set to be 180° more than the great-circle azimuth. Under this circumstance, if the ship followed the shortest path, it would always encounter head seas. Figure 5.2 and 5.3 demonstrate the wave directions, wave heights, and wave periods of the two groups of wave conditions over the prescribed ocean area.

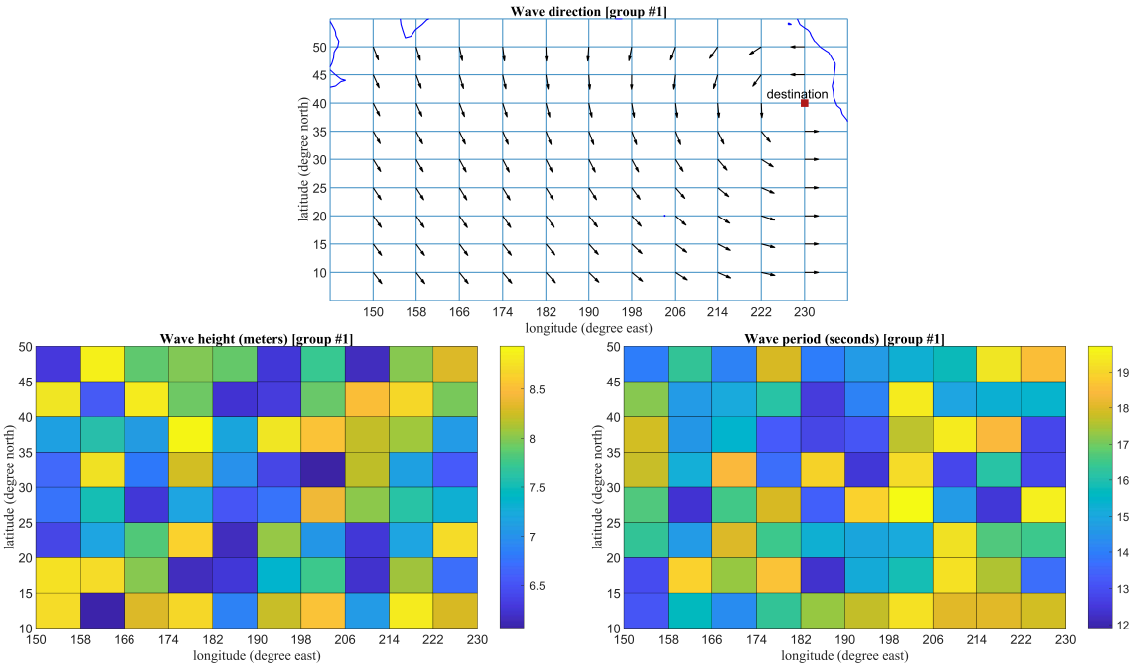


Figure 5.2: The first group of wave conditions

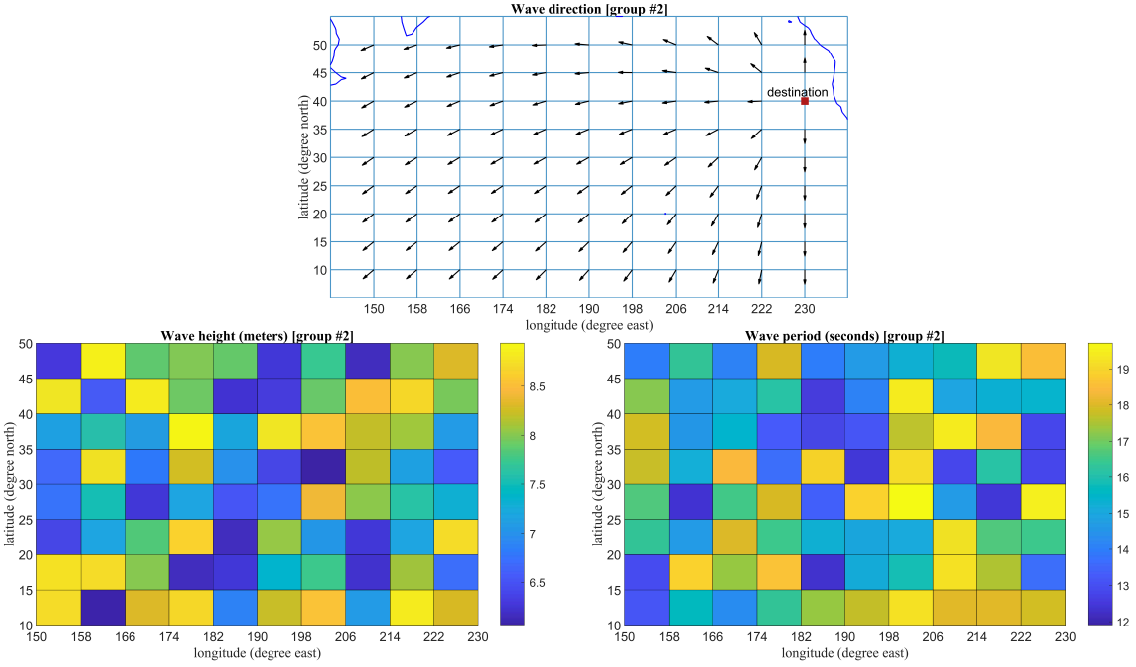


Figure 5.3: The second group of wave conditions

These two groups of wave conditions are used for testing the GS-MDP framework.

They are severe wave conditions that result in transit phenomena that are obvious and diverse. For example, if the wave conditions are too mild, the transit phenomena will only be dominated by the ship's intent of reaching the destination. Although the influence of ship motions has been incorporated in the framework, designers will find it difficult to observe the interactions or phenomena caused by seakeeping. Given extreme wave conditions, all the influential factors of the transit may take effect, and designers can control the relative importance of seakeeping by adjusting the values of $\lambda$ and $\alpha$, which will be discussed. Transit phenomena that highlight and ignore the seakeeping impact will both be attainable in this case study. The reason for this approach is to provide a logical way to test the framework based on the circumstances where designers can have some anticipations. For instance, in light of the first group of wave conditions, there is a high probability of encountering beam seas along the shortest transit trajectories so that designers may predict the roll motion as an issue. Similarly, they may predict the pitch motion as an issue when simulating the ship under the second group of wave conditions. Then, the designers can check if the results from the GS-MDP framework fit their anticipations. Moreover, if there are some inconsistencies, the examination of the framework will go deeper to check whether the unexpected results can be justified.

### 5.1.2 Seakeeping Impact Parameters

In this case study, a University of Michigan seakeeping software named SPP (*Parsons*, 2018) has been used to estimate the seakeeping responses. This software applies the strip theory and long-crested wave assumptions in the frequency domain. SPP offers reliable estimations of seakeeping responses given ship main hull parameters and sea spectrum profiles. According to the parameters mentioned in Table 5.1, SPP has the capability to approximate a sectional curve and a waterline curve via mathematical models, and then depict the hull sections at each station by Lewis Form. The role

of the sea spectrum is to represent the real irregular waves where transit operations occur. ISSC spectrum is an option to characterize the fully developed wave conditions of the North Pacific Ocean. This spectrum is a two-parameter spectrum that depends on the significant wave height $H_s$ in meters and the mean wave period $T$ in seconds, whose formula is shown below. In Equation (5.1), $\omega$ is the wave frequency in radians per second. Finally, as mentioned before in Equation (3.6), the corresponding energy spectrum $S_{motion}(\omega_E)$ offers the necessary seakeeping references.

$$S_W(\omega) = \frac{173.6 H_s^2 T^{-4}}{\omega^5} exp(-694.4 T^{-4} \omega^{-4}) \tag{5.1}$$

Figure 5.4 demonstrates the inputs, the major procedure, and the outputs of SPP. This case study considered the impact of roll, pitch, and heave, respectively. These three motions are common focuses when evaluating the operability of a container ship because they are relevant to cargo loss, onboard equipment applicability, personnel effectiveness, and many other shipping aspects (*Ghaemi and Olszewski*, 2017).

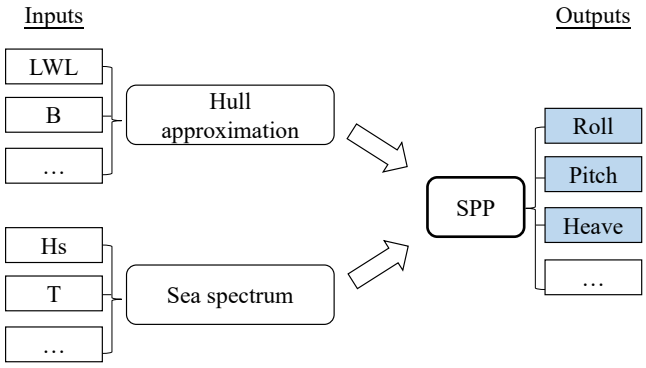


Figure 5.4: Major procedures and components of SPP

The impact levels of a given ship motion were represented by the combinations of $\lambda$ and $\alpha$ values. Parameter $\lambda$ modifies the seakeeping impact on the action of moving on. A smaller $\lambda$ value represents stricter constrain, meaning that the movements are more likely to be impeded by certain motion amplitudes. Parameter $\alpha$ modifies the

seakeeping impact on the action of adjusting the heading, and larger values correspond to more difficulties in overcoming certain motion amplitudes during the adjustment. First of all, a pretty large $\lambda$ and zero $\alpha$ represent no seakeeping impact. Then, if the seakeeping impact is considered, it will come from either roll, pitch, or heave. For each ship motion, this case study assigned three values to $\lambda$ and three values to $\alpha$ in order to signify the low, medium, and high impact levels. The low impact level determined by parameter $\lambda$ should be a value large enough to tolerate almost all the motion amplitudes. Then, medium and high levels of $\lambda$ were the values at the same magnitude of existing operational criteria (*Stevens and Parsons*, 2002; *Ghaemi and Olszewski*, 2017). To be specific, $\lambda$=180°, 8°, and 4° for roll; $\lambda$=90°, 3°, and 1.5° for pitch; $\lambda$=100m, 2m, and 1m for heave. For all three motions, $\alpha$ values were selected as 0.01, 0.4, and 0.7 to stand for the impact levels from low to high. In total, each motion had 9 combinations of $\lambda$ and $\alpha$ values, so 27 combinations were created after respectively considering roll, pitch, and heave. Including the combination that represents no seakeeping impact, all 28 combinations of $\lambda$ and $\alpha$ values are summarized in Table 5.2.

According to the case setups discussed above, the operation ensemble created by the GS-MDP framework covers $1+1\times2\times27=55$ transit scenarios. Furthermore, the ocean grid defined here contains 99 locations. Except for the destination, the other 98 locations are valid for aggregating directional decisions from every transit scenario, and 8 directional decisions exist at each location. As such, this operation ensemble extensively contains $8\times98\times55=43120$ directional decisions to help the designers understand the conceptual design, and simultaneously testify the usefulness of the GS-MDP framework.

Table 5.2: The combinations of $\lambda$ and $\alpha$ values to vary seakeeping impact

| No. | Ship motion | $\lambda$ | $\alpha$ |
|---|---|---|---|
| 1 | none | 1 000 000° | 0 |
| 2 | roll | 180° | 0.01 |
| 3 | roll | 180° | 0.4 |
| 4 | roll | 180° | 0.7 |
| 5 | roll | 8° | 0.01 |
| 6 | roll | 8° | 0.4 |
| 7 | roll | 8° | 0.7 |
| 8 | roll | 4° | 0.01 |
| 9 | roll | 4° | 0.4 |
| 10 | roll | 4° | 0.7 |
| 11 | pitch | 90° | 0.01 |
| 12 | pitch | 90° | 0.4 |
| 13 | pitch | 90° | 0.7 |
| 14 | pitch | 3° | 0.01 |
| 15 | pitch | 3° | 0.4 |
| 16 | pitch | 3° | 0.7 |
| 17 | pitch | 1.5° | 0.01 |
| 18 | pitch | 1.5° | 0.4 |
| 19 | pitch | 1.5° | 0.7 |
| 20 | heave | 100m | 0.01 |
| 21 | heave | 100m | 0.4 |
| 22 | heave | 100m | 0.7 |
| 23 | heave | 2m | 0.01 |
| 24 | heave | 2m | 0.4 |
| 25 | heave | 2m | 0.7 |
| 26 | heave | 1m | 0.01 |
| 27 | heave | 1m | 0.4 |
| 28 | heave | 1m | 0.7 |

## 5.2 Case Results

### 5.2.1 Main Contributor Identification

Descriptive statistics, especially the mean, of the metrics generalizes the overall transit potentials from the operation ensemble. Thus this case study chooses to

use the mean values to represent the results of different metrics. *Metric(C)* is the primary indicator of how idealized a ship can operate, and designers can quickly find undesirable operational outcomes by only observing this metric. In general, Table 5.3 summarizes the values of *metric(C)* for different wave conditions and different ship motions.

Table 5.3: *Metric(C)* for different wave conditions and different ship motions

| | wave environment #1 "beam seas to shortest path" | wave environment #2 "head seas to shortest path" |
|---|---|---|
| w/o | 1 | 1 |
| roll | 0.561 | 0.559 |
| pitch | 0.914 | 0.647 |
| heave | 0.848 | 0.822 |

The first row of *metric(C)* values corresponds to the circumstances without the seakeeping impact, so it is labeled as w/o. *Metric(C)* is always 1 at this row, and it should be 1 because the ideal transit is the transit without seakeeping itself. The last three rows show the *metric(C)* values that are affected by roll, pitch, or heave. According to the comparison of them under two different groups of wave conditions, it is feasible to infer which motion is the contributor to undesirable transit outcomes.

- Wave environment #1: Considering the roll impact leads to the lowest *metric(C)*, which is 0.561, while the values associated with the other two motions are relatively close to 1. Therefore, the main contributor that causes non-ideal transit outcomes in this environment is the roll motion. Moreover, identifying this negative influence from the roll motion is consistent with the anticipations mentioned in Section 5.1.1.

- Wave environment #2: 0.647 and 0.559 are both undesirable values, which indicate that there are two main contributors. Pitch and roll motions both de-

viate the ship away from the ideal transit in this environment, and roll motions even cause more adverse deviations. Pitch motions are the anticipated issue in this environment, while the reason why roll motions also worsen the transit performances needs to be investigated.

- Different groups of wave conditions demonstrate almost the same and little heave impact on the variations of *metric(C)*. The reason could be that SPP is a simplified estimation of each motion separately, excluding the consideration of coupled motions. However, heave is typically coupled with other motions. Replacing SPP with a better tool may improve the consideration of heave impact but will not change the GS-MDP framework. This change is not within the scope of this thesis, and it will be identified in future work.

The impact of ship motions is controlled by $\lambda$ and $\alpha$. To further understand the causation relationships between ship motions and transit performances, designers can dig into the influence of $\lambda$ and $\alpha$ on *metric(C)* as follows.

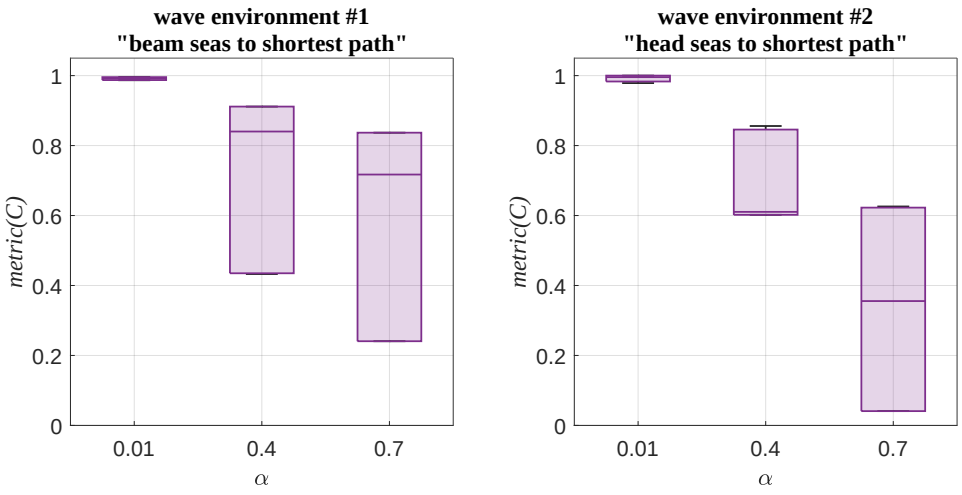


Figure 5.5: The distribution of *metric(C)* versus each $\alpha$ value under different wave conditions

Figure 5.5 summarizes the influence of $\alpha$ on *metric(C)* independent of the ship motion to be considered, so this figure reveals findings that involve all the motions.

The box plot on the left side shows how *metric(C)* values distribute based on different $\alpha$ values when the transit simulations occur in the first group of wave environments, and the right-side box plot depicts the *metric(C)* values from the second group of wave environments.

- Regardless of the wave environments, *metric(C)* is close to 1 as long as $\alpha$ is 0.01. In fact, an $\alpha$ value of 0.01 is equivalent to relaxing the seakeeping impact on adjusting the ship's heading. Although there is still another parameter $\lambda$ defined in the framework, the seakeeping impact that $\lambda$ imposes has been overwritten. As such, the *metric(C)* values seem idealized and do not present any seakeeping impact.

- On the left side, the distributions of *metric(C)* plotted based on $\alpha$ values 0.4 and 0.7 change but still have a broad overlap. It indicates that *metric(C)* is not sensitive to $\alpha$ in this weather environment.

- On the right side, the distributions of *metric(C)* under different $\alpha$ values are distinct intervals. It is hard to see overlaps between different distributions. In this weather environment, parameter $\alpha$ largely dominates the transit outcomes.

After identifying $\alpha$ as a contributor to *metric(C)* variations in the second group of wave environments, designers can say that the non-ideal transit outcomes related to the roll impact result from roll motions blocking the adjustment of heading directions. To be specific, the ship wants to adjust its heading to the ideal direction whenever possible. However, if the ship is more than 90° away from the ideal direction, it needs to handle some intermediate adjustment experiences that include beam seas and adverse roll amplitudes. Even worse, it will be less likely for the ship to go through such intermediate roll motions when larger $\alpha$ values are used to amplify this hardship.

Figure 5.6 and 5.7 expands all the combinations of the seakeeping impact related to roll and pitch. The 18 combinations are ranked based on their *metric(C)* values. Figure 5.6 shows the ranking results with respect to the first group of wave conditions, and Figure 5.7 corresponds to the second group. These results are also helpful in revealing the influence of ship motions.

| wave environment #1 | | | | |
|---|---|---|---|---|
| "beam seas to shortest path" | | | | |
| ranking | *metric(C)* | ship motion | λ | α |
| 1 | 0.996 | pitch | 90 | 0.01 |
| 2 | 0.996 | pitch | 3 | 0.01 |
| 3 | 0.992 | pitch | 1.5 | 0.01 |
| 4 | 0.987 | roll | 180 | 0.01 |
| 5 | 0.987 | roll | 8 | 0.01 |
| 6 | 0.987 | roll | 4 | 0.01 |
| 7 | 0.911 | pitch | 90 | 0.4 |
| 8 | 0.911 | pitch | 3 | 0.4 |
| 9 | 0.911 | pitch | 1.5 | 0.4 |
| 10 | 0.837 | pitch | 90 | 0.7 |
| 11 | 0.837 | pitch | 3 | 0.7 |
| 12 | 0.837 | pitch | 1.5 | 0.7 |
| 13 | 0.435 | roll | 180 | 0.4 |
| 14 | 0.435 | roll | 8 | 0.4 |
| 15 | 0.433 | roll | 4 | 0.4 |
| 16 | 0.241 | roll | 180 | 0.7 |
| 17 | 0.241 | roll | 8 | 0.7 |
| 18 | 0.241 | roll | 4 | 0.7 |

Figure 5.6: Ranking different combinations of the seakeeping impact based on their associated *metric(C)* values (wave environment #1)

Three observations need to be highlighted in Figure 5.6.

- Firstly, the general trend of color variation from top to bottom is from orange to blue. Orange stands for the pitch impact; blue stands for the roll impact. There is a rough tendency that roll motions cause more negative effects than pitch motions.

- Secondly, the ranking range that a certain motion covers also reflects the extent to which this motion negatively impacts transit outcomes. The lowest ranking related to the pitch impact is 12, with a metric value of 0.837. The lowest ranking related to the roll impact is meanwhile the lowest ranking overall. Even

worse, suppose that *metric(C)* less than 0.5 means low performances, and then all the low performances are caused by the roll impact.

- Thirdly, in regard to a particular $\alpha$ value, 0.01, 0.4, or 0.7, the metric values influenced by the pitch impact basically have higher rankings than the ones associated with the roll impact.

These three observations consistently show that *metric(C)* becomes smaller when the ship motion to be considered changes from pitch to roll. Here is the reason why roll motions induce undesirable transit outcomes. Due to the manually specified wave conditions, almost all the ideal $a_1$-directional decisions force the ship to go along beam seas, thus creating adverse roll amplitudes. As long as the roll impact is seriously considered, it will be the main contributor that deviates the ship away from the shortest trajectories. To be noticed, from rank 4 to 6, their metric values are still close to 1. These values mean that if the roll impact is not seriously considered, the ship can stay on the ideal trajectories.

| wave environment #2 | | | | |
|---|---|---|---|---|
| "head seas to shortest path" | | | | |
| ranking | *metric(C)* | ship motion | λ | α |
| 1 | 1 | roll | 180 | 0.01 |
| 2 | 1 | roll | 8 | 0.01 |
| 3 | 1 | roll | 4 | 0.01 |
| 4 | 0.983 | pitch | 90 | 0.01 |
| 5 | 0.983 | pitch | 3 | 0.01 |
| 6 | 0.983 | pitch | 1.5 | 0.01 |
| 7 | 0.610 | roll | 180 | 0.4 |
| 8 | 0.610 | roll | 8 | 0.4 |
| 9 | 0.604 | roll | 4 | 0.4 |
| 10 | 0.602 | pitch | 90 | 0.4 |
| 11 | 0.602 | pitch | 3 | 0.4 |
| 12 | 0.602 | pitch | 1.5 | 0.4 |
| 13 | 0.355 | pitch | 90 | 0.7 |
| 14 | 0.355 | pitch | 3 | 0.7 |
| 15 | 0.355 | pitch | 1.5 | 0.7 |
| 16 | 0.041 | roll | 180 | 0.7 |
| 17 | 0.041 | roll | 8 | 0.7 |
| 18 | 0.041 | roll | 4 | 0.7 |

Figure 5.7: Ranking different combinations of the seakeeping impact based on their associated *metric(C)* values (wave environment #2)

In general, Figure 5.7 looks different from Figure 5.6, and the differences existing in the two figures show that wave conditions do have an influence on the ship's reactions. The three aspects observed in Figure 5.6 are again the focus of this figure.

- The two colors do not present clear sequential patterns. The blue and orange colors occupy the bottom area of the figure together.

- *Metric(C)* ranges from 0.355 to 0.983 when the pitch motion influences the transit, and the range becomes 0.041 to 1 if the seakeeping consideration is the roll motion. Both pitch and roll motions can induce low *metric(C)* values, and the values smaller than 0.5 come from either pitch or roll impact.

- When $\alpha$ equals 0.7, *metric(C)* values are always lower than 0.5, which are influenced by the pitch or roll impact.

Therefore, the observations from Figure 5.7 also consistently support an inference. Both the pitch and roll motion can severely deviate the ship away from the ideal transit when it operates under the second group of wave conditions. The reason why pitch motions worsen the transit here is similar to why roll motions are problematic in the first environmental conditions. In short, there exist predictable difficulties in maintaining the ideal directions, which is to transit into the head seas and handle large pitch motions. This difficulty makes the pitch motion a concern to the transit. Additionally, the degree of impact that roll motions impose on the transit significantly depends on the value of $\alpha$. When $\alpha$ equals 0.01, *metric(C)* values based on the roll impact are even the highest. As $\alpha$ gets larger, roll motions start to affect the transit worse, and the undesirable *metric(C)* values gradually emerge. This finding is consistent with what has been discussed in Figure 5.5.

Parameter $\lambda$ is also a potential contributor, which can influence the transit outcomes. It controls the seakeeping impact on the ship's movements. Observe Figure 5.6 and 5.7 again, these two figures have not demonstrated all the digits but displayed

the ranking orders instead. The following tendency can be extracted. Given certain ship motion and $\alpha$ value, when $\lambda$ decreases, the ship is more likely to be impeded by certain motion amplitudes and fails in moving forward. Therefore *metric(C)* is also probable to decrease. However, the contribution of $\lambda$ to *metric(C)* variations cannot be identified until many fractional digits, meaning that it is not a contributor as significant as $\alpha$.

### 5.2.2 Underlying Context Explanation

Every $a_1$-directional decision generated by the GS-MDP framework has an underlying context about why it exists. Within the transit scenarios simulated in the framework, some of the directional decisions more or less present certain underlying contexts in common. Generally speaking, the underlying contexts can be categorized into three basic types. The first category includes the $a_1$-directional decisions that follow the ideal transit. The second category includes the ones that slightly deviate from the ideal transit. The last category covers the ones that severely deviate from the ideal transit and cause detours. This section uses the transit scenario shown in Figure 5.8 as an example, and explores the contexts of the $a_1$-directional decisions.

Figure 5.8 displays the $a_1$-directional decisions via black arrows. The top panel shows the simulation results of transiting to location "California" (230E,40N) with the consideration of pitch impact based on a $\lambda$ value of 1.5° and an $\alpha$ value of 0.7. The transit weather is what has been assumed in the second group of wave conditions. The bottom panel illustrates the corresponding ideal transit to the same destination.

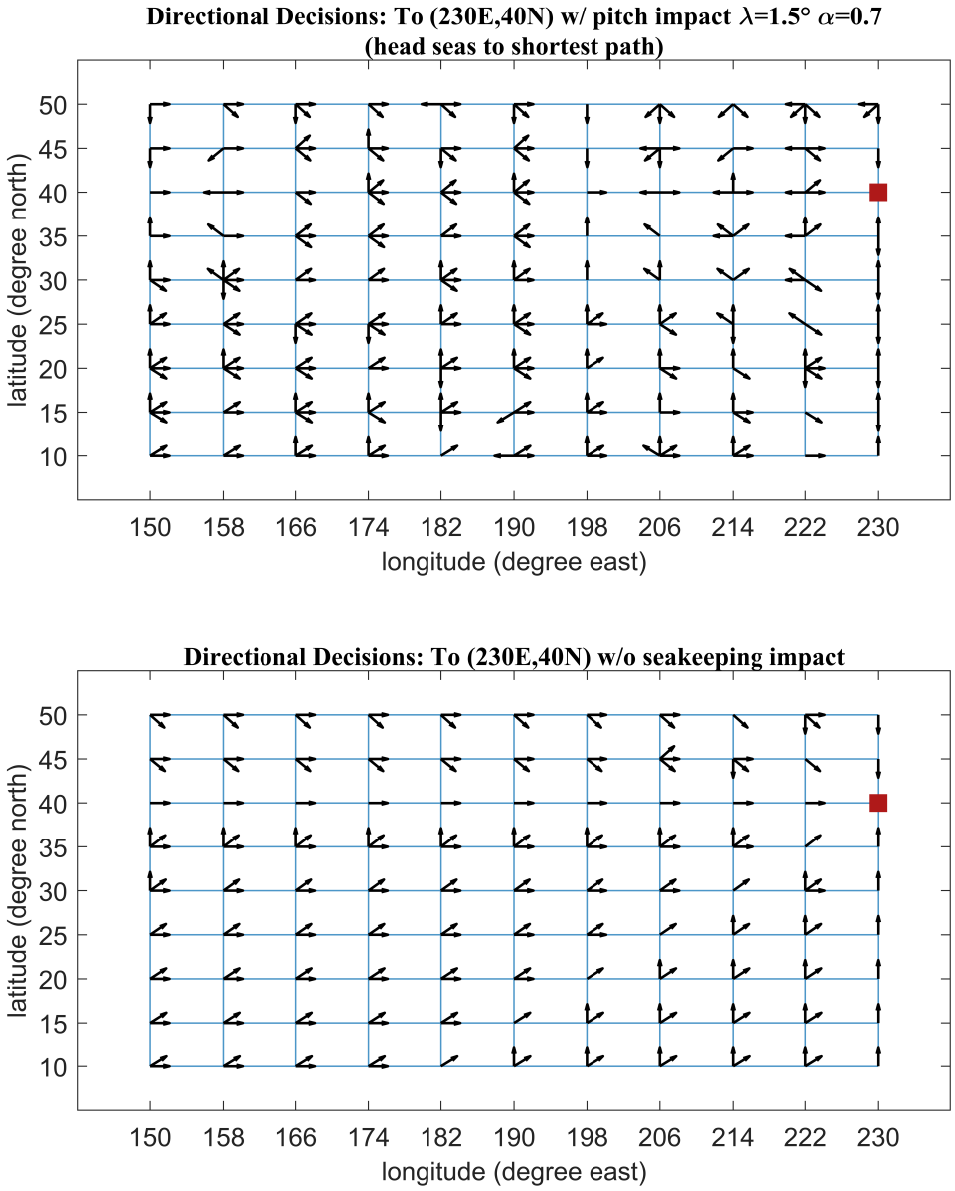


Figure 5.8: Simulation results of a transit scenario to (230E,40N), with pitch impact, $\lambda$=1.5°, $\alpha$=0.7, under the second group of wave environments & the simulation results to (230E,40N) without seakeeping impact

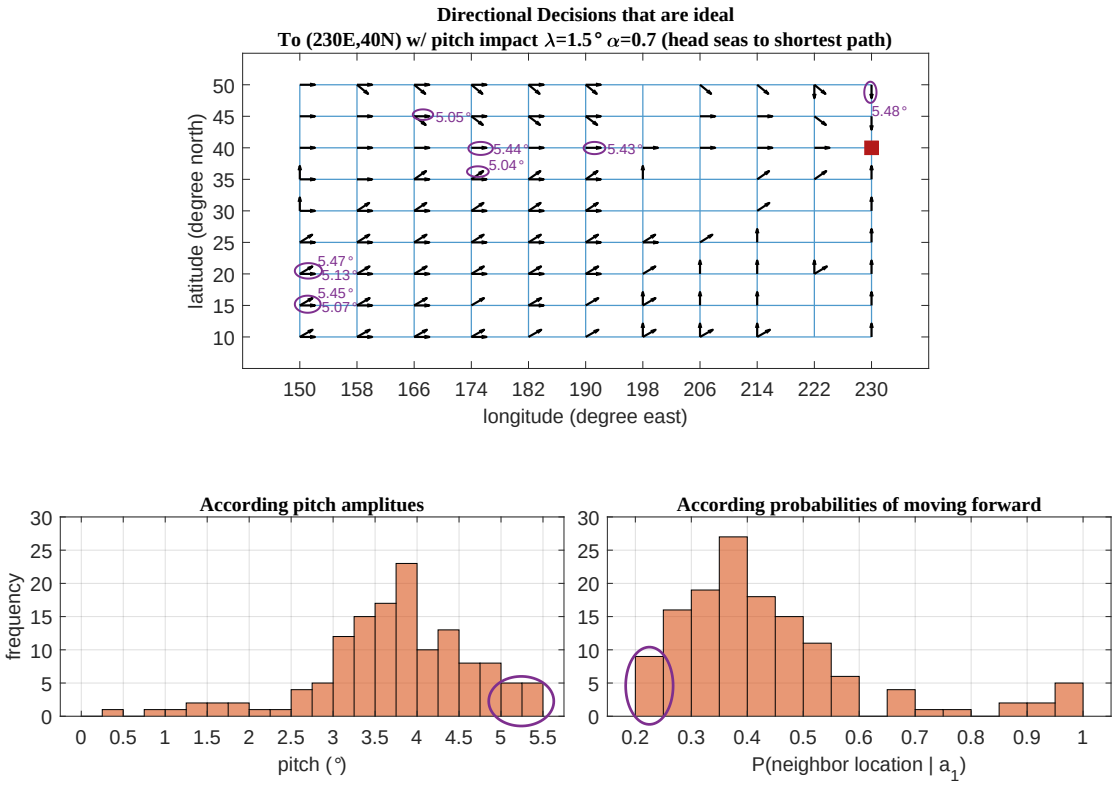


Figure 5.9: The first category: $a_1$-directional decisions that are ideal; and underlying context related to the first category: histograms of the according pitch amplitudes and transition probabilities

The $a_1$-directional decisions that are the same as the ideal transit can be collected together, and they belong to the first category. In this category, even though the pitch motions are undesirable, the motive of pursuing the shortest path still dominates the ship's actions. To be specific, Figure 5.9 demonstrates all these $a_1$-directional decisions, relevant pitch amplitudes, and according transition probabilities extracted from the MDP structure. The threshold value $\lambda$, which tends to constrain the pitch amplitudes along with the ship's movements, is set as 1.5°. However, the histogram of pitch amplitudes shows that most amplitude values distribute in the range from 2.5° to 5.5° and the peak frequency corresponds to the interval [3.75°, 4°]. These relatively large amplitudes thus lead to low transition probabilities of successfully accomplishing the movements. The according transition probabilities seldom get greater than 0.7.

The ship's movements that are activated by these $a_1$-directional decisions often just have a success rate of approximately 40%. As shown in Figure 5.9, there are nine instances with pitch motions larger than 5° and transition probabilities smaller than 0.25. Given the definitions within the GS-MDP framework, they can be regarded as possible reactions to adverse motion amplitudes. As long as the transition probability of moving forward is above zero, the framework will analyze and even determine the action of moving on. However, such underlying context illustrates that the ship indeed takes substantial risks to pursue ideal transit. For evaluating operational performances, designers may primarily focus on the number of $a_1$-directional decisions in this category. Nevertheless, it would be equally important to understand the risk behind these movements. This is a unique design insight enabled by the GS-MDP framework.

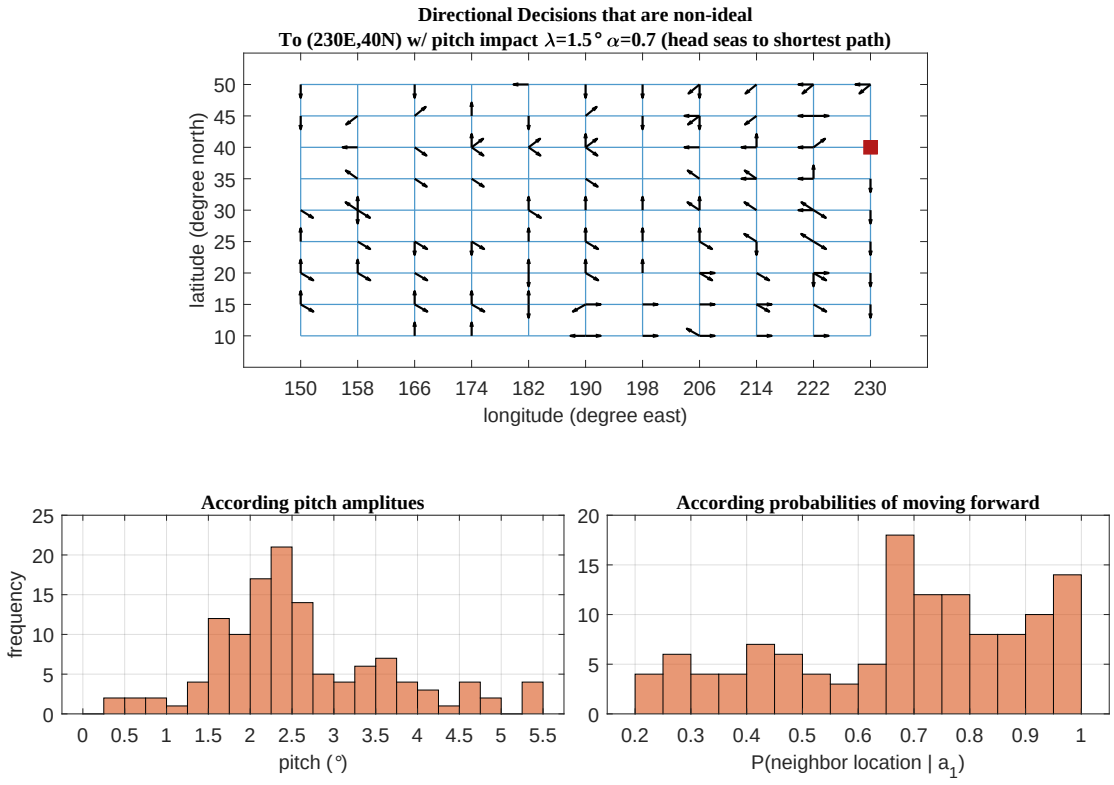


Figure 5.10: Underlying context of the non-ideal $a_1$-directional decisions: histograms of the according pitch amplitudes and transition probabilities

The next two categories of $a_1$-directional decisions center on the non-ideal ones. Before discussing each of them separately, their overall pitch amplitudes and transition probabilities of moving forward are summarized in Figure 5.10. By comparing the histograms in Figure 5.9 and 5.10, people can see the differences in the underlying contexts between the ideal and non-ideal $a_1$-directional decisions. As for the non-ideal ones, they are associated with relatively moderate pitch amplitudes, and the amplitude interval with the peak frequency now drifts to [2.25°, 2.5°], which becomes closer to the threshold value 1.5°. Additionally, the probabilities of successfully executing the movements are improved. In short, the non-ideal $a_1$-directional decisions aim to prevent sea transport from undesirable pitch motions. Meanwhile, some trade-offs, such as zigzags or detours, might be demonstrated on the transit trajectory. The two categories of non-ideal $a_1$-directional decisions are classified based on their different effect on the trajectory.

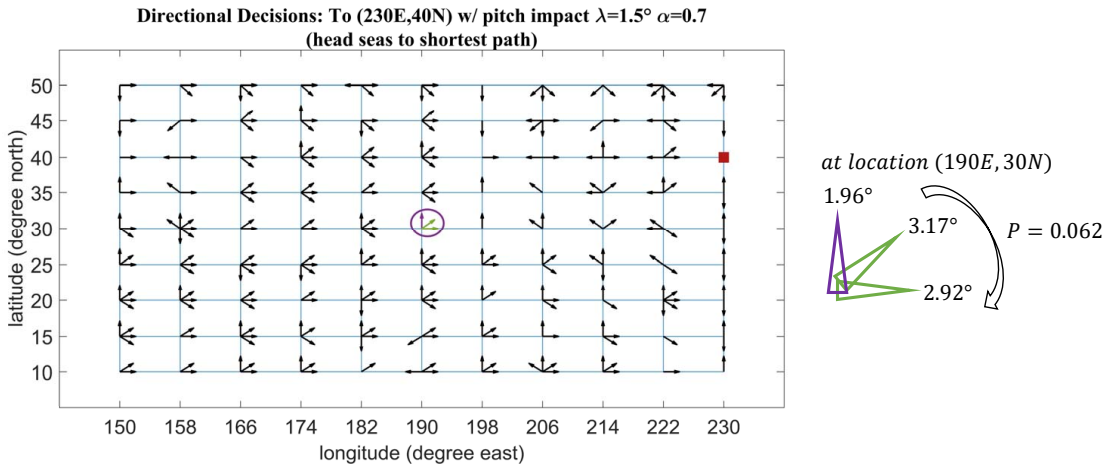


Figure 5.11: An example of $a_1$-directional decisions belonging to the second category

Some non-ideal $a_1$-directional decisions can still lead the ship closer to the destination. Even though they do not maintain the transit on the shortest trajectory, they still positively promote the transit without detours. These $a_1$-directional decisions are gathered in the second category. Figure 5.11 shows an example of them in a purple

arrow, which is an $a_1$-directional decision determined at location (190E,30N) toward the north. The other two green arrows are the ideal $a_1$-directional decisions that exist at this location. This example illustrates a typical situation of why such an $a_1$-directional decision can be selected. For one reason, its associated motion is relatively small to enable movement. Among the three $a_1$-directional decisions existing at the exemplified location, the smallest motion amplitude that they cause is actually 1.96°, which is associated with the non-ideal $a_1$-directional decision. For another reason, the adjustment to the ideal directions is relatively difficult. If the ship gives up the north direction, there will be only 6.2% of adjusting to the ideal directions. After balancing the efforts in the ship's movement and heading adjustment, an $a_1$-directional decision in the second group would be generated from the framework.

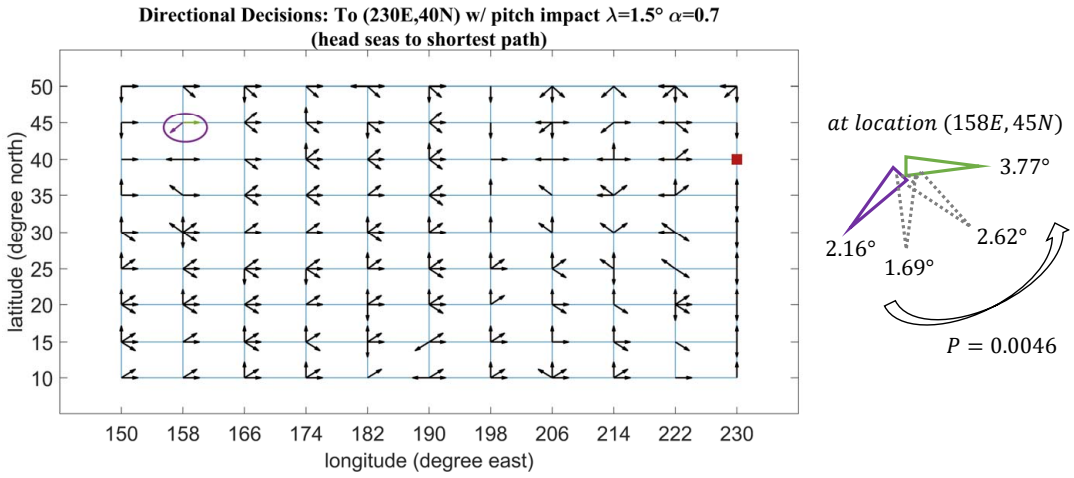


Figure 5.12: An example of $a_1$-directional decisions belonging to the third category

The last category contains the non-ideal $a_1$-directional decisions that make the ship farther away from the destination. Figure 5.12 uses a purple arrow to illustrate an exemplified $a_1$-directional decision belonging to the third category, which is at location (158E,45N) and approximately toward the southwest. The green arrow is an ideal $a_1$-directional decision that is also allowed at (158E,45N). The existence of the non-ideal $a_1$-directional decision at this location is mainly due to the difficulty in

adjusting the heading direction. To adjust from the non-ideal direction to the existing ideal direction, the pitch motions that the ship experiences change from 2.16°, 1.69°, 2.62° to 3.77°. Given that the ship is more willing to shift to heading directions related to smaller motions, most steps of this adjustment are difficult to achieve. Thus, the probability of making this adjustment is as low as 0.0046. As mentioned before in Section 5.2.1, $\alpha$ is an important contributor that influences the transit outcomes by incorporating seakeeping implications into the ship's heading adjustment. The underlying contexts of an $a_1$-directional decision discussed in this category support the previous findings of $\alpha$.

This section has illustrated three basic types of underlying contexts to explain why certain $a_1$-directional decisions exist. Additionally, the GS-MDP framework is based on the MDP structure, so the directional decisions are not generated from this framework in isolation. They may have dependencies with each other until a ship reaches the destination. Sometimes the underlying contexts and dynamics of certain directional decisions may not be as explicit as the examples shown in this section. However, it is still possible to make a reasonable exploration according to the three basic types of underlying contexts and the knowledge of the MDP structure. Meanwhile, understanding the causation relationships behind the $a_1$-directional decisions can improve the designer's ability to use the *COEM* metrics to evaluate a ship design.

### 5.2.3 Insights from *COEM* Metrics

An advantage of the operation ensemble is that designers can either use it as a whole or extract part of it for a particular analysis. As a demonstration, this section here concentrates on a part of the operation ensemble, which is with medium $\lambda$ and $\alpha$ values, and evaluates the *COEM* metrics for the extracted part. In terms of the roll motion, a medium level of impact means a $\lambda$ value of 8° and an $\alpha$ value of 0.4. As for the pitch motion, a medium level of impact means a $\lambda$ value of 3° and an $\alpha$ value of

0.4. After combining the two weather conditions, four transit scenarios are included to analyze different operational metrics, which are all summarized in Table 5.4.

Table 5.4: Summary of *COEM* metrics of four extracted transit scenarios

| | *metric(C)* | *metric(O)* | *metric(E)* | *metric(M)* |
|---|---|---|---|---|
| w/o seakeepping impact | 1 | 0.235 | 1 | 1 |
| wave environment #1 | | | | |
| roll | 0.435 | 0.385 | 0.858 | 0.803 |
| pitch | 0.911 | 0.225 | 0.992 | 0.993 |
| wave environment #2 | | | | |
| roll | 0.610 | 0.281 | 0.794 | 0.806 |
| pitch | 0.602 | 0.304 | 0.880 | 0.931 |

In this table, *metric(C)*, *metric(E)*, and *metric(M)* are the primary concerns to learn the operational potentials of a conceptual design. They can reflect the ideal degree, the positive degree, and the smooth degree of the ship's transit. Moreover, they have the same tendency of signifying poor potentials through small values. As for *metric(O)*, it describes the percent of $a_1$-directional decisions at a location and reflects the selections to promote the transit. The magnitude of this metric cannot signify desirable or undesirable potentials directly, but it can assist designers in inferring the underlying contexts of the transit when it is analyzed with other metrics together. Moreover, when there are conflicting observations among the other three metrics, *metric(O)* will be useful to provide explanations.

First of all, the results independent of the seakeeping impact are the idealized performances that designers expect the ship design to have. The values of *metric(C)*, *metric(E)*, and *metric(M)* all equal 1; *metric(O)* is 0.235. Thus there are on average $0.235 \times 8 = 1.88$ directions that allow the ship to move forward at a location. As long as it moves forward, it will always get closer to the destination along smooth trajectories.

When the seakeeping impact is incorporated, *metric(C)*, *metric(E)*, and *metric(M)*

all decrease. The minimum values of *metric(C)* and *metric(M)* are 0.435 and 0.803, which occur in the same transit scenario. Compared to the ideal scenario, this transit scenario demonstrates a large decrease in *metric(C)*, meaning that most $a_1$-directional decisions do not follow the ideal directions. Since the results of *metric(E)* and *metric(M)* are undesirable, designers can further identify the negative impact of roll motions. The roll motions cause many severe detours during the transit process.

Under the second group of wave conditions, some observations seem conflicting. The values of *metric(C)* with roll and pitch impact are similar, which are 0.610 and 0.602, and thus designers would expect *metric(E)* and *metric(M)* to be similar as well. However, these two metrics present different results. *Metric(E)* and *metric(M)* are higher for pitch than roll, indicating that the ship has better transit efficiency and easier course changes with regards to pitch. Then the designers would be interested in the reason why conflicting results occur in these three metrics. There are clues in *metric(O)*. It can be observed that *metric(O)* is higher for pitch. Designers can infer that the transit scenario with pitch impact involves more non-ideal $a_1$-directional decisions, which cause the *metric(C)* lower than the result with roll impact. In other words, when the transit is influenced by pitch motions, there are more available $a_1$-directional decisions, but they are not ideal. Thus transiting to the destination is easier than that with roll impact, but there are more deviations away from the ideal trajectories.

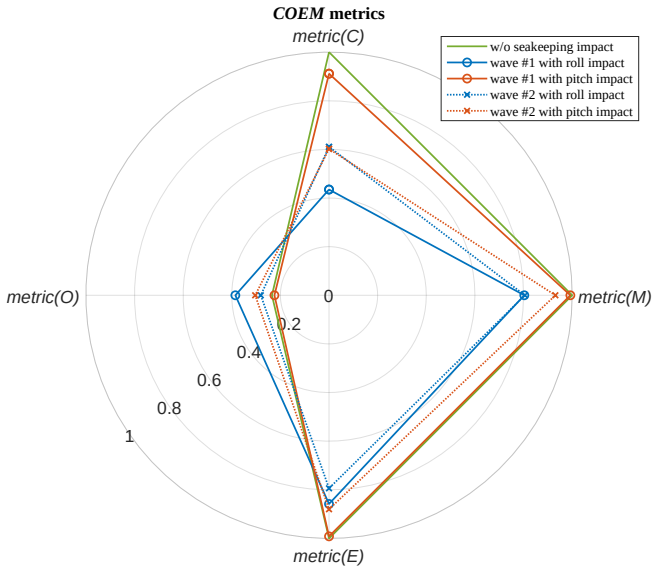


Figure 5.13: A graphical representation of the *COEM* metrics

For a convenient observation, the *COEM* metrics can be illustrated in a graph such as Figure 5.13. For each transit scenario, the values of the four metrics form a quadrilateral, and the right-side area is determined by *metric(C)*, *metric(E)*, and *metric(M)*. Larger areas of the right side correspond to better overall operational potentials. Designers can find that the areas related to the roll impact are smaller than those with the pitch impact, indicating that roll motions would be a major issue to be solved for this conceptual design. This finding is consistent with what has been discussed throughout this chapter, but it is intuitively convenient for the designers to use this figure and grasp the information. If only using one metric to evaluate the operational performances, *metric(C)* can be the representative. The variations in this metric for different scenarios are more recognizable than the other metrics, and the ranking order of this metric almost reflects how large the right-side area is. In short, this graphical representation concisely conveys reliable evaluation results, which can help designers condense critical knowledge for decision-making quickly.

## 5.3 Conclusions

This chapter has demonstrated the GS-MDP framework on a conceptual ship design that was faced with presumed weather challenges.

First, the results of this case study have supplemented an important aspect for appropriately utilizing the GS-MDP framework. The physical analysis codes influence the application of this framework. This case study chose the SPP tool to provide ship motion estimations. This tool adequately supported the incorporation of roll and pitch motions into the sea transport, but had some limitations in considering heave motions. However, the GS-MDP framework allows flexible modifications in connecting the MDP to any other physical analysis. Thus, such limitations can be addressed by finding the proper analysis for heave motions, which should be the continued work of this thesis.

Then, this case study has properly verified and validated the GS-MDP framework through the manually specified waves. According to the operation ensemble and a focus on *metric(C)*, the case results identified the ship motion contributors, which were the expected or explainable ones corresponding to the manually specified weather challenges. The mechanism of how ship motions influenced the movements and heading direction adjustments was analyzed based on an exploration of various $\lambda$ and $\alpha$ values. The insights obtained from this exploration may facilitate the selection of suitable $\lambda$ and $\alpha$ in the future use of this framework. Moreover, an in-depth analysis was carried out to investigate the contexts behind the metric values and the directional decisions. The data extraction, including motion amplitudes and transition probabilities for specific directional decisions, allowed the designers to know the detailed trade-offs among distinct disciplines. Finally, the evaluation of this ship design was expanded to all four metrics, and the *COEM* metrics generated knowledge for designers in an intuitively convenient way.

From the design perspective, the GS-MDP framework basically shows two advan-

tages. Firstly, it enables design knowledge layers and layers deeper, and its systematic pattern of looking for causation relationships through the operation ensemble can be reused for any other ship designs. Secondly, the metrics defined for this framework are reliable and convenient for designers to abstract an operational profile of a conceptual design.

# CHAPTER VI

# Case Study 2: Evaluating an Offshore Construction Vessel Design

Vessels specialized for marine operations, such as the Offshore Construction Vessel (OCV), are often unique designs made to perform specific operations, such as lifting, drilling, or towing. To ensure the implementation of these operations, researchers have developed criteria and methods to evaluate conceptual ship designs based on their on-site operational performances. However, the transit events between ports and offshore sites have been reduced in the current evaluation methods, which are indeed an important part of understanding the OCV designs. Thus, as stated by *Sandvik et al.* (2018), "including the influence of rough weather on transit could yield further insights of the overall performance of the OCV". Since the GS-MDP framework offers a thin abstraction of ship operations, both the on-site and transit events of a ship design can be modeled and highlighted in this framework. This chapter achieves the following three objectives and compares the GS-MDP framework with an existing evaluation method (*Sandvik et al.*, 2018).

- Applying the GS-MDP framework to the simulation of on-site operations;
- Reflecting weather challenges and susceptibility during marine operations;
- Exploring the effect of ship design parameters on operational performances.

## 6.1 Thin Abstraction Mapped to Different Ship Operations

As discussed in Chapter I, a framework established based on thinness "can be mapped onto several situations, all of which share the same relevant features, even if irrelevant features make them appear dissimilar" (*Folger and Turillo*, 1999). The way that the GS-MDP framework abstracts transit operations is to focus on if a ship stays on the anticipated trajectories or not. Broadly speaking, this abstraction of the transit can also be described as a ship maintaining or not maintaining the expected status for the operation. This is a common feature that most ship operations share. As for the on-site operations, thin abstractions focus on if a ship keeps stationary enough at a fixed location toward a fixed direction. The difference between the transit and on-site operations is that the former tracks the vessel's status over a certain ocean area while the latter cares about how the vessel's status changes through a certain time period. With the main definitions of $< \mathcal{S}, \mathcal{A}, \mathcal{P}, \mathcal{R} >$ unchanged, the GS-MDP framework can demonstrate both the transit and the on-site operations. The modeling process of transit events has been introduced previously, so this case study starts with explaining how the existing $< \mathcal{S}, \mathcal{A}, \mathcal{P}, \mathcal{R} >$ definitions stand for the on-site operations.

### 6.1.1 States

When the vessel performs lifting, drilling, or other tasks at the offshore engineering site, this case study assumes that it can change its heading direction but not its location. In other words, people can observe the vessel toward different directions at different time steps, but it will always be at the offshore engineering location. Thus, a state $s$ in the set $\mathcal{S}$ now becomes "a ship toward $\theta_i$ at a certain time step $t_k$". The determination of $\theta_i$ where $i$=1,2...,8 still relies on Equation (3.5). The time step $t_k$ depends on how a time period is assigned for the operational simulation. For example, a state could be "a ship toward $\theta_1$ at $t_1$", which is illustrated in yellow in Figure 6.1.

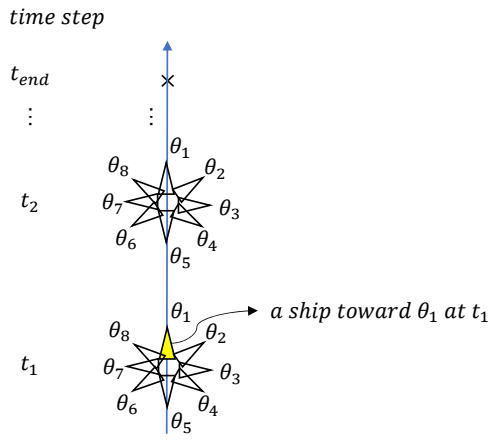


Figure 6.1: Modeling on-site operations, an exemplified state "a ship toward $\theta_1$ at $t_1$"

### 6.1.2 Actions

The actions previously defined for the ship were to move on or adjust the heading direction. Since the ship now conducts on-site operations at a fixed location, moving on is no longer a relevant action to change its status. Thus this case study refines the first action $a_1$ as maintaining the heading, and the second action $a_2$ is still adjusting the heading. No matter which action is executed, the ship will be at the next time step, but the ship's heading direction may have different changes depending on the action. The transitions related to $a_1$ or $a_2$ are described as follows and are concretely illustrated through an exemplified state in Figure 6.2.

- Action 1: If $a_1$ is executed at state $s$, namely "a ship toward $\theta_i$ at $t_k$", the ship will maintain its current heading direction $\theta_i$ until the next time step $t_{k+1}$. Thus, the next state $s'|s, a_1$ should be "a ship toward $\theta_i$ at $t_{k+1}$".

- Action 2: If $a_2$ is executed, the ship will possibly head any of the eight directions until the next time step $t_{k+1}$. Thus, the next state $s'|s, a_2$ would be "a ship toward $\theta_{j=1,2,...8}$ at $t_{k+1}$".

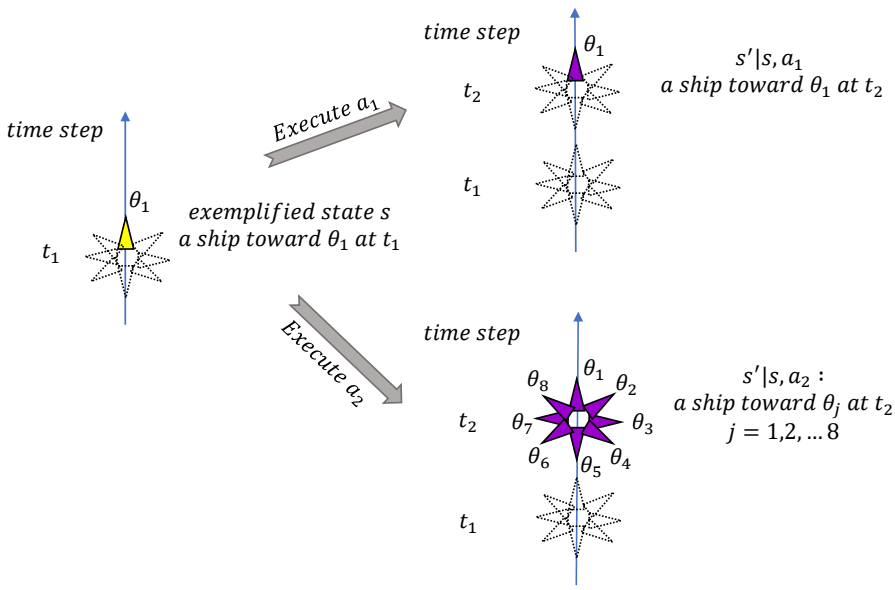


Figure 6.2: Modeling on-site operations, an illustration of the transitions caused by two different actions

### 6.1.3 Transition Probabilities

Calculating the probabilities of the transitions depicted in Figure 6.2 reuses most of the calculation process defined for the transit operations.

First, the only outcome of $a_1$ is to make the ship pose a certain heading direction unchanged until the next time step, and the time steps just sequentially proceed without any randomness. Due to this fact, $P(s'|s, a_1)$ should always have a deterministic value of 1. Equation (6.1) is shown as follows to emphasize that $P(s'|s, a_1)$ has a newly defined value for the on-site operations. Compared to the previous calculation of $P(s'|s, a_1)$, the determination here is actually a reduced version, which skips all the equations and parameters defined in Section 3.2.3. Knowing the value of $P(s'|s, a_1)$ becomes straightforward, but this value does not convey any seakeeping implications that were previously demonstrated by the parameter $\lambda$. It was a threshold value that represented the risk tolerance for a given ship motion. The previous intent of introducing $\lambda$ was to show how the ship's movements could be impeded when the

associated motion amplitudes were larger than $\lambda$. The on-site operations also need to model a similar intent. To be specific, the motion amplitude induced by a heading direction can impose difficulties in controlling the direction unchanged. This case study still uses parameter $\lambda$ to express this intent but finds it more appropriate to be added to rewards, which will be shown in the next section.

$$\begin{gathered} P(s'|s, a_1) = 1 \\ s = \text{“a ship toward } \theta_i \text{ at } t_k\text{”}, \quad s' = \text{“a ship toward } \theta_i \text{ at } t_{k+1}\text{”} \end{gathered} \tag{6.1}$$

Second, the outcomes of $a_2$ created by the on-site operations involve one focus on the time step and another on the ship's heading direction. As mentioned above, the changes in the time step are natural and deterministic, such as from $t_1$ to $t_2$, from $t_2$ to $t_3$, and so on, which do not influence the determination of transition probabilities. Thus, analyzing which direction the ship may shift to becomes the only focus of calculating $P(s'|s, a_2)$. This calculation follows the same mechanism of "adjusting heading directions based on relative variations of the ship motions", which has been established in Section 3.2.3. Designers can refer to the equations developed for this mechanism. They can then figure out how different adjustment outcomes and the corresponding probabilities occur at a location when the ship decides to adjust its heading direction. Moreover, the parameter $\alpha$ embedded in the calculation of $P(s'|s, a_2)$ still controls the level of seakeeping impact on the adjustment of heading directions.

### 6.1.4 Rewards

If the ship selects $a_1$, which is to maintain its heading direction at a time step, it needs to handle the difficulties caused by ship motions to ensure the direction unchanged. As a representation of the ability to maintain the heading direction, parameter $\lambda$ and its underlying intent can be applied here to determine a value for

$R(s'|s, a_1)$. Specifically speaking, when a given ship motion exceeds the value of $\lambda$, the ship has to overcome seakeeping difficulties and maintain the heading direction unchanged under such circumstances. This case study modifies Equation (3.7), which calculates the likelihood of these circumstances based on the threshold value $\lambda$, and converts the likelihood to a negative value. Then the $R(s'|s, a_1)$ for on-site operations can be redefined as follows. Equation (6.2) shows that larger motions will cause worse values of $R(s'|s, a_1)$. Additionally, $\lambda$ and $RMS$ in Equation (6.2) are the same as what they mean in Equation (3.7).

$$\begin{gathered} R(s'|s, a_1) = -exp(-\frac{\lambda^2}{2 \times RMS^2}) \\ s = \text{“}a\ ship\ toward\ \theta_i\ at\ t_k\text{”}, \quad s' = \text{“}a\ ship\ toward\ \theta_i\ at\ t_{k+1}\text{”} \end{gathered} \tag{6.2}$$

When the ship selects $a_2$, which is to adjust its heading direction, Equation (3.17) is totally suitable to calculate $R(s'|s, a_2)$. What this equation expresses for the on-site operations is that larger angles cause worse $R(s'|s, a_2)$ values.

### 6.1.5 *Metric(W)* for Evaluating On-site Operations

After updating the states, actions, transition probabilities, and rewards, it is feasible for designers to use the GS-MDP framework and simulate a scenario of the on-site operations at an engineering location over a time period. At a certain state $s$ “a ship toward $\theta_i$ at $t_k$”, the output from the MDP structure is $\pi(s)$, which optimizes whether $\theta_i$ is maintained or adjusted at time step $t_k$. In this case study, $\pi(s)$ and $\pi(\theta_i, t_k)$ will be used interchangeably and denote the same meaning. Suppose that the ship should keep stationary to support the on-site operational tasks. When the optimal action is $a_1$, the ship can be regarded as stationary. However, an optional action of $a_2$ indicates that the ship is not in a stationary status. For the convenience of evaluating on-site performances, this case study further assumes that the ship keeps working when $\pi(\theta_i, t_k)$ equals $a_1$, while not working if $\pi(\theta_i, t_k)$ equals $a_2$. Therefore,

designers can focus on each of the 8 heading directions and observe how often a certain direction is maintained, so that they can evaluate the ship's on-site operational potentials. To this end, this case study newly develops a metric called *metric(W)* to quantify the percent of working status to the overall time period. In Equation (6.3), $N$ represents the end step of the time period, thus leading to $N$-1 intervals, and $\theta$ is the heading direction to be observed, which should be one of $\theta_{i=1,2,...8}$.

$$metric(W) = \frac{|\{t_k : \pi(\theta, t_k) = a_1,\ t_1 \leq t_k < t_N\}|}{N-1}$$
$$0 \leq metric(W) \leq 1 \tag{6.3}$$

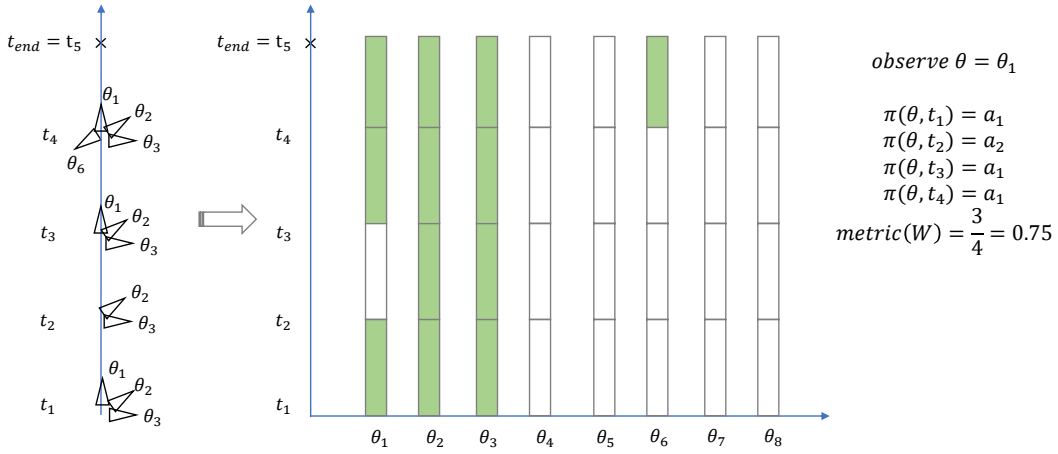


| $\theta$ | $\theta_1$ | $\theta_2$ | $\theta_3$ | $\theta_4$ | $\theta_5$ | $\theta_6$ | $\theta_7$ | $\theta_8$ |
|---|---|---|---|---|---|---|---|---|
| $metric(W)$ | 0.75 | 1 | 1 | 0 | 0 | 0.25 | 0 | 0 |

Figure 6.3: An example of calculating *metric(W)*

Figure 6.3 shows an example of the outputs for an on-site scenario, which includes $N$=5 time steps and $N$-1=5-1=4 time intervals in total. During this period, the working status of the ship associated with all 8 heading directions is expanded on the right side. For instance, when observing $\theta_1$, this direction is not maintained only in one interval from $t_2$ to $t_3$, so the corresponding *metric(W)* is 0.75. In addition, larger values of *metric(W)* reflect longer working status and more desirable on-site

performances. The heading directions associated with larger *metric(W)* values are more suitable to conduct operational tasks.

Similar to the other metrics defined within the GS-MDP framework, the evaluation of *metric(W)* also depends on an operation ensemble, which should cover a variety of on-site scenarios. The four operational setups that define the on-site scenarios are the engineering locations, weather conditions, $\lambda$ values, and $\alpha$ values. Based on adequate combinations of these setups, designers can again analyze *metric(W)* through reliable statistics.

Until now, the GS-MDP framework has finished the modeling of the on-site operations with the same definitions of $< \mathcal{S}, \mathcal{A}, \mathcal{P}, \mathcal{R} >$ applied to transit operations. During the modeling process above, there are some changes in the literal descriptions of how the defined $\mathcal{S}$ and $\mathcal{A}$ translate specific operations, and some modifications in the values of $\mathcal{P}$ and $\mathcal{R}$. Nevertheless, the mathematical representations of the two operations are the same in the GS-MDP framework.

## 6.2 Case Setups

This case study originated from an existing assessment of a conceptual OCV design that was expected to conduct on-site operations in the Norwegian Sea (*Sandvik et al.*, 2018). In the reference paper, *Sandvik et al.* (2018) used discrete-event simulations to evaluate the OCV design. They focused on the on-site operational evaluations but reduced the transit considerations. The reference paper incorporated physics only in the on-site simulations, while the GS-MDP framework can consider physics in both transit and on-site simulations. The basic setups of this case study are similar to the reference paper, so that it is reasonable to compare the results between the GS-MDP framework and the existing assessment of the OCV design. This case study can help the designers understand how the GS-MDP framework enables thin abstractions of ship operations and provides useful evaluations of a vessel design.

Table 6.1: Main hull parameters of a conceptual OCV design

| Parameter | Value |
|---|---|
| Hull length, L(m) | 120 |
| Beam, B(m) | 24.3 |
| Draft, T(m) | 7.5 |
| Block coefficient, $C_B$ | 0.755 |
| Displacement, $\nabla$ (tonne) | 15334 |

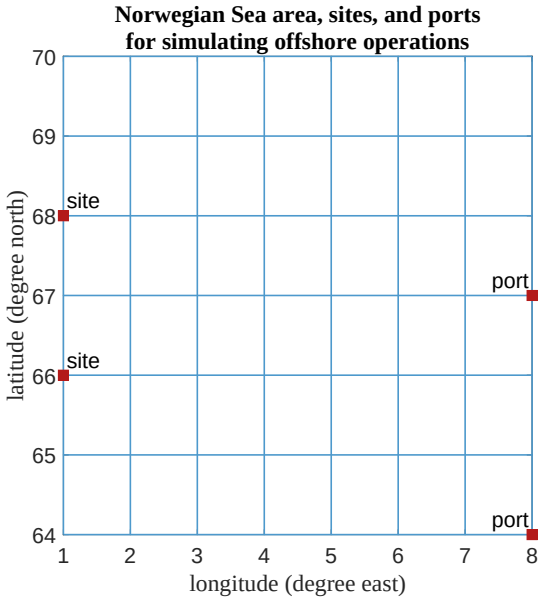


Figure 6.4: Ocean grid for the offshore operations

Table 6.1 demonstrates the main hull parameters of this conceptual OCV design. The design speed of this vessel is 12 knots. This case study generated the ocean grid with a focus on the Haltenbanken area, which was the site for operations mentioned in the reference paper. The ocean grid in Figure 6.4 represents the area for offshore operations, with a longitude range from 1E to 8E and a latitude range from 64N to 70N; the resolutions along the longitude and latitude are both 1 degree. For the completion of offshore operations, the ship first needs to transit across the prescribed ocean area between ports and offshore engineering sites, and then stay at the on-site

locations to execute the operational tasks. The GS-MDP framework can simulate and evaluate the transit and on-site operations separately. Moreover, if an overall operational evaluation is needed, the separate analyses of different operations can be combined together.

### 6.2.1 Transit Operations

Destinations, weather conditions, $\lambda$ values, and $\alpha$ values determine the transit scenarios to be simulated and gathered in the operation ensemble.

Firstly, this case study designated two locations near the coastline as ports and two locations away from the continent as offshore engineering sites. As shown in Figure 6.4, all these four locations, namely (8E,64N), (8E,67N), (1E,66N), and (1E,68N), served as the destinations of the transit.

Secondly, to embody various weather conditions, monthly wave data in the year 2010 was extracted from the European Center for Medium-Range Weather Forecasts (*ECMWF*, 2010) and assigned to transit simulations. For example, Figure 6.5 demonstrates the significant wave height, mean wave period, and mean wave direction over the specified ocean area in January. Additionally, the other months also presented their wave conditions. In general, at the beginning of a year, such as January and February, the wave conditions were relatively severe due to the winter season. Then the wave conditions became relatively mild during spring and summer and got severe again approximately from September to December.

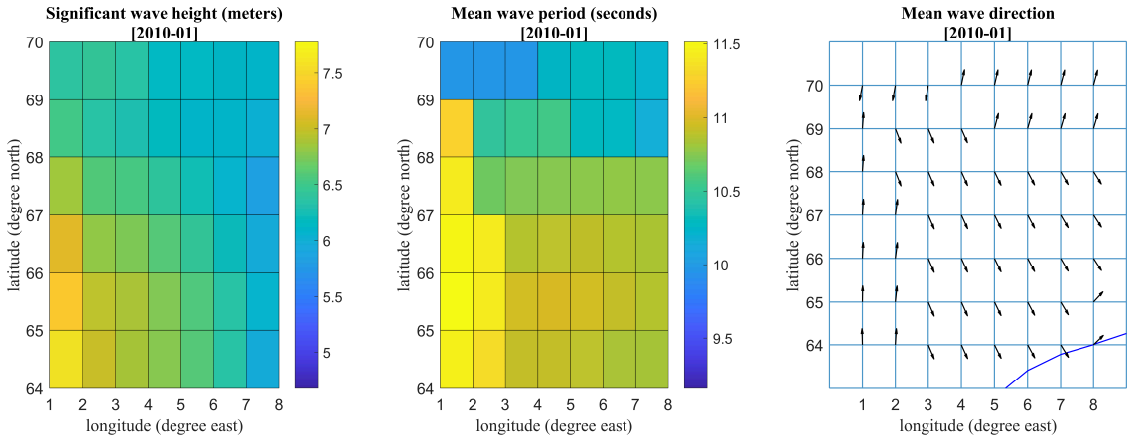


Figure 6.5: Wave conditions in January 2010 based on a public dataset (*ECMWF*, 2010)

In terms of seakeeping considerations, the SPP tool was used again. However, the previous case study in Chapter V has found that there might be some limitations of using the SPP for heave motions. Thus this case study kept the focus just on roll and pitch motions. Relevant $\lambda$ and $\alpha$ values for these two motions are listed in Table 6.2. They were derived from the operational criteria specified for Significant Single Amplitude (SSA) of roll and pitch (*Ghaemi and Olszewski*, 2017). Moreover, these combinations of $\lambda$ and $\alpha$ have already been tested in the previous case study and shown effectiveness to impose seakeeping impact on the ship's transit.

Table 6.2: $\lambda$ and $\alpha$ values for transit simulations

| Ship motion | $\lambda$ | $\alpha$ |
|---|---|---|
| roll | 8° | 0.4 |
| pitch | 3° | 0.4 |

### 6.2.2 On-site Operations

The parameters that modify the on-site scenarios are the offshore engineering sites, weather conditions, $\lambda$ values, and $\alpha$ values. The specification of offshore engi-

neering sites has some connections with the transit destinations, while the other three parameters are independent of the transit scenarios. Weather conditions describe the wave variations at an on-site location during a time period; $\lambda$ and $\alpha$ values should be consistent with the on-site operational requirements. In addition, the speed of the vessel should be 0 when simulating on-site operations.

Firstly, as mentioned in Section 6.2.1, (1E,66N) and (1E,68N) were selected as two offshore engineering sites. Thus all the on-site simulations centered on these two locations.

Secondly, this case study assumed that each on-site scenario would last for a whole day, starting from 0 o'clock and ending at 21 o'clock. Meanwhile, according to the data availability of ECMWF, the wave variations at an on-site location were obtained based on a temporal increment of 3 hours. In other words, the time period to be simulated included 8 time steps and 7 intervals within a day, and each time step was related to certain wave data. Moreover, wave data from multiple days was extracted to enrich the weather conditions for on-site simulations. This case study selected six days for each month and regarded the wave data from these days as a representation of the monthly on-site weather conditions. Figure 6.6 is an example of the on-site weather conditions in January, occurring at location (1E,66N).

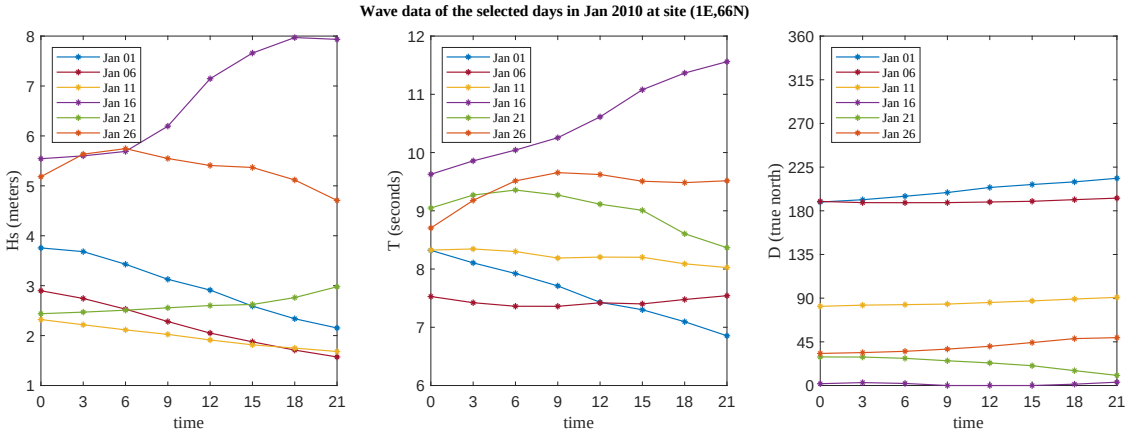


Figure 6.6: On-site wave conditions in January at location (1E,66N)

Table 6.3: $\lambda$ and $\alpha$ values for on-site simulations

| Ship motion | $\lambda$ | $\alpha$ |
|---|---|---|
| roll | 2° | 0.4 |
| pitch | 1.2° | 0.4 |

Finally, $\lambda$ and $\alpha$ values for the on-site simulations are listed in Table 6.3. The determination of the $\lambda$ values is explained as follows. In the reference paper that evaluated the OCV design, researchers had exploited limiting criteria that concentrated on the RMS of motion amplitudes. The RMS limit was set as 1° for roll and 0.6° for pitch. According to the assumption that ship motion amplitudes follow the Rayleigh distribution (*Molland*, 2008), the RMS value represents the amplitude with the highest frequency. However, it may not be an appropriate threshold to identify where the majority distributes. The SSA value, which should be twice as large as the RMS, can better signify the majority of motion amplitudes. To be specific, when the RMS limit was set as 1° or 0.6°, it implied the majority of motion amplitudes under 2° or 1.2°. Thus, this framework defined the $\lambda$ values as 2° for roll and 1.2° for pitch. Then the limits on the ship motions were maintained similar to the reference paper.

## 6.3 Case Results

Before demonstrating the results obtained from this case study, it is helpful to briefly review the three operational metrics that were used in the reference paper to assess the OCV design. As such, designers can refer to the results in the reference paper and build a robust understanding of the design insights that the GS-MDP framework can provide.

- %OP: percentage operability, "the percentage of time during which the ship is operational (*Fonseca and Guedes Soares*, 2002)".

- IOF: integrated operability factor, "a quantification of response-based operability of offshore vessels (*Sandvik et al.*, 2018)", which can be calculated based on %OP.

- RRO: "the ratio between the number of performed operations and feasible number operations (*Sandvik et al.*, 2018)", which can be regarded as a generalized version of %OP that includes weather window requirements.

The only thing that designers need to know about these metrics is that larger values represent more desirable operational performances.

### 6.3.1 On-site Operational Evaluations

In the GS-MDP framework, *metric(W)* is the metric used to evaluate on-site operations. Table 6.4 generally compares the results of *metric(W)* and the other three metrics for the presented OCV design.

Table 6.4: Comparison of *metric(W)* and other metrics (%OP, IOF, and RRO) that are from the reference paper

| | *metric(W)* | %OP | IOF | RRO |
|---|---|---|---|---|
| roll | 0.842 | 0.633 | 0.362 | 0.809 |
| pitch | 0.553 | 0.205 | 0.086 | 0.369 |

- The calculation of *metric(W)* is based on the operation ensemble that contains various on-site scenarios. When the roll impact is considered, *metric(W)* equals 0.842, which is a value close to 1. However, when incorporating the pitch impact, *metric(W)* is as small as 0.533, meaning that pitch motions negatively influence the on-site performances. Thus, compared to roll motions, pitch motions are the main contributor to poor performances when the ship is working at the offshore sites.

- The values of the %OP, IOF, and RRO are directly extracted from the paper that previously assessed this OCV design. These three metrics also show that pitch motions lead to smaller values than roll motions, meaning that the impact of pitch is worse than roll.

Based on all four metrics, they consistently identify pitch motions as the main issue of on-site operations for this OCV design. This observation suggests that it is suitable to apply *metric(W)* from the GS-MDP framework to the on-site evaluations.

In addition to the overall *metric(W)* values listed in Table 6.4 above, the design data can also expose the *metric(W)* variations based on different seasons. To convert the monthly data to seasonal variations, March, April, and May are gathered together to represent spring season; June, July, and August together represent summer; September, October, and November correspond to fall; the remaining months are in the winter season. Figure 6.7 demonstrates the seasonal variations in *metric(W)* under the impact of either roll or pitch motions. This figure can help designers analyze weather challenges and susceptibility that the vessel design may encounter during the on-site period.

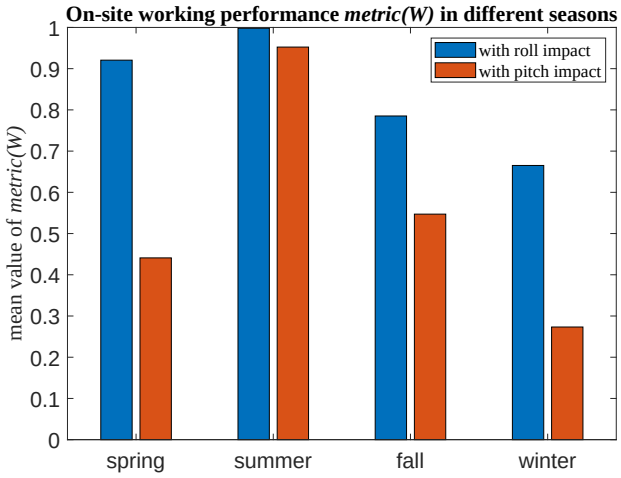


Figure 6.7: The variations of *metric(W)* based on different seasons

First, in all four seasons, *metric(W)* with pitch impact is always lower than that

with roll impact. This observation confirms that pitch motions are the main issue.

Second, *metric(W)* follows the intuition of seasonal weather conditions. The maximum occurs in summer, the time of the year when weather conditions are mild. When fall and winter come, the weather gets severe, and *metric(W)* decreases.

- With roll impact: *metric(W)* is not susceptible to weather changes. While the general tendency of *metric(W)* is what has been described above, the differences in *metric(W)* values between different seasons are not obvious. To be specific, the maximum is 1, and the minimum is still greater than 0.6. Hence, the biggest difference does not exceed 0.4, which is incurred by the extreme weather conditions in summer and winter.

- With pitch impact: *metric(W)* is susceptible to weather changes. The value of *metric(W)* in summer is almost 1, indicating that pitch motions no longer worsen the execution of on-site tasks. However, once the weather conditions are not as desirable as summer, *metric(W)* decreases below 0.5, and the lowest value is approximately 0.3.

Moreover, since the operation ensemble that enables the calculation of *metric(W)* covers all the heading directions, the magnitude of *metric(W)* can reflect weather susceptibility from a unique perspective.

- When the *metric(W)* value is close to 1, the on-site operations can proceed independent of the ship's heading direction. It also implies that weather challenges do not exist because the weather does not impact the determination of suitable heading directions. For example, on-site operations in summer with roll or pitch impact belong to this situation.

- When the *metric(W)* decreases and gets smaller than 1, it indicates that fewer heading directions can support the on-site operations, and more interruptions

occur during the operational process. Even worse, there are also circumstances where *metric(W)*is close to 0, signifying the emergence of great weather challenges. The ship's relative heading angles against the wave must be appropriately managed. Specifically, designers need to delve into the results of *metric(W)* in winter.

The next step of analysis further exploits the advantage of the operation ensemble and evaluates the on-site performances based on the ship's relative heading angles against the wave. Figure 6.8 illustrates the variations in *metric(W)* based on different relative heading angles in each season given roll or pitch impact. The relative heading angle is a continuous variable, and for convenience, it is represented by 18 equally distributed intervals in this figure. Each square of this figure is the average of the *metric(W)* values that have the same seakeeping impact, season, and relative heading angle. The squares with *metric(W)* greater than 0.8 are highlighted as a demonstration of desirable on-site performances. The 8 rows concretely show how *metric(W)* changes according to different relative heading angles. Based on this figure, designers are able to uncover the implications from the perspective of thin abstractions.

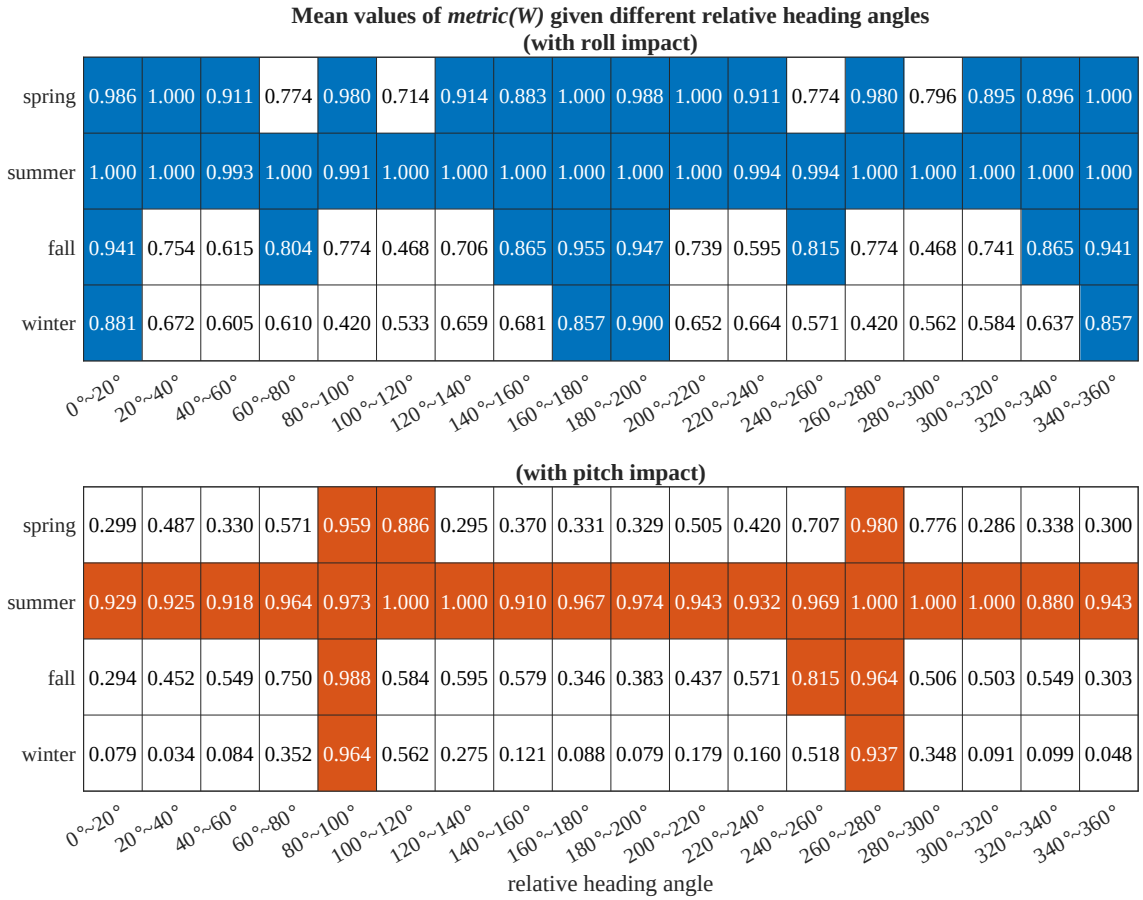


Figure 6.8: The variations of *metric(W)* based on different seasons and different relative heading angles

First of all, what Figure 6.8 demonstrates is consistent with the aforementioned findings. When *metric(W)* is expanded under the roll impact, more than half of the squares show values greater than 0.8. However, there are fewer highlighted squares when *metric(W)* is expanded under the pitch impact. Comparing the number of highlighted squares demonstrates that pitch motions more often create challenges for on-site operations. Additionally, the mild weather in summer allows the ship to conduct operations toward all relative heading angles, while the on-site performances are sensitive to the relative heading angles in other seasons.

Furthermore, Figure 6.8 can further help designers to identify the relative heading angles that should be preferred or avoided under different considerations of seakeeping

impact.

- With roll impact: The relative heading angles from the intervals of 0° to 20°, 160° to 200°, and 340° to 360° are helpful for the completion of on-site operations in all the seasons. In fall, the relative heading angles ranging from 100° to 120° and from 280° to 300° need to be avoided. The range of unsuitable relative heading angles enlarges in winter.

- With pitch impact: Except for summer, the other seasons seem to demonstrate limited ranges of suitable relative heading angles, which are from 80° to 100° and from 260° to 280°.

- With roll and pitch impact: This figure enables the designers to analyze roll and pitch impact together and understand their trade-offs. In winter, it is hard to alleviate the roll and pitch impact simultaneously. For example, if the relative heading angles are selected to handle roll impact, such as 0° to 20°, the ship will be severely influenced by pitch motions, leading to a *metric(W)* value as low as 0.079. Then, for relative heading angles between 100° to 120°, *metric(W)* values in winter with different seakeeping impact are around 0.5, which are both somewhat undesirable. It can be inferred that if the roll and pitch motions are coupled, the on-site performances associated with such relative heading angles may be substantially worse or better.

In general, the GS-MDP framework creates thin abstractions that enable new design insights. Most of the design insights above have not been achieved from the thick abstractions in the reference paper. The *metric(W)*, its associated variations, and relevant factors behind this metric serve as leading indicators to help designers understand the on-site operational performances.

### 6.3.2 Integrated Operational Evaluations

The transit operations between the sites and ports are also simulated by the GS-MDP framework. The evaluations mentioned in Chapter V can all be applied depending on the need. In this case study *metric(C)* is used as a representative to exhibit transit performances. The integrated operational performances of this OCV design are defined as a combination of *metric(C)* and *metric(W)*, which are shown in Table 6.5.

Table 6.5: Integrated operational performances based on *metric(C)* and *metric(W)*

| | *metric(C)+metric(W)* | *metric(C)* | *metric(W)* |
|---|---|---|---|
| roll | 1.276 | 0.434 | 0.842 |
| pitch | 1.196 | 0.642 | 0.553 |

According to Table 6.5, the metric values of the integrated operational performances show that pitch motions impose more negative influence than roll motions overall. However, the small difference in 1.196 and 1.276 makes it hard to identify pitch motions as the only issue. Roll motions should also be regarded as a main contributor to the undesirable integrated performances. As shown above, *metric(C)* equaling 0.434 indicates that the roll impact is severe and adverse during the transit across the sea. Moreover, a deeper understanding of the roll impact can be obtained through the seasonal variations of *metric(C)*.

Figure 6.9 contains a demonstration of how *metric(C)* varies in different seasons. *Metric(C)* is not sensitive to weather conditions. The values of *metric(C)* with pitch impact are approximately 0.6, and the values with roll impact are approximately 0.4. In addition, *metric(C)* values influenced by the roll motions are always lower in all four seasons. Thus it is noticeable that roll motions are the major cause of deviating the vessel away from ideal transit trajectories. If designers need to investigate the

underlying contexts of the transit outcomes, they can apply the analysis procedures that have been examined in Chapter V.

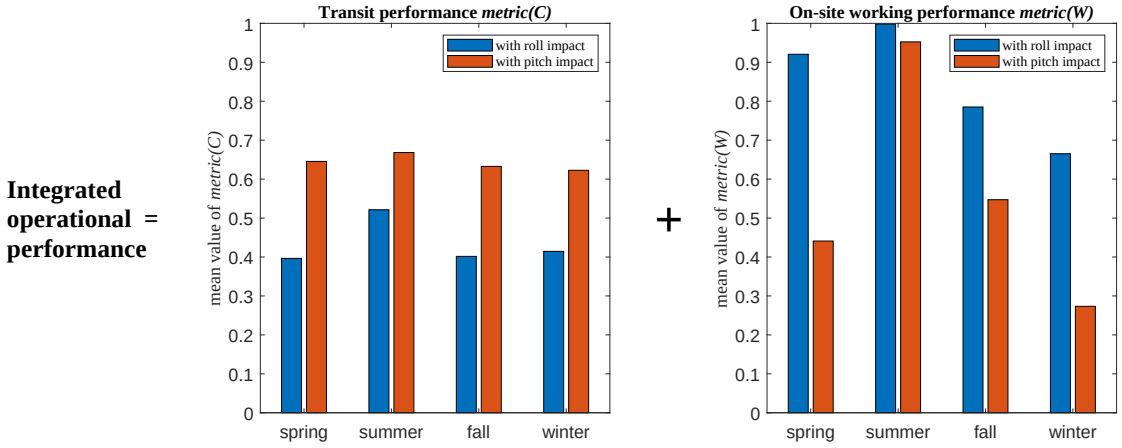


Figure 6.9: Seasonal variations of *metric(C)* and *metric(W)*

Table 6.6: Seasonal variations of *metric(C)*+*metric(W)*

| | spring | summer | fall | winter |
|---|---|---|---|---|
| roll | 1.317 | 1.519 | 1.187 | 1.080 |
| pitch | 1.086 | 1.621 | 1.180 | 0.896 |

Another purpose of putting Figure 6.9 here is to help designers review the seasonal variations of *metric(C)* and *metric(W)* separately before combining them together. Table 6.6 exhibits the values of the integrated operational performance in different seasons. The best value of the integrated operational performance is 2. Except for the values in summer, most of the values in the other seasons are just near 1. Generally speaking, this vessel is somewhat far from the idealized performances. Improvements should focus on alleviating the roll motion amplitudes during the transit and mitigating the pitch motion amplitudes during the on-site operating process. To be noticed, such design insights cannot be attainable without the GS-MDP framework, which

offers the evaluations of both transit and on-site operations based on *metric(C)* and *metric(W)*.

As the last analysis, this case study referred to the data from (*Sandvik et al.*, 2018; *Gutsch et al.*, 2020), which homogeneously scaled the hull geometry of this OCV vessel, and carried out a parametric design variation in ship length. The main particulars of the parametric designs are presented in Table 6.7.

Table 6.7: Scale the hull geometry based on ship length

| Parameter | baseline | | | | |
|---|---|---|---|---|---|
| Hull length, L(m) | 80 | 100 | 120 | 140 | 160 |
| Beam, B(m) | 18.3 | 21.4 | 24.3 | 27.3 | 30.4 |
| Draft, T(m) | 7.5 | 7.5 | 7.5 | 7.5 | 7.5 |
| Block coefficient, $C_B$ | 0.755 | 0.755 | 0.755 | 0.755 | 0.755 |
| Displacement, $\nabla$ (tonne) | 7699 | 11253 | 15334 | 20833 | 25575 |

Figure 6.10 shows the integrated operational performances, transit performances, and on-site performances for all parametric designs in different seasons. The metric values with roll and pitch impact are both illustrated. As expected, the results in fall and winter reflect more challenging conditions to improve the vessel's operational performances than spring and summer. The detailed observations are as follows.

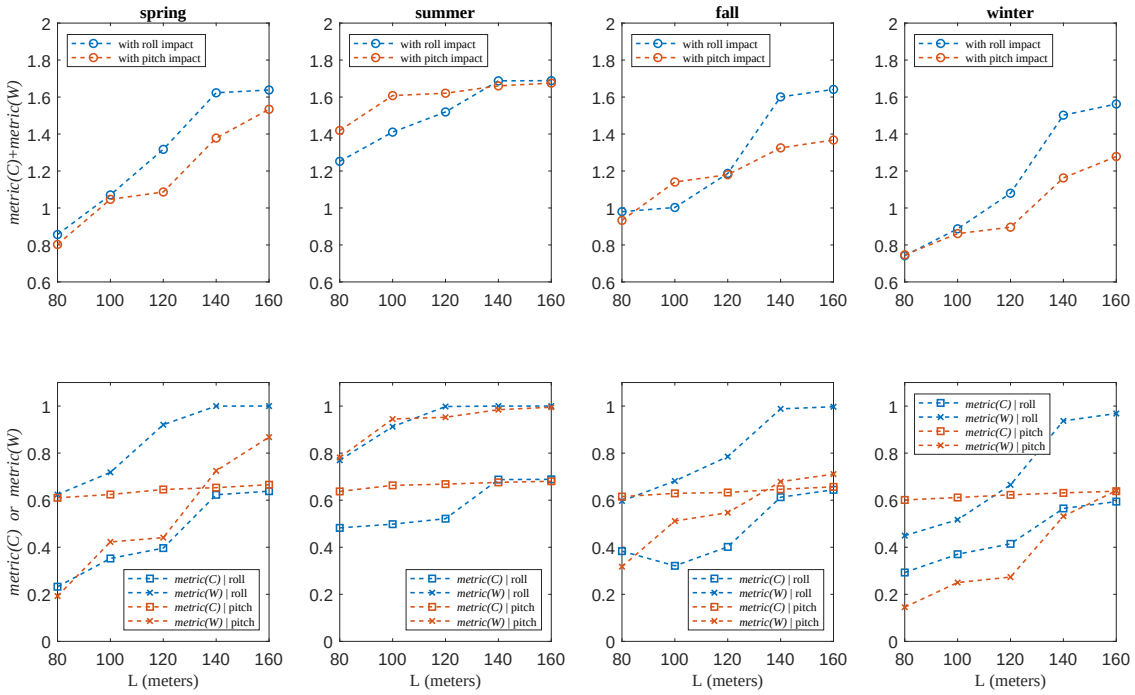


Figure 6.10: Results of the operational performances for all parametric designs in different seasons

- As the ship length increases, *metric(C)+metric(W)*, *metric(C)*, and *metric(W)* basically all become larger, indicating better operational performances. The maximum value of the integrated operational performances is approximately 1.6. The transit and on-site performances can be as large as 1 and 0.6, respectively.

- Based on the variations of *metric(C)+metric(W)*, designers are able to infer how the design decision of ship length influences the integrated operational performances. With roll impact, the integrated performances of the vessel achieve substantial improvement when ship length changes from 80m to 140m. Then there is little performance improvement for ship length beyond 140m. With pitch impact, longer ships present better performances except for summer.

- There is one observation that seems counter-intuitive and needs further explanation. The values of *metric(C)* with pitch impact are about 0.6 regardless

of the ship length. It seems counter-intuitive that *metric(C)* demonstrates no sensitivity to the ship length. The reason why *metric(C)* remains at 0.6 lies in the parameter $\alpha$. When $\alpha$ value is not large enough, the GS-MDP framework cannot distinguish the difficulties in adjusting the heading for different ship designs.

Table 6.8: *Metric(C)* with pitch impact in winter when $\alpha$=0.7

| Hull length (meters) | 80 | 120 | 160 |
|---|---|---|---|
| *Metric(C)* | 0.483 | 0.550 | 0.613 |

To check the effect of parameter $\alpha$ on transit evaluations, this case study modified the $\alpha$ value from 0.4 to 0.7 and simulated the transit operations again for three ship designs (L=80m, 120m, and 160m) with pitch impact in winter. Table 6.8 shows the corresponding simulation results, indicating that *metric(C)* does present sensitivity to ship length variations given a relatively large $\alpha$ value. Therefore, from the design perspective, it will be necessary to conduct a parametric analysis of $\alpha$ combined with the variations in ship design decisions.

## 6.4 Conclusions

This chapter has verified and validated the extension of thin abstractions from transit to on-site operations. The presented case study concretely illustrated the feasibility and value of the GS-MDP framework for on-site operations through the comparison with a reference paper. First of all, both this case study and the reference paper suggest the same contributor that influences the on-site performances, indicating the validity of extending the GS-MDP framework to the on-site simulations. Then, the operation ensemble generated from the GS-MDP framework allows designers to

expand the on-site operational evaluations from various dimensions. Analyzing how the on-site performances change based on different seasons can inform designers of potential weather challenges and susceptibility that this vessel may experience. Uncovering the on-site operational performances with respect to all the relative heading angles can provide leading indicators for designers to understand this vessel design. Furthermore, the GS-MDP framework enables the combination of the transit and on-site evaluation results as the integrated performances. Thus, designers can discover the contributors, seasonal tendencies, or any other insights related to the vessel's transit and consider design activities to improve the overall execution of ship operations. Last but not least, this case study has conducted a parametric design in ship length and presented how the GS-MDP framework and corresponding metrics create appropriate knowledge to differentiate the choices of a design decision. In this case study, the influence of modifying ship length on operational performances has been presented as an example to testify the framework's ability. A more comprehensive parametric study will be needed in the future if designers want to enrich their understandings of all the critical design decisions relevant to the OCV.

The major takeaway from this chapter is the versatile application of the thin abstraction. Abstracting ship operations from the thinness perspective not only enables generic evaluations independent of specific cases, but also allows different operation events to be represented under the same framework without loss or sacrifices of their essential features. This develops a new mindset for designers to handle the complexity and multidisciplinary interactions of a ship design in an effective way, even during the concept stage.

# CHAPTER VII

# Conclusion

This thesis has presented a novel perspective of generating knowledge for concept designs by initiating the GS-MDP framework. The focus of knowledge generation shifted from thick abstractions, which were traditionally used and mainly offered case-specific design insights, to thin abstractions, which were more likely to create generalized design insights. To promote the understanding of operational performances from the thinness perspective, the GS-MDP framework abstracted and presented ship operations through an operation ensemble, a concept that was uniquely defined in this thesis. The operation ensemble is the key contribution to assisting early-stage decision-making. It can involve multidisciplinary considerations related to ship operations systematically and flexibly, which allows designers to break down the complexity of ship designs in the concept stage. Moreover, it can provide in-depth knowledge for designers, including not only the operational outcomes but also the causation relationships and leading indicators.

## 7.1 Review of Contributions

For the purpose of aiding conceptual ship design, this research has made the following contributions.

1. *Identified the need for thin abstractions in ship design.*

(1) Clarified the thick and thin abstractions and their different values in the marine design domain for the first time, which initiated a new mindset to instruct design activities.

(2) Clarified the usefulness of the thin abstraction, which was especially suitable to discover design insights in the concept stage.

2. *Enabled the thin abstraction for ship operations based on directional decisions and operation ensembles as the key factors.*

(1) Developed directional decisions to decompose ship operations.

(2) Developed operation ensembles to emphasize what was essential and generic and ignore what was singular and incidental.

3. *Created the GS-MDP framework to achieve thin abstractions.* This framework handles the operational cases, situations, and scenarios that share similar features, by just modifying constants within the framework while keeping the main definitions of the framework unchanged. The primary contributions of this framework are listed below.

(1) Developed a novel ocean gridding approach to eliminate the need for a specific route, which supported the aggregation of directional decisions and the formation of an operation ensemble.

(2) Developed the MDP states and actions to represent and understand all potential routes and transit status.

(3) Developed a systematic mechanism of tying the implications of ship motions to operational simulations within the MDP transition probabilities.

(4) Enabled the modification of different seakeeping impact levels by defining parameters $\lambda$ and $\alpha$.

(5) Presented the feature of desirable ship operations through the MDP rewards and Bellman equation.

4. *Created unique metrics to enable multi-attribute operational evaluations.*

   (1) Identified the principles that new metrics should follow to ensure their applicability and meanwhile reserve the possibility of adding more metrics whenever necessary.

   (2) Developed new metrics to analyze sea transport operations, reflecting transit selections, efficiency, robustness, and on-site working status.

   (3) Utilized the newly defined metrics to benchmark ideal ship operations and understand negative physical influence.

5. *Enabled deep investigation of operational outcomes.* This involves the contributions in terms of supporting iterative investigation from the what perspective to the why perspective.

   (1) Utilized MDP as a tool of generating operation-related data rather than just calculating optimal solutions.

   (2) Enabled the ability to track the emergence of operational phenomena and explore the underlying dynamics and causal contexts.

   (3) Enabled the ability to uncover leading indicators and help designers know the potential operational challenges.

6. *Demonstrated the GS-MDP framework via two representative case studies.*

   (1) Illustrated a manual on how to exploit the value of directional decisions and operation ensembles.

   (2) Introduced a template of how to extend the thin abstraction from transit to on-site operations.

## 7.2 Future Work

While this research has made many contributions to early-state operational considerations, there still remain several topics that deserve to be explored in the future. The future topics may include the following ones.

1. *Modify the tool to be used for other engineering considerations.* The incorporation of physics into the GS-MDP framework depends on making suitable connections with certain physical analysis tools. As mentioned in Chapter V, the consideration of heave motions needs to be improved by a more appropriate seakeeping tool. Moreover, the physical factors to be considered are not limited to seakeeping responses. For example, they could also be structural fatigue analysis, which has an influence on the vessel's lifetime maintenance costs. The GS-MDP framework should be extended to incorporate other analysis tools.

2. *Improve the reward functions in the areas of logistics and economics.* The operational evaluations for different design problems may involve some logistics or economic considerations beyond what has been currently included in the GS-MDP framework. There is a need to update the rewards in MDP with corresponding estimations of these disciplines.

3. *Extend the use of this thin abstraction to more ship operations.* Currently, the transit and offshore engineering operations have been modeled through the GS-MDP framework. If needed, designers should apply this framework to other operations, such as the operations occurring at the port.

4. *Explore a comprehensive parametric study of design decisions.* The variations in metric values can help designers distinguish the choices of a design decision. As a demonstration, the case study in Chapter VI examined the influence of varying ship lengths on operational performances. In the future, it is necessary

to conduct a comprehensive parametric study including all the critical design decisions related to the design concept. Moreover, the parametric analyses also need to include parameters $\lambda$ and $\alpha$ in combination with the variations in ship design decisions.

# BIBLIOGRAPHY

# BIBLIOGRAPHY


Bellman, R. (1957), *Dynamic Programming*, Princeton University Press, Princeton, NJ.

Bertram, V. (2012), Chapter 4 - ship seakeeping, in *Practical Ship Hydrodynamics (Second Edition)*, edited by V. Bertram, second edition ed., pp. 143–204, Butterworth-Heinemann, Oxford, doi:10.1016/B978-0-08-097150-6.10004-1.

Broughton, S. A., and K. M. Bryan (2008), *Discrete Fourier analysis and wavelets: Applications to signal and image processing*, John Wiley & Sons.

Castillo, J., S. Steinberg, and P. J. Roache (1987), Mathematical aspects of variational grid generation ii, *Journal of Computational and Applied Mathematics*, *20*, 127 – 135, doi:https://doi.org/10.1016/0377-0427(87)90130-0.

Chen, C., H. Liu, and R. C. Beardsley (2003), An unstructured grid, finite-volume, three-dimensional, primitive equations ocean model: Application to coastal ocean and estuaries, *Journal of Atmospheric and Oceanic Technology*, *20*(1), 159 – 186, doi:10.1175/1520-0426(2003)020⟨0159:AUGFVT⟩2.0.CO;2.

Couser, P. (2000), Seakeeping analysis for preliminary design, in *Proceedings of the 4th Ausmarine Conference, Fremantle, Australia*.

Debreu, L., C. Vouland, and E. Blayo (2008), Agrif: Adaptive grid refinement in fortran, *Computers & Geosciences*, *34*(1), 8–13, doi:https://doi.org/10.1016/j.cageo.2007.01.009.

Dictionary.com (n.d.), Definition of abstraction, `https://www.dictionary.com/browse/abstraction`, accessed: May 19, 2021.

ECMWF (2010), European center for medium-range weather forecasts.

Fiorini, M., A. Capata, and D. D. Bloisi (2016), Ais data visualization for maritime spatial planning (msp), *International Journal of e-Navigation and Maritime Economy*, *5*, 45–60, doi:https://doi.org/10.1016/j.enavi.2016.12.004.

Folger, R., and C. J. Turillo (1999), Theorizing as the thickness of thin abstraction, *The Academy of Management Review*, *24*(4), 742–758.

Fonseca, N., and C. Guedes Soares (2002), Sensitivity of the expected ships availability to different seakeeping criteria, in *Proceedings of the International Conference on Offshore Mechanics and Arctic Engineering - OMAE*, vol. 4, doi: 10.1115/OMAE2002-28542.

Fox-Kemper, B., et al. (2019), Challenges and prospects in ocean circulation models, *Frontiers in Marine Science*, *6*, 65, doi:10.3389/fmars.2019.00065.

Freund, R. J., W. J. Wilson, and D. L. Mohr (2010), Chapter 1 - data and statistics, in *Statistical Methods (Third Edition)*, edited by R. J. Freund, W. J. Wilson, and D. L. Mohr, third edition ed., pp. 1–65, Academic Press, Boston, doi:10.1016/B978-0-12-374970-3.00001-9.

Gale, P. A. (2003), Chapter 5: The ship design process, in *Ship design and construction*, Society of Naval Architects and Marine Engineers.

Ghaemi, M. H., and H. Olszewski (2017), Total ship operability –review, concept and criteria, *Polish Maritime Research*, *24*(s1), 74–81, doi:10.1515/pomr-2017-0024.

Goldthorpe, J. H. (2001), Causation, statistics, and sociology, *European sociological review*, *17*(1), 1–20.

Gregor, S., O. Müller, and S. Seidel (2013), Reflection, abstraction and theorizing in design and development research, in *European Conference on Information Systems*.

Gutsch, M., S. Steen, and F. Sprenger (2020), Operability robustness index as seakeeping performance criterion for offshore vessels, *Ocean Engineering*, *217*, 107,931, doi:10.1016/j.oceaneng.2020.107931.

Kamarudin, K. M., K. Ridgway, and N. Ismail (2016), Abstraction and generalization in conceptual design process: Involving safety principles in triz-sda environment, *Procedia CIRP*, *39*, 16–21, doi:10.1016/j.procir.2016.01.038, structured Innovation with TRIZ in Science and Industry: Creating Value for Customers and Society.

Kana, A. A., and K. Droste (2019), An early-stage design model for estimating ship evacuation patterns using the ship-centric markov decision process, *Proceedings of the Institution of Mechanical Engineers, Part M: Journal of Engineering for the Maritime Environment*, *233*, 138–149.

Kana, A. A., and D. J. Singer (2016), A ship egress analysis method using spectral markov decision processes, in *Proceedings of PRADS*.

Kim, S. P. (2011), Cfd as a seakeeping tool for ship design, *International Journal of Naval Architecture and Ocean Engineering*, *3*(1), 65–71, doi:https://doi.org/10.2478/IJNAOE-2013-0046.

Kolb, D. A. (2014), *Experiential learning: Experience as the source of learning and development*, FT press.

Lane, E., R. Walters, P. Gillibrand, and M. Uddstrom (2009), Operational forecasting of sea level height using an unstructured grid ocean model, *Ocean Modelling*, *28*(1), 88–96, doi:10.1016/j.ocemod.2008.11.004, the Sixth International Workshop on Unstructured Mesh Numerical Modelling of Coastal, Shelf and Ocean Flows.

Lee, W. T., S. L. Bales, and S. E. Sowby (1985), Standardized wind and wave environments for north pacific ocean areas, *Tech. rep.*, David W Taylor Naval Ship Research And Development Center.

Lexico.com (n.d.), Definition of abstraction, `https://www.lexico.com/definition/abstraction`, accessed: May 19, 2021.

MarineTraffic (n.d.), Maunawili, `https://www.marinetraffic.com/en/ais/details/ships/shipid:445163/mmsi:367438000/imo:9268538/vessel:MAUNAWILI`, accessed: May 29, 2021.

Mavriplis, D. J. (1996), Chapter 7 - mesh generation and adaptivity for complex geometries and flows, in *Handbook of Computational Fluid Mechanics*, edited by R. Peyret, pp. 417 – 459, Academic Press, London, doi:https://doi.org/10.1016/B978-012553010-1/50008-6.

McLean, A. A., and W. E. Biles (2008), A simulation approach to the evaluation of operational costs and performance in liner shipping operations, in *2008 Winter Simulation Conference*, pp. 2577–2584, doi:10.1109/WSC.2008.4736370.

Merriam-Webster (n.d.), Definition of abstraction, `https://www.merriam-webster.com/dictionary/abstraction`, accessed: May 19, 2021.

Michalski, J. (2014), Parametric method for evaluating optimal ship deadweight, *Polish Maritime Research*, *21*(2(82)), 3–8.

Molland, A. F. (2008), *The Maritime Engineering Reference Book*, chap. 7, pp. 483 – 577, Butterworth-Heinemann, Oxford.

Niese, N. D. (2012), Life cycle evaluation under uncertain environmental policies using a ship-centric markov decision process framework, Ph.D. thesis, University of Michigan.

Niese, N. D., and D. J. Singer (2013), Strategic life cycle decision-making for the management of complex systems subject to uncertain environmental policy, *Ocean Engineering*, *72*, 365 – 374.

Niese, N. D., and D. J. Singer (2014), Assessing changeability under uncertain exogenous disturbance, *Res Eng Design*, *25*, 241–258.

Niese, N. D., A. A. Kana, and D. J. Singer (2015), Ship design evaluation subject to carbon emission policymaking using a markov decision process framework, *Ocean Engineering*, *106*, 371–385.

Paik, J. K., and A. K. Thayamballi (2007), Appendix 3 - probability of sea states at various ocean regions, in *Ship-Shaped Offshore Installations: Design, Building, and Operation*, Cambridge University Press, Cambridge, doi:10.1017/CBO9780511546082.

Parsons, M. G. (2018), Advanced marine design (informal course notes), *Tech. rep.*, Department of Naval Architecture and Marine Engineering, University of Michigan.

Pinker, S. (1997), *How the mind works*, 1st ed. ed., Norton.

Prochazka, V., and R. Adland (2019), Ocean mesh grid: Applications in shipping modeling, in *2019 IEEE International Conference on Industrial Engineering and Engineering Management (IEEM)*, pp. 330–334.

Puterman, M. L. (1994), *Markov decision processes: discrete stochastic dynamic programming*, John Wiley & Sons, Inc, Hoboken, New Jersey.

Rawson, K., and E. Tupper (2001), 15 - ship design, in *Basic Ship Theory (Fifth Edition)*, fifth edition ed., pp. 617–654, Butterworth-Heinemann, Oxford, doi:10.1016/B978-075065398-5/50018-2.

Reymen, I. (2001), *Improving design processes through structured reflection : a domain-independent approach*, SAI Reports, Technische Universiteit Eindhoven. Stan Ackermans Instituut.

Robelin, C.-A., and S. M. Madanat (2007), History-dependent bridge deck maintenance and replacement optimization with markov decision processes, *Journal of Infrastructure Systems*, *13*(3), 195–201.

Russell, S. J., and P. Norvig (2010), *Artificial intelligence: a modern approach*, chap. 17, pp. 645 – 693, 3rd ed., Pearson Education, Inc., Upper Saddle River, New Jersey.

Sandvik, E., M. Gutsch, and B. Asbjørnslett (2018), A simulation-based ship design methodology for evaluating susceptibility to weather-induced delays during marine operations, *Ship Technology Research*, *65*, 1–16, doi:10.1080/09377255.2018.1473236.

Sharlanova, V. (2004), Experiential learning, *Trakia Journal of Sciences Trakia Journal of Sciences*, *2*, 36–39.

Shchepetkin, A. F., and J. C. McWilliams (2005), The regional oceanic modeling system (roms): a split-explicit, free-surface, topography-following-coordinate oceanic model, *Ocean Modelling*, *9*(4), 347–404, doi:https://doi.org/10.1016/j.ocemod.2004.08.002.

Simon, H. A. (1954), Spurious correlation: A causal interpretation, *Journal of the American statistical Association*, *49*(267), 467–479.

Simon, H. A., and Y. Iwasaki (1988), Causal ordering, comparative statics, and near decomposability, *Journal of Econometrics*, *39*, 149–173.

Stevens, S., and M. Parsons (2002), Effects of motion at sea on crew performance: A survey, *Marine Technology*, *39*, 29–47, doi:10.5957/mt1.2002.39.1.29.

Suppes, P. (1970), *A probabilistic theory of causality*, North-Holland.

Trotta, F., E. Fenu, N. Pinardi, D. Bruciaferri, L. Giacomelli, I. Federico, and G. Coppini (2016), A structured and unstructured grid relocatable ocean platform for forecasting (surf), *Deep Sea Research Part II: Topical Studies in Oceanography*, *133*, 54 – 75, doi:https://doi.org/10.1016/j.dsr2.2016.05.004.

Tupper, E. C. (2013), Chapter 14 - ship design, in *Introduction to Naval Architecture (Fifth Edition)*, edited by E. C. Tupper, fifth edition ed., pp. 343–377, Butterworth-Heinemann, Oxford, doi:10.1016/B978-0-08-098237-3.00014-X.

Urquhart, C., H. Lehmann, and M. D. Myers (2010), Putting the theory back into grounded theory: guidelines for grounded theory studies in information systems, *Information Systems Journal*, *20*(4), 357–381, doi:10.1111/j.1365-2575.2009.00328.x.

Wood Daudelin, M. (1996), Learning from experience through reflection, *Organizational Dynamics*, *24*(3), 36–48, doi:10.1016/S0090-2616(96)90004-2.

Wu, L., Y.-J. Xu, Q. Wang, F. Wang, and Z. Xu (2017), Mapping global shipping density from ais data, *Journal of Navigation*, *70*, 67–81, doi:10.1017/S0373463316000345.